ÇUKUROVA UNIVERSITY
INSTITUTE OF NATURAL AND APPLIED SCIENCES

MSc. THESIS

Durmuş Can ACER

THE EFFECT OF ADDITIVES ON THE LOW VELOCITY IMPACT PROPERTIES OF LOW DENSITY FIBER SANDWICH PANELS

DEPARTMENT OF MECHANICAL ENGINEERING

ADANA-2019

ÇUKUROVA UNIVERSITY
INSTITUTE OF NATURAL AND APPLIED SCIENCES

THE EFFECT OF ADDITIVES ON THE LOW VELOCITY IMPACT PROPERTIES OF LOW DENSITY FIBER SANDWICH PANELS

Durmuş Can ACER

MSc. THESIS

DEPARTMENT OF MECHANICAL ENGINEERING

We certified that the thesis titled above was reviewed and approved for the award degree of the master of mechanical engineering by the board of jury on 23/07/2019

…………………………….   …………………………………...   ………………………

Prof. Dr. Necdet GEREN   Prof. Dr. Melih BAYRAMOĞLU   Prof. Dr. Uğur EŞME
SUPERVISOR   MEMBER   MEMBER

This M Sc. Thesis is performed in Department of Mechanical Engineering of the Institute of Natural and Applied Sciences of Çukurova University.
Registration No:

Prof. Dr. Mustafa GÖK
Director
Institute of Natural and Applied Science

ABSTRACT

MSc. THESIS

THE EFFECT OF ADDITIVES ON THE LOW VELOCITY IMPACT PROPERTIES OF LOW DENSITY FIBER SANDWICH PANELS

Durmuş Can ACER

ÇUKUROVA UNIVERSITY
INSTITUTE OF NATURAL AND APPLIED SCIENCES
DEPARTMENT OF MECHANICAL ENGINEERING

Supervisor	: Prof. Dr. Necdet GEREN
	Year: 2019, Page: 145
Jury	: Prof. Dr. Necdet GEREN
	: Prof. Dr. Melih BAYRAMOĞLU
	: Prof. Dr. Uğur EŞME

Sandwich structures with carbon fiber-epoxy face sheets and polyvinyl chloride foam core material are known for their high strength and flexural stiffness despite their low weight. However, poor impact characteristics make it difficult to operate these materials under impact load without failure. In this thesis work, it is aimed to increase the impact resistance of low weight composite sandwich structures. The focus is on the epoxy matrix, which has a brittle structure, because the improvement in impact properties is intended to be achieved without significant weight gain. Graphene, boron carbide and kaolin were used as additives in this study for the application of matrix toughening method. 2%, 5% and 10% by weight additives were mixed into epoxy matrix and sandwich structures were produced by hand lay-up and vacuum bagging method. All configurations were subjected to a low velocity drop weight impact test at three different energy levels (10 J, 17.5 J and 25 J). The results obtained from the experiments and the images of the post-impact damage of the sandwich structures are presented comparatively. According to the test results, configurations containing boron carbide additive were the most resistant to impact load. It has been observed that graphene additive increases impact resistance at low additive ratios, while kaolin additive has no significant effect on impact resistance.

Keywords: sandwich structures, drop weight impact, matrix toughening, graphene, boron carbide, kaolin

ÖZ

YÜKSEK LİSANS TEZİ

THE EFFECT OF ADDITIVES ON THE LOW VELOCITY IMPACT PROPERTIES OF LOW DENSITY FIBER SANDWICH PANELS

Durmuş Can ACER

ÇUKUROVA ÜNİVERSİTESİ
FEN BİLİMLERİ ENSTİTÜSÜ
MAKİNA MÜHENDİSLİĞİ ANABİLİM DALI

Karbon fiber-epoksi yüzey tabakalı ve polivinil klorid köpük çekirdek malzemeli sandviç yapılar sahip oldukları düşük ağırlığa rağmen sundukları yüksek mukavemet ve eğilme dayanımı ile bilinirler. Buna rağmen darbe özelliklerinin zayıf olması bu malzemelerin darbe yükü altında hatasız çalışmasını zorlaştırmaktadır. Bu tez çalışmasında düşük ağırlıklı kompozit sandviç yapıların darbe dirençlerini artırmaya yönelik çalışılmıştır. Darbe özelliklerinde iyileşmenin önemli miktarda ağırlık artışı olmadan yapılması istendiğinden dolayı kırılgan bir yapıya sahip olan epoksi matris üzerine odaklanılmıştır. Matris güçlendirme yönteminin uygulandığı bu çalışmada katkı maddesi olarak grafen, boron karbid ve kaolin kullanılmıştır. Ağırlıkça %2, %5 ve %10 oranlarındaki katkı maddeleri epoksi matrise karıştırılmış, el yatırması ve vakum torbalama yöntemiyle sandviç yapılar üretilmiştir. Tüm konfigürasyonlar üç farklı enerji seviyesinde (10 J, 17,5 J ve 25 J) düşük hızda ağırlık düşürmeli darbe testine tabi tutulmuştur. Deneylerden elde edilen sonuçlar ve sandviç yapıların darbe sonrası hasarlarının görüntüleri karşılaştırmalı olarak sunulmuştur. Test sonuçlarına göre boron karbid katkısı içeren konfigürasyonların darbe yüküne en dayanıklı seçenek olduğu görülmüştür. Grafen katkısının düşük katkı oranlarında darbe dayanımını artırdığı, kaolin katkısının ise darbe dayanımına anlamlı bir etkisinin olmadığı görülmüştür.

Anahtar Kelimeler: sandviç yapılar, düşük hızda ağırlık düşürmeli darbe, matris güçlendirme, grafen, boron karbid, kaolin

II

EXTENDED ABSTRACT

Fiber reinforced composite materials have become very popular especially in the last century due to their low weight, high stiffness and strength properties. With the introduction of fiber-reinforced composite materials, structures such as lighter transportation vehicles and wind turbine blades were built and a significant amount of energy efficiency was achieved. In addition, it has been possible to make lighter sporting goods and military equipment. Composite materials have found its place in many industries.

The composite materials consist of the reinforcement elements and the binding elements that hold the reinforcement elements together. The reinforcement element and the binding element vary depending on where the material is to be used. For example, when high tensile strength and low weight are desired, carbon fiber can be selected as the reinforcing material. On the other hand, when the cost is considered, glass fiber can be selected as the reinforcement. Aramid fiber (Kevlar) should be used if ballistic performance is expected. Sandwich structures with carbon fiber face sheets and polyvinyl chloride (PVC) core material are used when high bending stiffness is desired with a lighter material. Carbon fiber reinforced epoxy matrix composite structure used as face sheet has very high tensile and compressive strength despite its low density. However, the impact resistance is low due to the brittle nature of the material.

In this study, impact resistance of sandwich structures produced from carbon fiber reinforced epoxy matrix face sheets and PVC core material were studied. In areas where sandwich structures will be subjected to impact load, metal sheets are generally preferred as face sheets and metal foams as core material. However, in this case there is a significant weight increase. Instead, matrix toughening method, which is performed for laminated composites in the literature, was applied to sandwich structures. The matrix toughening method is applied for toughening the brittle structure of the matrix material. In this method, micro or

nano size additives are mixed into the matrix. Thus, it is aimed to significantly increase the impact resistance of the sandwich structure without significant weight increase.

High strength carbon fiber with a density of 200 g/m^2 as reinforcement material, Hexion MGS L160 epoxy resin and MGS H160 hardener as matrix material, closed cell PVC foam with a density of 48 kg/m^3 having a thickness of 10 mm as core material, while graphene, boron carbide and kaolin were used as additives in this study. Each of three different additive materials were mixed into the matrix material in three different proportions (2%, 5% and 10%) by weight, and a total of 10 different configurations were produced with the reference configuration without additive material. These 10 different configurations were tested under 10 J, 17.5 J and 25 J impact energy.

According to ASTM D7136 / D7136M-12 standard, 100x150 mm sample size was determined for each sample to be subjected to low velocity drop weight impact test. Furthermore, according to the relevant standard, each experiment should be repeated five times. Therefore, it is necessary to produce at least 15 samples from each configuration in order to perform five replicated impact tests at three different energy levels. With the backup productions, 18 samples were produced for each configuration and a total of 180 samples were produced for all configurations in this thesis.

Sandwich panels with additive material were produced by hand lay-up and vacuum bagging method. This method provides a flexible and cost-effective production for low number of productions. Each face sheet of the sandwich panel is made of four layers of carbon fiber. After determining the dimensions of sandwich panels to be produced according to ASTM test standard, sufficient number of carbon fiber fabrics, PVC foams and vacuum bags were cut with suitable tools. Additive materials, epoxy resin and hardener to be used as matrix material were weighed in predetermined proportions. A total of 500 grams of epoxy/hardener mixture is required for 18 samples of each configuration. The ratio of this mixture

is 100 grams of hardener for 400 grams of epoxy resin in accordance with the information obtained from the manufacturer. An appropriate amount of the additive material was mixed into the 500 grams of matrix material by using an ultrasonic homogenizer. Then, each layer of the face sheet and the core material were wetted with the filled matrix material and stacked in a suitable order. Prepared sandwich structures with release film, breather and spiral hose was taken into vacuum bag. Curing was completed in 24 hours under vacuum atmosphere. Thus, excess resin and air are evacuated, which causes weakening of the mechanical properties of the sandwich structure. In addition, the samples were allowed to stand at room temperature and atmospheric pressure for a further seven days after curing under vacuum to ensure complete curing of the samples.

The low velocity impact test was performed with Ceast Fractovis Plus drop weight impact device according to the ASTM D7136/D7136M-12 test standard. Tests were performed at three different energy levels (10 J, 17.5 J, and 25 J) to investigate the response of the samples at different energy levels. Time, impact force, striker tip position and energy values were obtained from the software of the impact device. With these values, "force-time", "energy-time" and "force-displacement" curves were obtained and plotted. The force-time curve exhibits the time-dependent force during the contact of the striking tip to the sample. Because the samples are sandwich structure, the curve peaks twice. The energy-time curve shows the impact energy, the energy absorbed by the sample, and the energy of the striking tip bounces back from the sample. The force-displacement curve shows the change in force according to the position of the striking tip during impact. This chart provides information on whether the sample is punctured. In addition to the curves, the maximum force values (for the first and second peaks), the energy values absorbed by the sandwich structure and the indentation depth of the striker tip obtained from the low velocity impact test are given in the tables. In addition, the experimental results are compared with each other according to the material type and the amount of material in the graphs, and the results are also given in

tables. In these comparisons, the percentage contribution of the configurations was determined by reference to the sandwich structure made with neat epoxy. Finally, the damage of the sandwich structures after the impact is shown in photos obtained during the tests.

According to the obtained results, it was determined that when the graphene additive were added to the sandwich structure at 2% and 5% by weight of the matrix, the reaction force increased up to 35.6%. However, it was observed that the sandwich structure containing 10% graphene by weight of the matrix became weaker against impact load. Samples containing 2% and 5% graphene additive were not punctured completely, but samples containing 10% graphene additive and the reference samples were punctured at 25 J impact energy level.

Samples containing boron carbide additive were the configuration with the highest increase in reaction forces (up to 63.8%). Unlike sandwich structures containing graphene, it has been observed that boron carbide additive increases the impact resistance of the sandwich structure in all three additive ratios (2%, 5% and 10%). Specimens containing neat epoxy matrix were punctured at 25 J impact energy, but samples containing boron carbide additives were not punctured.

There was no significant change in the impact strength of the configuration containing kaolin additive. Samples containing the kaolin additive were completely punctured just like samples containing neat epoxy matrix at 25 J impact energy.

GENİŞLETİLMİŞ ÖZET

Fiber takviyeli kompozit malzemeler sahip oldukları düşük ağırlık, yüksek rijitlik ve dayanım değerleri sayesinde özellikle son yüzyılda oldukça popüler hale gelmiştir. Fiber takviyeli kompozit malzemelerin kullanılmaya başlanmasıyla daha hafif ulaşım araçları ve rüzgar türbini kanatları yapılmış ve önemli miktarda enerji verimliliği sağlanmıştır. Ayrıca daha hafif spor aletleri ve askeri donanımlar yapmak mümkün olmuştur. Kompozit malzemeler birçok sektörde kendisine yer bulmuştur.

Kompozit malzemeler taşıyıcı elemanlar ve taşıyıcı elemanları bir arada tutan bağlayıcı elemanlardan oluşur. Malzemenin kullanılacağı alana göre taşıyıcı eleman ve bağlayıcı eleman değişiklik gösterir. Örneğin yüksek çekme dayanımı ve düşük ağırlık istenen bir çalışma yapılıyorsa takviye malzemesi olarak karbon fiber seçilebilir. Diğer bir yandan maliyet ön plana çıkıyorsa cam fiber takviye malzemesi olarak seçilebilir. Balistik bir performans bekleniyorsa aramid fiber (Kevlar) kullanılması gerekir. Karbon fiber yüzey tabakalı ve polivinil klorid (PVC) çekirdek malzemeli sandviç yapılar ise yüksek eğilme rijitliğinin daha hafif bir malzeme ile elde edilmesi arzu edildiğinde kullanılmaktadır. Yüzey tabakası olarak kullanılan karbon fiber takviyeli epoksi matrisli kompozit yapının düşük yoğunluğuna rağmen çok yüksek çekme ve basma mukavemeti vardır. Ancak darbe direnci malzemenin kırılgan doğasından dolayı düşüktür.

Bu çalışmada karbon fiber takviyeli epoksi matrisli yüzey tabakaları ve PVC çekirdek malzemesinden üretilen sandviç yapıların darbe dirençleri ele alınmıştır. Sandviç panellerin darbe yüküne maruz kalacağı alanlarda genellikle metal saclar yüzey tabakaları olarak ve metal köpükler çekirdek malzeme olarak tercih edilmektedir. Ancak bu durumda önemli miktarda ağırlık artışı olmaktadır. Bunun yerine literatürde de tabakalı kompozit malzemeler için çeşitli çalışmalara konu olan matris toklaştırma yöntemi, bu çalışmada geliştirilen sandviç yapılara uygulanmıştır. Matris toklaştırma yöntemi matris malzemenin kırılgan yapısını

toklaştırma amacıyla uygulanmaktadır. Bu yöntemde mikro veya nano boyuttaki katkı malzemeleri matris içerisine karıştırılmaktadır. Bu sayede önemli bir ağırlık artışı olmadan, sandviç yapının darbe direncinin önemli miktarda artırılması hedeflenmektedir.

Bu çalışmada takviye malzemesi olarak 200 gr/m^2 yoğunluğa sahip yüksek mukavemetli karbon fiber, matris malzeme olarak Hexion MGS L160 epoksi reçine ile MGS H160 sertleştirici, çekirdek malzeme olarak 10 mm kalınlığa sahip 48 kg/m^3 yoğunluklu kapalı hücreli PVC köpük ve katkı malzemesi olarak ise grafen, boron karbid ve kaolin kullanılmıştır. Bu üç farklı katkı malzemesinin her biri matris malzemeye ağırlıkça üç farklı oranda (%2, %5 ve %10) karıştırılmış, katkı malzemesi içermeyen referans konfigürasyonla birlikte toplamda 10 farklı konfigürasyon üretilmiştir. Bu 10 farklı konfigürasyon 10 J, 17,5 J ve 25 J darbe enerjisine tabi tutulmuştur.

ASTM D7136/D7136M-12 standardına göre düşük hızda ağırlık düşürmeli darbe testine tabi tutulacak her bir numune için 100x150 mm numune ölçüsü belirlenmiştir. Ayrıca ilgili standarda göre her bir deneyin beş defa tekrarlanması gerekmektedir. Bu yüzden her bir numuneden üç farklı enerji seviyesinde darbe testi ve beş replikasyon yapabilmek için en az 15 numune üretimi gerekmektedir. Yedek yapılan üretimlerle birlikte bu tez çalışmasının her bir konfigürasyonu için 18 numune, tüm konfigürasyonlar için toplamda 180 numune üretilmiştir.

Katkı malzemeli sandviç panellerin üretimi el yatırması, vakum torbalama yöntemiyle yapılmıştır. Bu yöntem düşük sayıda yapılan üretimler için esnek ve düşük maliyetli bir üretim sağlamaktadır. Sandviç panelin her bir yüzey tabakası dört kat karbon fiberden üretilmektedir. İlgili deney standardına göre üretilecek sandviç panellerin boyutları belirlendikten sonra yeterli sayıda karbon fiber kumaşlar, PVC köpükler ve vakum torbaları uygun araçlarla kesilmiştir. Matris malzeme olarak kullanılacak katkı malzemeleri, epoksi reçine ve sertleştirici önceden belirlenen oranlarda tartılmıştır. Her bir konfigürasyonun 18 numunesi için toplamda 500 gram epoksi/sertleştirici karışımı gerekmektedir. Bu karışımın

oranı üreticiden alınan bilgi doğrultusunda 400 gram epoksi reçine için 100 gram sertleştiricidir. Toplamda 500 grama ulaşan matris malzeme için uygun ağırlıklardaki katkı malzemesi ultrasonik homojenizatör kullanılarak yapıya karıştırılmıştır. Sonrasında yüzey tabakasının her bir katmanı ve çekirdek malzeme katkılı matris malzeme sürülerek uygun düzende üst üste dizilmiştir. Hazırlanan sandviç yapı ayırıcı film, vakum battaniyesi ve spiral hortum ile birlikte vakum torbasına alınmıştır. Kürlenme vakum atmosferi altında 24 saatte tamamlanmıştır. Bu sayede sandviç yapının mekanik özelliklerinin zayıflamasına sebep olan fazla reçine ve havanın tahliyesi sağlanmıştır. Ayrıca numunelerin tam kürlenmesinin sağlanması için vakum altında kürlenmeden sonra yedi gün daha oda sıcaklığında ve atmosfer basıncında bekletilmiştir.

Düşük hızda darbe testi ASTM D7136/D7136M-12 test standardına göre Ceast Fractovis Plus ağırlık düşürmeli darbe cihazı kullanılarak yapılmıştır. Numunelerin farklı enerji seviyelerindeki tepkilerini görmek için üç farklı enerji seviyesinde (10 J, 17,5 J, 25 J) testler yapılmıştır. Darbe cihazının yazılımı aracılığıyla zaman, darbe kuvveti, vurucu ucun konumu ve enerji değerleri elde edilmiştir. Elde edilen bu değerler ile "kuvvet-zaman", "enerji-zaman" ve "kuvvet-yer değiştirme" grafikleri çizilmiştir. Kuvvet-zaman grafiği vurucu ucun numuneye teması süresince kuvvetin zamana bağlı olarak değişimini göstermektedir. Numune sandviç panel olduğu için grafik iki defa pik yapmaktadır. Enerji-zaman grafiği çarpma enerjisini, numunenin absorbe ettiği enerjiyi ve numuneden geri tepen vurucu ucun enerjisini göstermektedir. Kuvvet-yer değiştirme grafiği vurucu ucun çarpma anındaki konumuna göre kuvvetteki değişimi göstermektedir. Bu grafik numunenin delinip delinmediği hakkında bilgi sahibi olunmasını sağlamaktadır. Grafiklere ek olarak düşük hızda darbe testinden elde edilen maksimum kuvvet değerleri (birinci ve ikinci pik için), sandviç yapı tarafından absorbe edilen enerji değerleri ve vurucu ucun batma derinliği tablolarla verilmiştir. Ayrıca elde edilen deneysel sonuçlar malzemeye ve malzeme miktarına göre birbirleriyle kıyaslanarak grafikler ve tablolarla verilmiştir. Bu kıyaslamalarda katkısız epoksiyle yapılan

sandviç yapı referans alınarak konfigürasyonların yüzdesel etkileri ortaya konulmuştur. Son olarak sandviç yapıların darbe sonrası fotoğraflanan görünümleri verilmiştir.

Elde edilen sonuçlara göre grafen katkı malzemesi içeren sandviç yapılar matris ağırlığınca %2 ve %5 oranlarında yapıya katıldığında reaksiyon kuvvetinde %35,6'ya kadar artış sağladığı tespit edilmiştir. Fakat matris ağırlığınca %10 grafen içeren sandviç yapının darbe yüküne karşı daha dayanıksız hale geldiği gözlemlenmiştir. 25 J darbe enerjisine tabi tutulan numunelerden %2 ve %5 grafen katkısı içeren numuneler tamamen delinmemesine rağmen katkı malzemesi içermeyen ve %10 grafen katkısı içeren numuneler delinmiştir.

Boron karbid katkısı içeren numuneler reaksiyon kuvvetlerinde en yüksek artışın görüldüğü (%63,8'e kadar) konfigurasyon olmuştur. Grafen katkısı içeren sandviç yapılardan farklı olarak boron karbid katkısının üç katkı oranında da (%2, %5 ve %10) yapının darbe dayanımını artırdığı gözlemlenmiştir. Katkısız matris içeren numuneler 25 J darbe enerjisinde tamamen delinmesine rağmen boron karbid katkısı içeren numuneler delinmemiştir.

Kaolin katkısı içeren numunelerin darbe dayanımlarında ise anlamlı bir değişiklik gözlemlenmemiştir. 25 J darbe enerjisinde kaolin katkısı içeren numuneler tıpkı katkısız matris içeren numuneler gibi tamamen delinmiştir.

ACKNOWLEDGEMENTS

Completing this thesis would not have been possible without the support and encouragement of several special people. Hence, I would like to take this opportunity to express my gratitude to those who have assisted me in countless ways.

I would first like to thank my supervisor Prof. Dr. Necdet GEREN of the Mechanical Engineering Department at Çukurova University. The door to Prof. GEREN office was always open whenever I ran into a trouble spot or had a question about my research or writing. He consistently allowed this paper to be my own work, but steered me in the right direction whenever he thought I needed it. Besides my supervisor, I would like to thank my thesis jury members Prof. Dr. Melih BAYRAMOĞLU and Prof. Dr. Uğur EŞME.

I thank my colleagues Çağrı UZAY, Metehan BOZTEPE and Ahmet ÇETİN in for the stimulating discussions, specimen manufacturing and performing experiments.

My sincere thanks also goes to Prof. Dr. Recep GÜNEŞ and Mr. Mevlüt HAKAN from Mechanical Engineering Department at Erciyes University for opening the door of their laboratory to me.

A very special thanks to Scientific Research Projects department (BAP) in Çukurova University for providing the funding for this thesis work.

My deep and sincere gratitude to the people who mean a lot to me, my mother and sisters for showing faith in me. I am grateful to a very special person, my wife, for her continued and unfailing love, help and support.

Dedicated to the memory of my father who passed away during the writing of this thesis. You always believed and supported me. You are gone but your belief in me has made this journey possible.

LIST OF FIGURES **PAGE**

XIV

XV

XVI

XVII

1. INTRODUCTION

Even the use of composite materials in daily life is based on centuries ago, it has become very widespread in the field of engineering in the last century. Especially automotive, marine, sporting goods, aeronautics, military, construction and military fields have increased the percentage use of composite materials significantly. This is because the higher stiffness and strength values desired in these areas are achieved with lower weight compared to conventional materials. In this way, serious losses of energy have been avoided especially in transportation, and consequently more payloads have been transported. Figure 1.1 illustrates the evolution of composite use in airplanes as an example to the use of it.
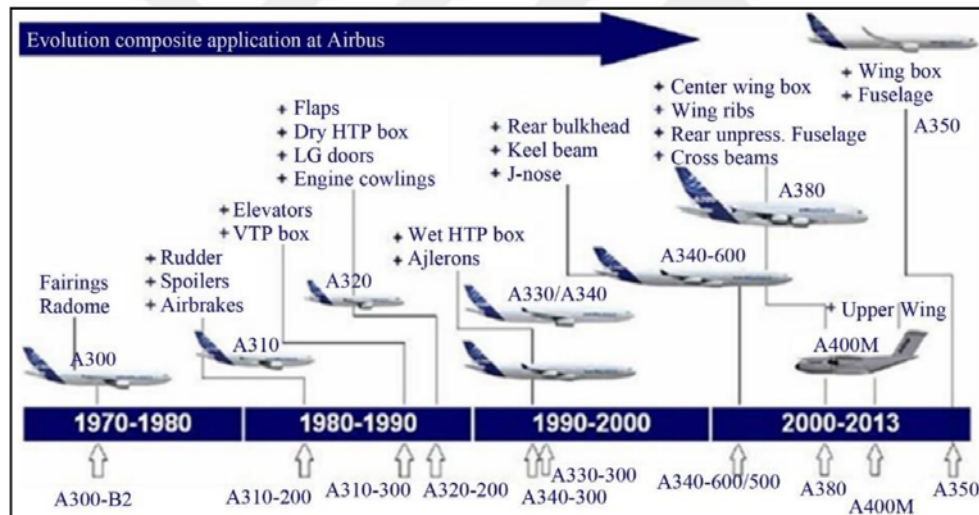
Figure 1.1. Using of composites in Airbus airplanes by years (Di Sante, 2015)

There are different definitions of composite materials in the literature. In general term, composite material is combination of two or more different material which have different properties to obtain a better material (Vasiliev and Morozov, 2007). On the other hand, almost all materials could be named as composite materials based on this definition. For instance, 2024 aluminum alloy consist

aluminum, copper, manganese and magnesium. All these materials are bonded together at the atomic level. However 2024 aluminum alloy cannot be named as composite material. So, the definition of composite materials could be a combination of more than one materials, which are distinct at a physical scale greater than about 1 μm and which are bonded together at the atomic and/or molecular levels (Tuttle, 2004).

Simply, a composite material contains at least one reinforcement to carry loads acting on the member, and a matrix material to hold together the reinforcement. Reinforcements and matrix materials, which have different shapes or materials, can be seen in composite applications. Composites can be classified as metal, ceramic and polymer matrix composites based on their matrix material or particulate, fibrous and laminate composites based on their reinforcement material structure.

One layer of fiber reinforcement called as laminae. The structure consisting of stacking of more than one laminae in the same or different orientations of the same or different materials is called laminate (Altenbach et al, 2004). In this work, sandwich structures, one of the laminated composite types, are studied.

Sandwich composites are based on laminated composite structures. As shown in Figure 1.2, high strength outer thin face sheets, and a low density core material are bonded together to obtain extremely high bending rigidity. Fiber reinforced laminates or metals can be used as face sheets and, woods, metal/polymeric foams or honeycomb structures can be used as core material. Sandwich structures are frequently used in weight critical areas because of their very high bending strength to weight ratio. Depending on the application area, the face sheet and the core material may vary (Uzay et al, 2019). When bending strength and weight are critical, fiber composite face sheets and non-metallic light weight foams or honeycomb core materials can be used. When cost is more critical, metallic face sheets and core materials can be used. Also, impact properties of the structure are directly affected by the face sheets and core materials. In this study,

carbon fiber reinforced polymer (CFRP) was chosen as face sheets, and polyvinyl chloride (PVC) closed cell foam was chosen as core material. This structural combination was chosen because automotive, aerospace and sports equipment demands new materials having superior bending strength to weight ratio.
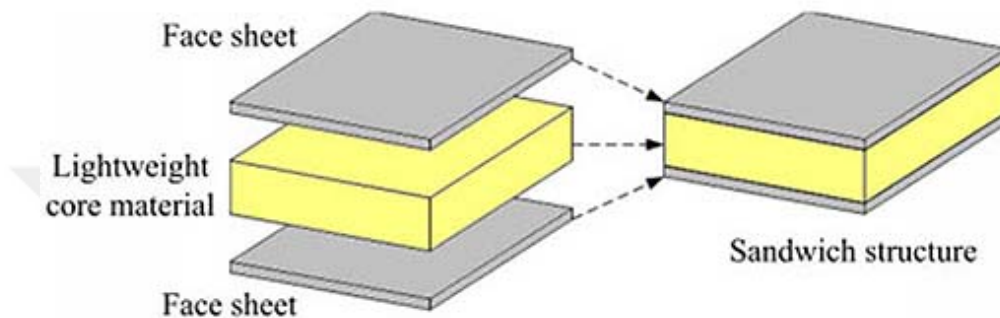
Figure 1.2. Basic schematics of sandwich structure

The application area of an engineering material is determined by the physical, mechanical, thermal, etc. properties of that material. In this thesis, the carbon fiber reinforced epoxy matrix composite structure, which was used as a face sheet, has very good yield strength, fatigue strength and density but the impact strength are not at desired levels. Impact strength can be described as the resistance of a material against sudden loads (Campo, 2008). Impact damage is a major problem in composite materials because most composites have brittle structure, unlike metal materials. In addition, composites can fail in different modes that are visible or invisible (Richardson and Wisheart, 1996). The resistance of the material against sudden loads is very important for an industrial composite structure, especially for safety and long service life.

Researchers have developed a number of methods to improve the impact resistance of laminated composite materials. Saghafi et al. (2018), reported that methods for improving impact resistance of composite laminates are Z-pinning, tufting, 3D weaving, stitching and matrix toughening. This is slightly different in

sandwich structures. Not only the face sheets but also the core material absorb some of the impact energy. When it is desired to increase the impact strength, it is possible to use a core material which has higher impact toughness, but this will cause the sandwich structure to be heavier.

The matrix toughening method is used to toughen matrix materials having brittle structure. It is aimed to increase the toughness of the composite structure by toughening the matrix material which acts as a binder in the composite structure. In this method, micro or nano sized additives are added to the matrix or particles, fibers or film are left between the layers (Saghafi et al., 2018). In this study, matrix toughening method was applied to CFRP face sheets by using micro sized additive materials.

In addition to these methods, it is possible to toughen the composite structure by making hybridization with tougher fiber fabrics or by using commercially available hybrid fabrics. The structure built by combining two or more different reinforcement or binding materials is called hybrid composite (Uzay et al., 2016). There are basically four types of hybrid composites in the literature. These are interply hybrid composites, intraply hybrid composites, interply-intraply hybrid composites and resin hybrid composites (Mallick, 2007). The hybrid made with different fibers in different layers is called interply hybrid composites. The hybrid made with two or more different fibers in one layer (hybrid fabric) is called intraply hybrid composites. The hybrid made with interply and intraply layers together is called interply-intraply hybrid composites. The hybrid made with different types of resins is called resin hybrid composites. Figure 1.3 shows the schematic representation of interply and intraply hybrid composites.
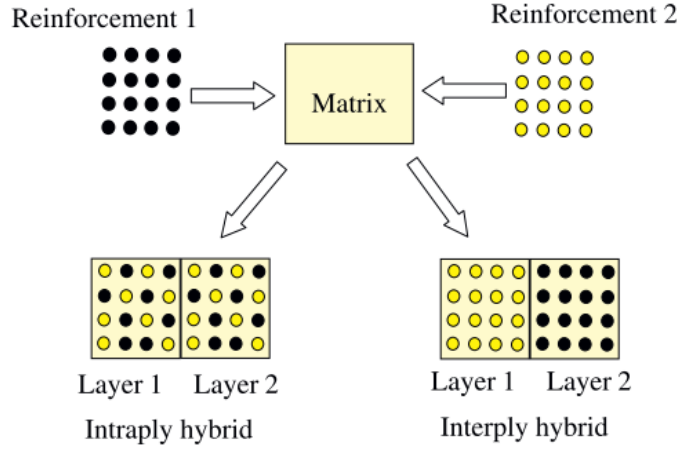
Figure 1.3.   Schematic wiev of intraply and interply hybrid composite (Ha et al., 2012)

1.1. Composite Notation

Notation of composite structures is necessary to know the stacking sequence of reinforcement materials. In the notation, the angles of the uni-directional (UD) fibers are written from the bottom ply to the top ply. For instance, a laminate consist of 0^0, -45^0 and 90^0 plies from bottom to top is notated as [0/-45/90]. In this illustration, the materials and thicknesses of all plies must be the same. When it is not the same, one of the following notations is used. In addition, a subscript "T" can be written at the end of the notation to indicate that all plies of laminate are written.

The subscript "S" can be written at the end of the notation to indicate that the stacking sequence continues symmetrically. For instance, a laminate consist of 0^0, 90^0, 90^0 and 0^0 plies from bottom to top is notated as $[0/90/90/0]_T$ or $[0/90]_S$.

When repetitive plies are present in the sequence, the notation can be shortened by writing the number of repetitions as a subscript. For instance, the sequence [0/90/90/0] may also be represented as $[0/90_2/0]_T$.

When the laminate contains plies of different materials, the upper index is used to indicate the materials. For instance, a hybrid laminate notation consisting of

5

two different materials is written as $[90^1/20^2/0^1/-20^2/90^1]_T$. Here, the plies indicated by the upper index 1 refer to the first material and the plies indicated by the upper index 2 represent the second material.

When the laminate contains plies of different thicknesses, the thickness of each ply should be specified as a subscript. For instance, a laminate notation consisting of plies with two different thickness is written as $[0_{t1}/45_{t2}/-45_{t2}/0_{t1}]_T$.

The above notations are used for UD fabrics but not for woven fabrics used in this thesis work. Woven fabrics can be considered as two UD fabrics knitted at right angles to each other. UD fabrics have high mechanical properties in the longitudinal direction but weak in the transverse direction. Woven fabrics contain fibers in both longitudinal (warp) and transverse (weft) directions as shown in Figure 1.4. Therefore, woven fabrics have good mechanical properties in both directions.
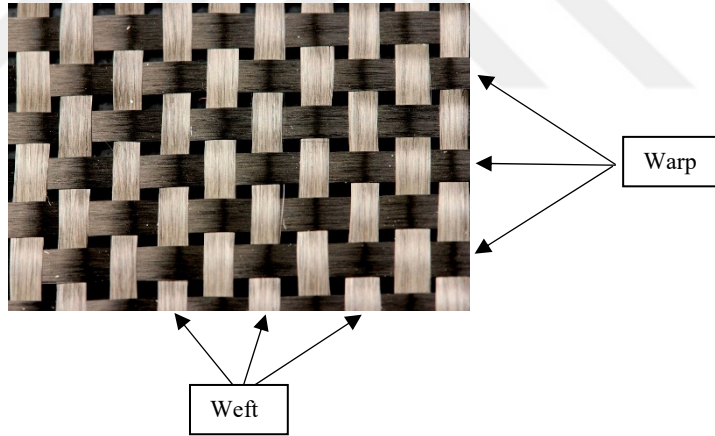

Figure 1.4. Woven carbon fiber fabric

1.2. Sandwich Structure Manufacturing Methods

The most commonly used sandwich production methods are wet lay-up, prepreg lay-up, adhesive bonding, liquid composite moulding, continuous

lamination, compression moulding and filament winding (Karlsson and Åström, 1997).

1.2.1. Wet Lay-Up

The wet lay-up method can be carried out as hand lay-up or spray-up. It is one of the oldest and most widely used methods for sandwich structures consisting of fiber composite surface layers (Karlsson and Åström, 1997). In the hand lay-up method, reinforcement fabrics wetted by brush or roller and core material are placed to the mould in the desired orientation and thickness as shown in Figure 1.5. After placing and resin impregnation of the layers is completed, curing process starts. Curing process is highly dependent on matrix material, ambient temperature and pressure. The curing process can be carried out at atmospheric pressure or under vacuum atmosphere with vacuum bag. When it is complete under vacuum, it is called as hand lay-up vacuum bagging method as shown in Figure 1.6. In the spray-up process, the matrix material and the chopped reinforcing material are sprayed onto the surface or mould by using a spray gun as shown in Figure 1.7. Spraying is continued until the desired thickness is achieved. The structure obtained after spraying process is left to complete the curing process. Wet lay-up method provides flexible and cost-effective production for low production rates. Labour skill has a significant effect on production quality.
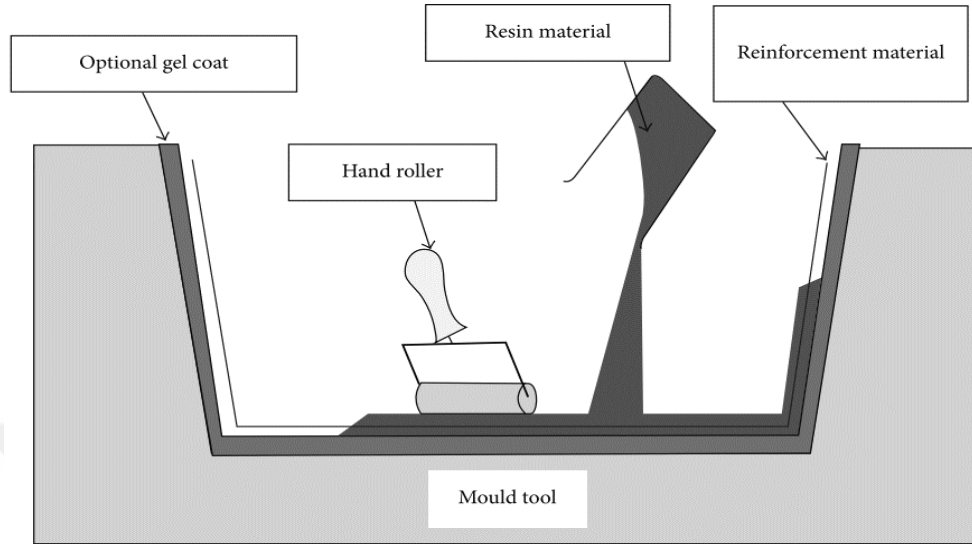
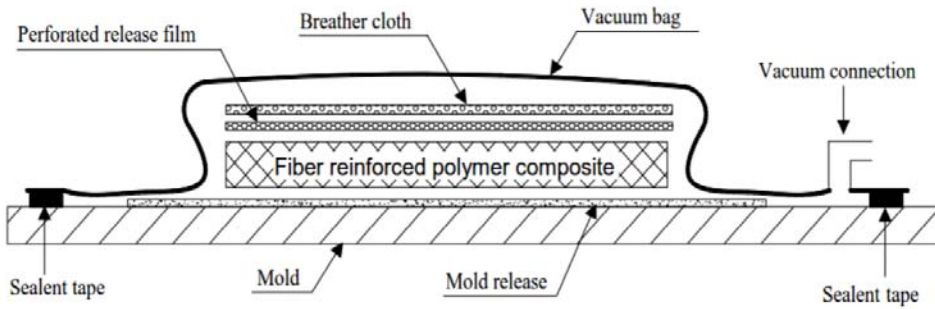Figure 1.5. Schematic view of hand lay-up process (Udupi and Rodrigues, 2016)

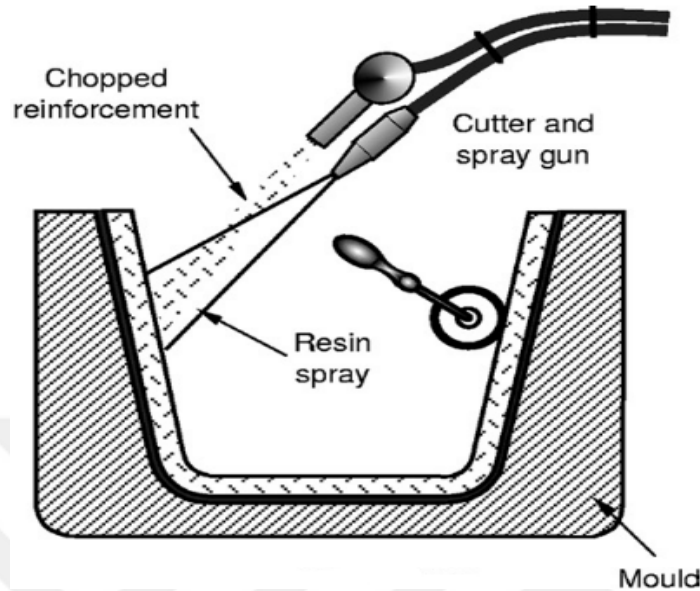Figure 1.6.   Schematic view of hand lay-up vacuum bagging method (Uzay et al, 2018)

Figure 1.7. Schematic view of spray-up process (Swift and Booker, 2013)

1.2.2. Prepreg Lay-Up

In general, the prepreg lay-up method is similar to the hand lay-up method. In the prepreg lay-up method, packed pre-impregnated (prepreg) fabrics are used unlike hand lay-up method. Prepreg fabrics should be stored in the cooler until the time of use in order to prevent curing before application. At the time of production, prepreg fabrics are unpacked and stacked on the mould in the desired orientation and thickness. Then, autoclave oven is used to cure under temperature and pressure. In this method, higher volume fiber ratio is obtained than hand lay-up method. In addition, prepreg lay-up method shortens the processing time and ensures a more homogenous production. However, the investment cost is high because of expensive curing equipment (Barbero, 2017)

1.2.3. Adhesive Bonding

In adhesive bonding method, sandwich structure is obtained by bonding surface layers and core material to each other. In particular, metal surface layer

sandwich structures are produced by this method. When the composite surface layer is to be used, the surface layer must be produced separately in the desired thickness and orientation. Subsequently, the surface layers and core material are cut to the desired size and bonded together with a suitable adhesive. After a good adhesive film is provided between the surface layers and the core material, the sandwich structure is allowed to cure. Usually a press or vacuum bag is used for better adhesion (Karlsson and Åström, 1997).

1.2.4. Liquid Moulding

Liquid moulding method can be carried out as resin transfer moulding (RTM), vacuum assisted resin transfer moulding (VARTM) and resin infusion method. RTM process requires male and female moulds. After the fabrics and core material are placed in the desired thickness and orientation, the moulds are closed and sealed. Then, the resin is transferred into the mould at a specific pressure and flow rate. End of the curing time, the final product is removed from the mould. In Figure 1.8, RTM production method is given simply.
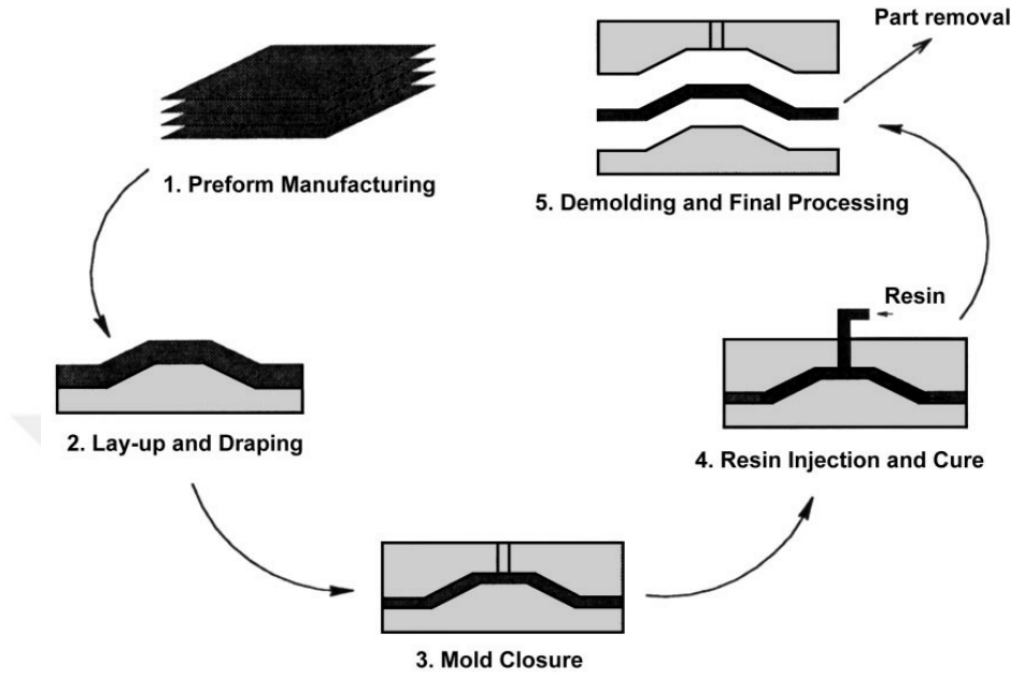
Figure 1.8. Schematic view of RTM method (Kelly, 2000)

In the VARTM production method, in addition to RTM method, the air remaining between the male and female moulds is discharged with a suitable vacuum pump. This ensures a better resin flow and reduces dry-spot formation in the final product (Kelly, 2000).

Resin infusion method requires one-sided mould. After the fabrics and core material are placed in the mould at the desired thickness and orientation, the mould is covered with a vacuum bag. Resin inlet from a suitable location of the mould and resin outlet with a vacuum pump from another suitable location are provided. Once the resin is fully impregnated, the resin inlet is stopped, but the vacuum is continued throughout the curing time. Figure 1.9 shows the steps of the resin infusion method.
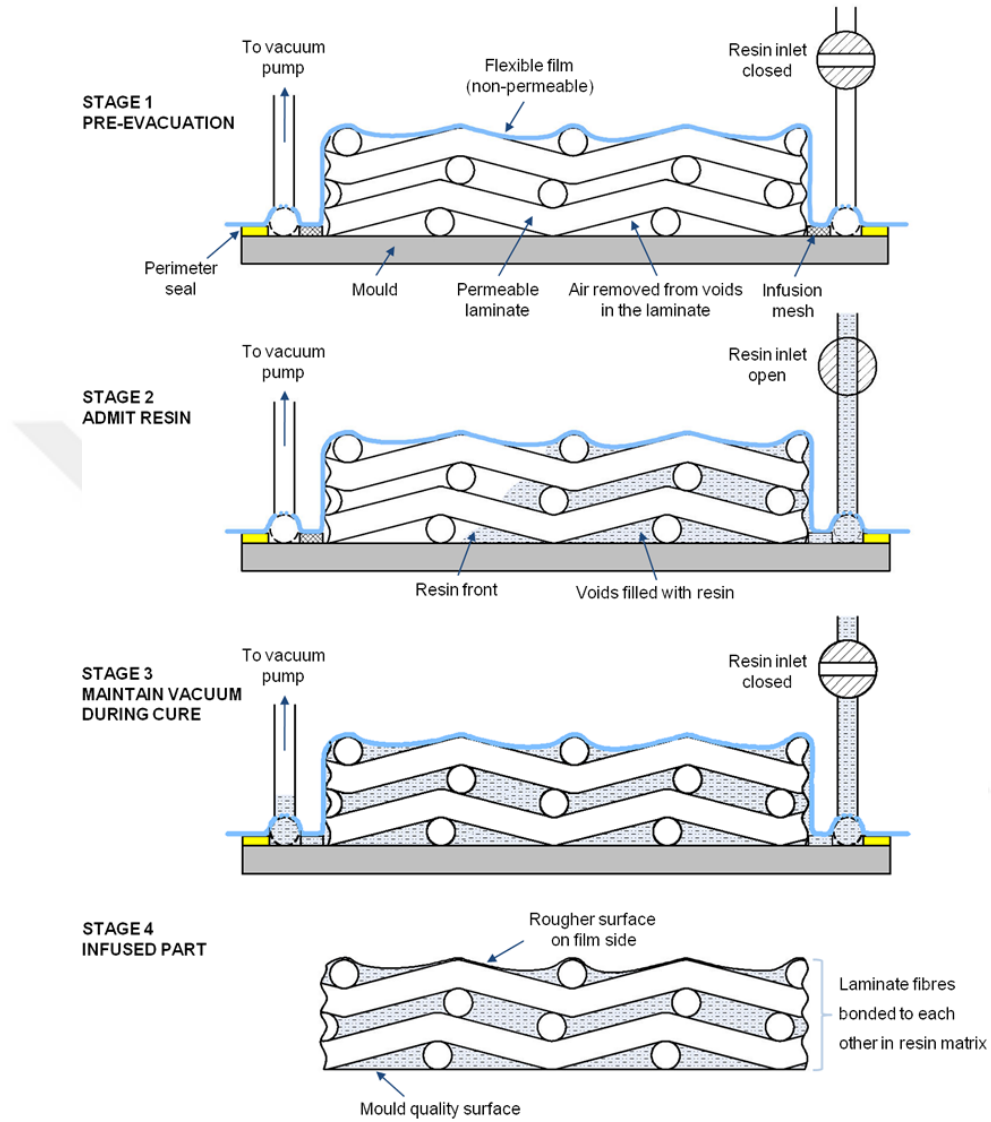
11

Figure 1.9. Production steps of resin infusion method (Vacmobiles, 2019)

1.2.5. Continuous Lamination

In the continuous lamination method, the upper and lower rolled surface layers are guided in between belts of press. The surface layers may be metal or composite. The core material along with the adhesive layers are aligned between

12

the two surface layers. Between the belts, the surface layers and core material stick to each other under a specific temperature and pressure (Karlsson and Åström, 1997). This method is generally used in the production of flat or fixed cross section sandwich panels. Continuous lamination method has high initial investment cost but low product cost. Suitable for high production rates. Continuous lamination production method is given simply in Figure 1.10.
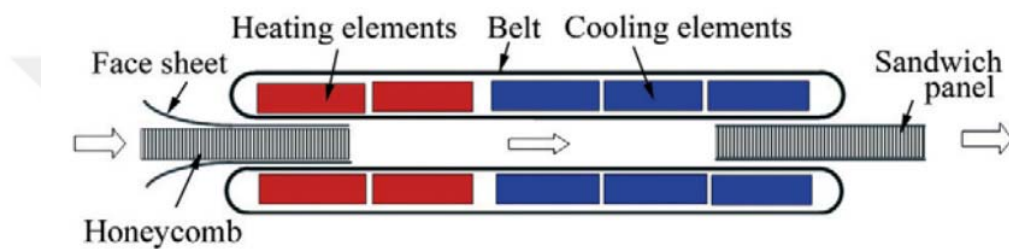
Figure 1.10. Schematic view of continuous lamination process (Xinyu et al., 2009)

1.2.6. Compression Moulding

In the compression moulding method, the composite structure can be produced by hand lay-up or prepreg lay-up method. The fabrics and core material are impregnated with resin and are placed in the mould at the desired thickness and orientation. Then a specific temperature and pressure is applied by using a press for curing process. Hydraulic press is generally used in this method. The composite structure takes the form of the mould under temperature and pressure. Figure 1.11 shows the schematic view of compression moulding process.
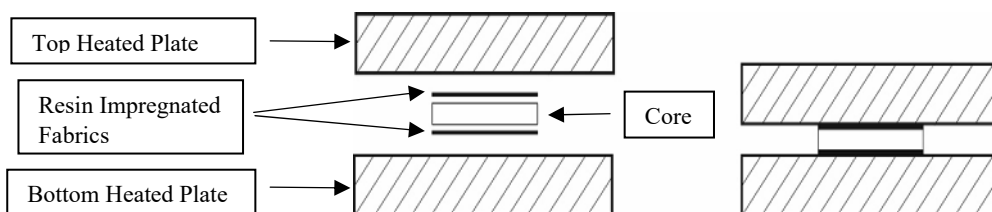

Figure 1.11. Schematic view of compression moulding process

13

1.2.7. Filament Winding

In filament winding method, resin impregnated fiber tows are wound on a mandrel. It is generally used for the production of cylindrical parts. When the part to be produced is sandwich structure, the inner surface layer is wound first. The preformed core is then placed on the inner surface layer. Then, the outer surface layer is wound on the core material (Karlsson and Åström, 1997). The mandrel is removed after curing. Figure 1.12 shows a sandwich pipe production.
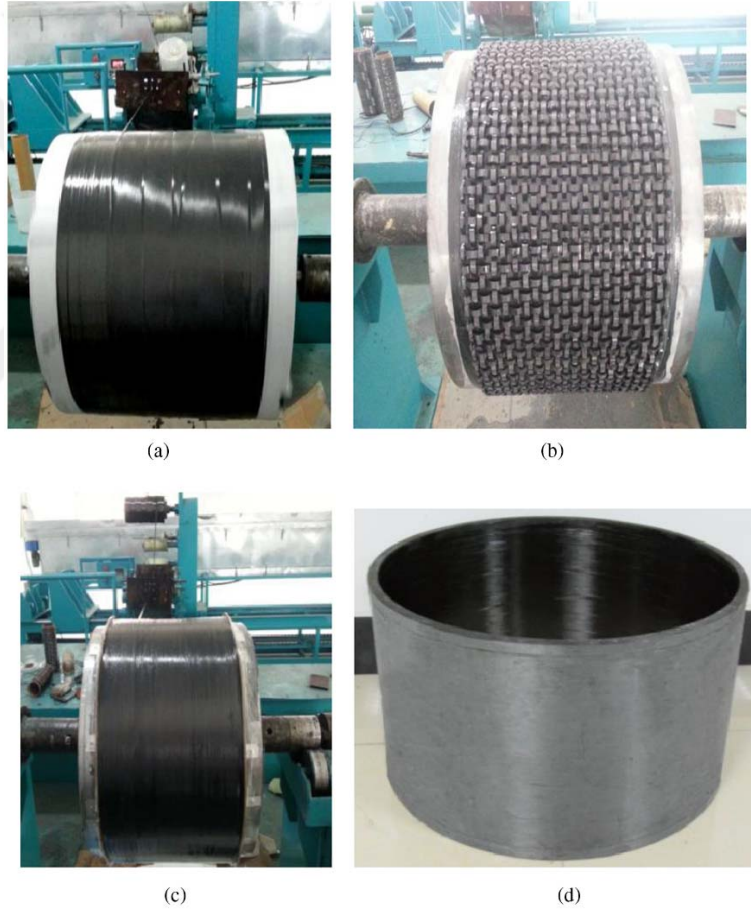

(a)

(b)

(c)

(d)

Figure 1.12. Sandwich cylinder produced by filament winding method: (a) winding inner face sheet; (b) placing core material; (c) winding outer face sheet; (d) finished product (Li et al., 2016)

1.3. Impact Tests

       Studies on the impact properties of composite materials have emerged with the introduction of carbon fiber fabrics. This is due to the fact that previously used glass fiber reinforced composites were able to work under impact loads, whereas carbon fiber reinforced composites were brittle (Adams, 2012).

       Impact tests for composite materials are divided into low and high velocity impact tests. Charpy, Izod and drop weight impact tests are called low velocity impact test, and ballistics impact test is called high velocity impact test (Navaranjan and Neitzert, 2017).

       Because low velocity impact load affects the performance of composite material, it can be considered as one of the most dangerous loads in composite structures (Safri et al., 2014). A number of test systems have been developed to simulate the low velocity loading type, as shown in Figure 1.13. In Charpy and Izod impact test systems, the sample is hit with a pendulum and the energy absorbed by the sample is calculated. Charpy (Figure 1.13(a)) and Izod (Figure 1.13(b)) can be used when comparing the impact toughness characteristics of different samples. In the drop weight impact (Figure 1.13(c)) test system, the striker with a certain weight is released from a certain height and hit to the sample with a set kinetic energy. It is possible to record data during the impact and obtain more information about the impact properties of the material. In this work, low velocity drop weight impact test was carried out to determine impact properties of specimens.
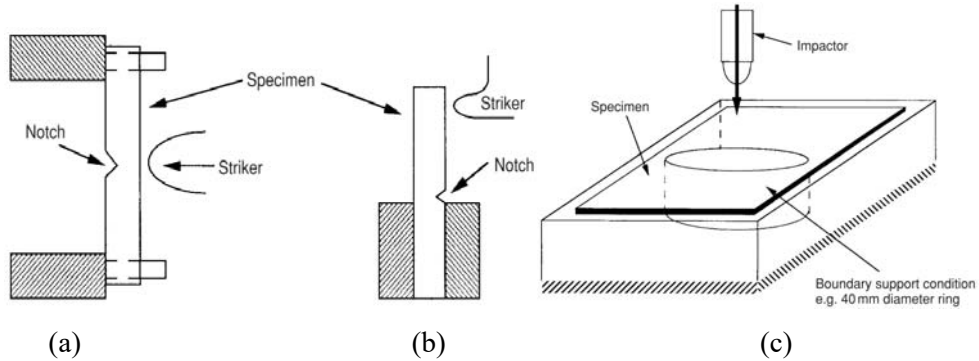
(a)   (b)   (c)

Figure 1.13. Low velocity impact test methods: (a) Charpy impact; (b) Izod impact;
            (c) Drop weight impact (Hogg and Bibo, 2000)

High velocity impact test systems are used to simulate high velocity loading to composite structures. Examples of high velocity impact load are bird and hail impact on the fuselage of an airplane. During the execution of the high velocity impact test, a lower weight projectile is used and the sample is hit at higher speeds, unlike the low velocity impact test. Some of the devices used for high velocity impact testing are electric heat gun (Yashiro et al, 2013), nitrogen gas gun (Villanueva and Cantwell, 2004) and single stage gas gun (Razali et al., 2014). Figure 1.14 shows an illustration of the high velocity impact test device.
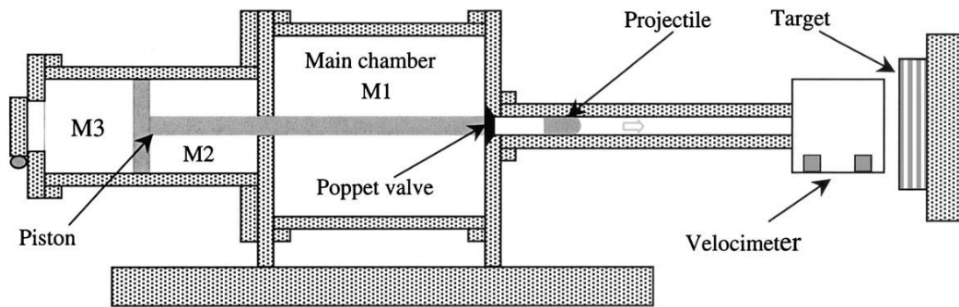
Figure 1.14. Schematic view of high velocity impact test (Villanueva and Cantwell, 2004)

2. PREVIOUS STUDIES

Besides the high tensile strength of fiber-reinforced composite structures, the weak impact resistance limits the use of these materials. The researchers investigated the impact properties of composite materials with different experimental methods such as low velocity drop weight impact (Shokrieh and Fakhar, 2012), Charpy impact (Ghasemnejad et al., 2010) and ballistic impact (Sevkat et al., 2009a), analytical models (Feli et al., 2016) and even using numerical methods such as finite element methods (Damanpack et al., 2013).

2.1. Laminated Composites

A wide variety of studies have been carried out to determine the impact properties of laminated composite structures. These studies were generally matrix toughening by using additives and hybridizing various types of fibers.

2.1.1. Matrix Toughening

Matrix toughening method has been used for decades to increase the toughness of the brittle matrix materials. The toughness of the matrix material directly affects the toughness of the composite structure. Argüelles et al. (2011), examined the effect of tough and brittle matrices on the fracture behaviour of the composite structure under static and dynamic mode I loading. They used AS4 type unidirectional carbon fiber as the reinforcement and modified Hexply® AS4/8552 (tough) and unmodified Hexply® AS4/3501-6 (brittle) as the matrix material. They found that the tough matrix material increased the static fracture energy value by roughly 230% as shown in Table 2.1

Table 2.1. Critical fracture energy of the AS4/8552 and AS4/3501-6 composites (MBT : Modified beam theory, CC : The compliance calibration, MCC : The modified compliance calibration) (Argüelles et al., 2011)

G_{IC} [J/m^2]	Material AS4/8552			Material AS4/3501-6		
Method	Mean	Standard deviation	Standard D. [%]	Mean	Standard deviation	Standard D. [%]
MBT	302,10	16,2	5,3	88,6	7,1	8,01
CC	319,53	19,3	6,01	99,13	5,9	5,95
MCC	298,08	12,1	4,06	90,63	7,8	8,6

The researchers added different type of micro and nano materials into the matrix in order to obtain a tougher composite structure and better fiber-matrix interface. Matadi Boumbimba et al. (2015), added 10% by weight of tri-block copolymers into the composite structure made with plain bidirectional glass fiber and epoxy matrix. They tested the composite plates with a low velocity impact test at three different energy levels (5.7 J, 9.6 J and 13.4 J). They did not see a significant difference at 5.7 J energy level but they obtained 13.7% and 12.6% increase in maximum reaction force at 9.6 J and 13.4 J respectively as shown in Figure 2.1 and Table 2.2 where corresponding force, displacement and energy values are provided.

Table 2.2. Low velocity impact test results (Matadi Boumbimba et al., 2015)

	F_{init} (N)	F_{max} (N)	Displacement D_{Fmax} (mm)	Absorbed energy (J)	Elastic energy (J)
EPO_FV (5.7J)	1050 ± 36	1385 ± 49	2.8 ± 0.5	4.9 ± 0.4	0.8 ± 0.05
EPONS_FV (5.7 J)	1190 ± 33	1387 ± 51	2.7 ± 0.4	4.8 ± 0.4	0.9 ± 0.1
EPO_FV (9.6 J)	1195 ± 30	1390 ± 43	2.9 ± 0.6	9.5 ± 0.2	0
EPONS_FV (9.6 J)	1530 ± 37	1665 ± 45	3.3 ± 0.8	8.6 ± 0.3	0.6 ± 0.05
EPO_FV (13.4 J)	1305 ± 29	1505 ± 37	3.6 ± 0.6	9.1 ± 0.3	—
EPONS_FV (13.4 J)	1565 ± 33	1695 ± 40	4.2 ± 0.5	10.9 ± 0.2	—
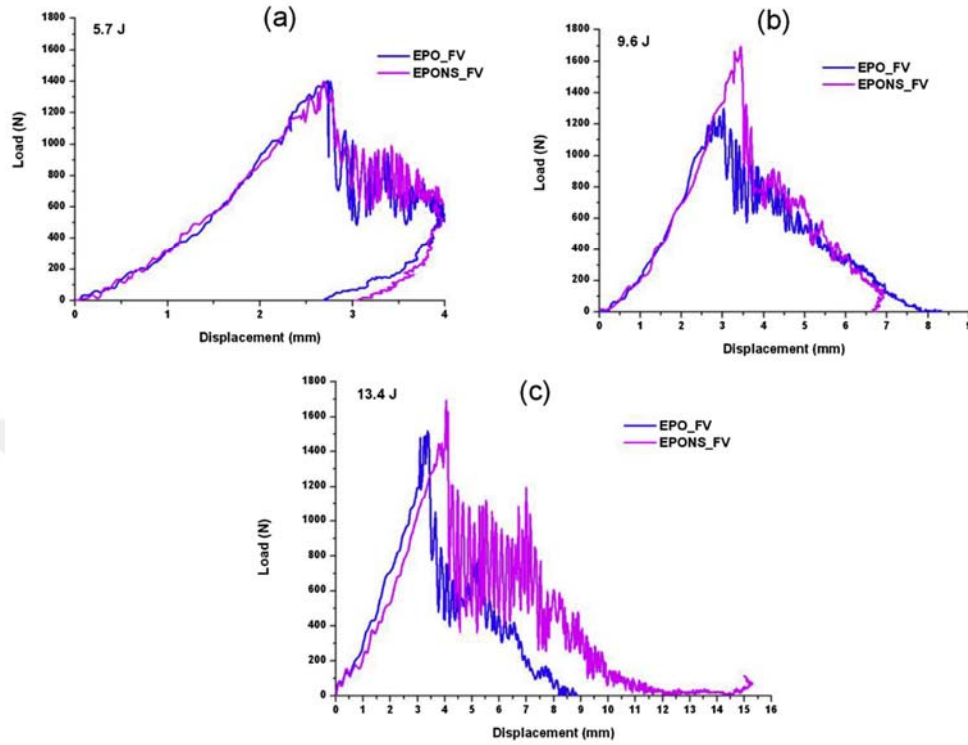
Figure 2.1. Load versus displacement curves at different impact energy levels (EPONS_FV: with additive, EPO_FV: without additive) (Matadi Boumbimba et al., 2015)

Zaman et al. (2011), investigated the mechanical properties of the matrix material by adding graphene and surface modified graphene into the diglycidyl ether of bisphenol A (DGEBA) epoxy resin. The mode 1 (transverse full thickness crack in longitudinal tension) fracture toughness (K_{1c}) of the graphene nano filled configuration increased until 2.5% additive level. However K_{1c} of the surface modified graphene nano filled configuration increased until 4% additive level. Energy release rate (G_{1c}) results increased up to 200% for the surface modified graphene filled configuration as shown in Figure 2.2.
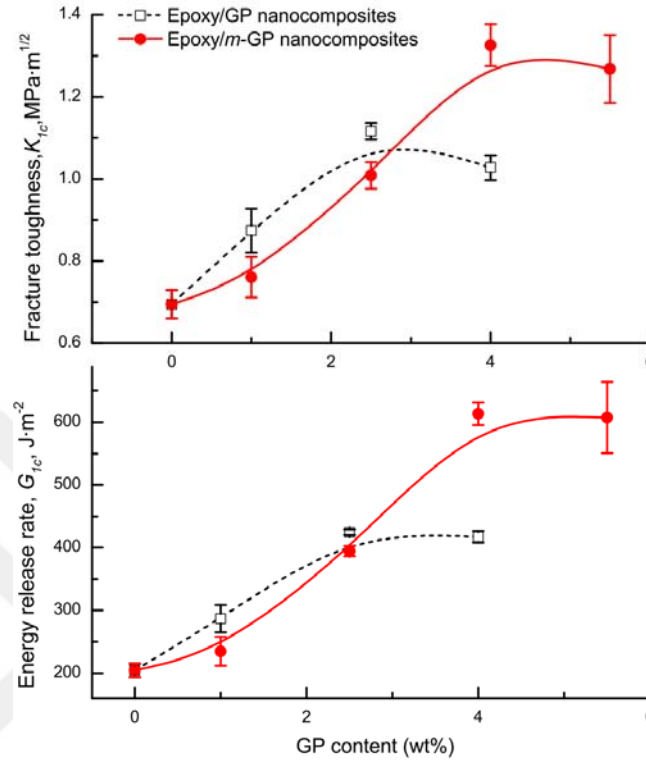
Figure 2.2.   Fracture toughness and energy release rate versus graphene content curves (Zaman et al., 2011)

Bulut (2017), added 0.1%, 0.2% and 0.3% by weight of graphene nano-pellets to basalt/epoxy composite laminates and examined their mechanical properties. According to Charpy impact test results, impact strength of 0.1% filled configuration was 16% higher compared to unfilled configuration, 5% higher compared to 0.2% filled configuration, 33% higher compared to 0.3% filled configuration as shown in Figure 2.3.
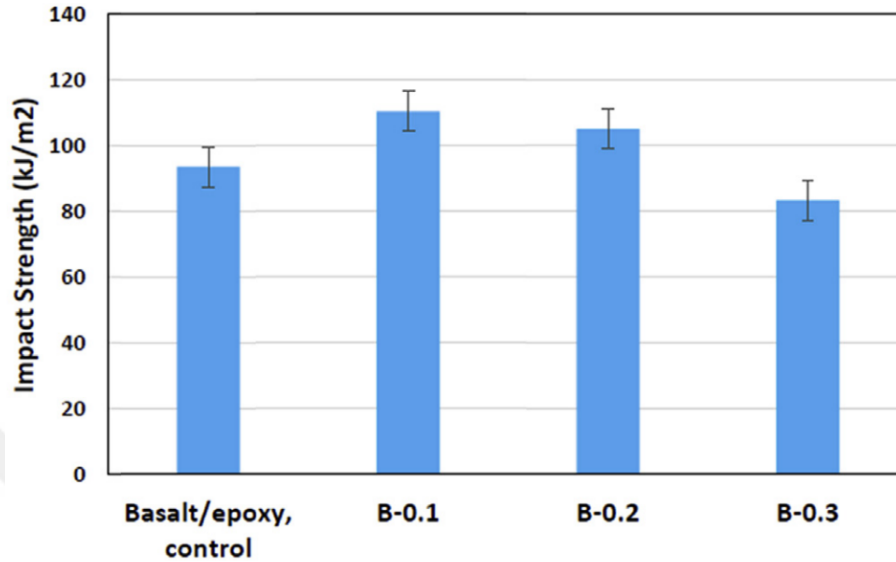
Figure 2.3. Impact strength versus graphene content results (Bulut, 2017)

Studies with boron carbide nano and micro particles were generally used as additives for metal matrices to increase wear resistance (Ahn et al., 2017; Shirvanimoghaddam et al., 2016). Also, it was used as additives for various purposes such as fire resistance (Rallini et al., 2013), nuclear protective material (Huang et al., 2013) etc. In addition, besides composite materials, boron particles have favourable effects on hardness and wear resistance of metallic materials (Boztepe et al., 2019).

Pekbey et al. (2017), filled nano-clays and cork powder into the Kevlar/epoxy composite structure and subjected to low velocity drop weight impact test at three different energy level (6, 12, 21 J). Maximum impact load increased about 4.5% for cork added structures, 10.4% for cork/clay added structures and 16.1% for clay added structures at 21 J impact energy respectively as shown in Figure 2.4.
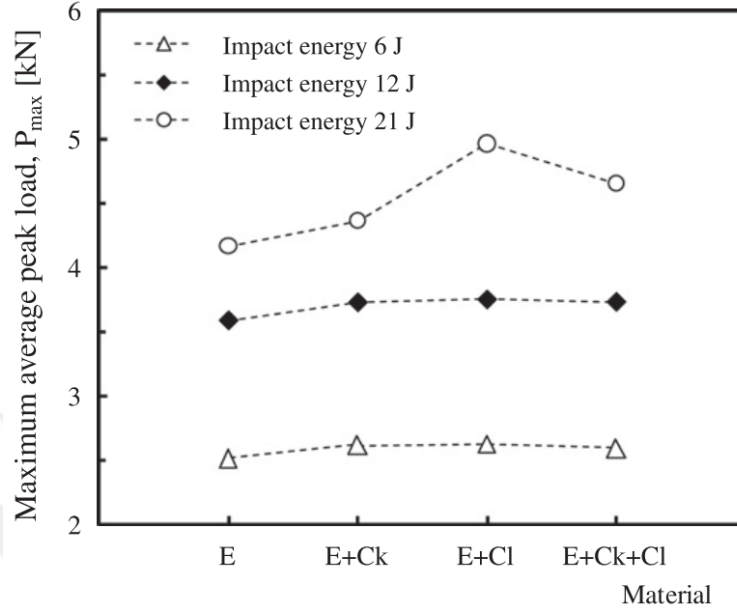
Figure 2.4. Maximum average peak loads of filled composites (E: neat epoxy, E+Ck: cork filled epoxy, E+Cl: nanoclay filled epoxy, E+Ck+Cl: cork and nanoclay filled epoxy) (Pekbey et al., 2017)

2.1.2. Hybridization

In order to increase the toughness of composite structures, the researchers did not only focus on the matrix but also aimed to increase the toughness of the composite structure by using different types of reinforcement materials together. (Sevkat et al. (2009b) made hybridization with woven glass fiber and woven graphite fiber fabrics at four different stacking sequences (glass/epoxy, glass-graphite-glass/epoxy, graphite-glass-graphite/epoxy and graphite/epoxy). They subjected composite structures to low velocity impact test at four different impact energy level (47, 60, 71, 122 J). According to the test results, non-hybrid glass/epoxy was the most resistant specimen against to the impact as shown in Figure 2.5. They observed delamination in hybrid configurations because of poor bonding between different layers.
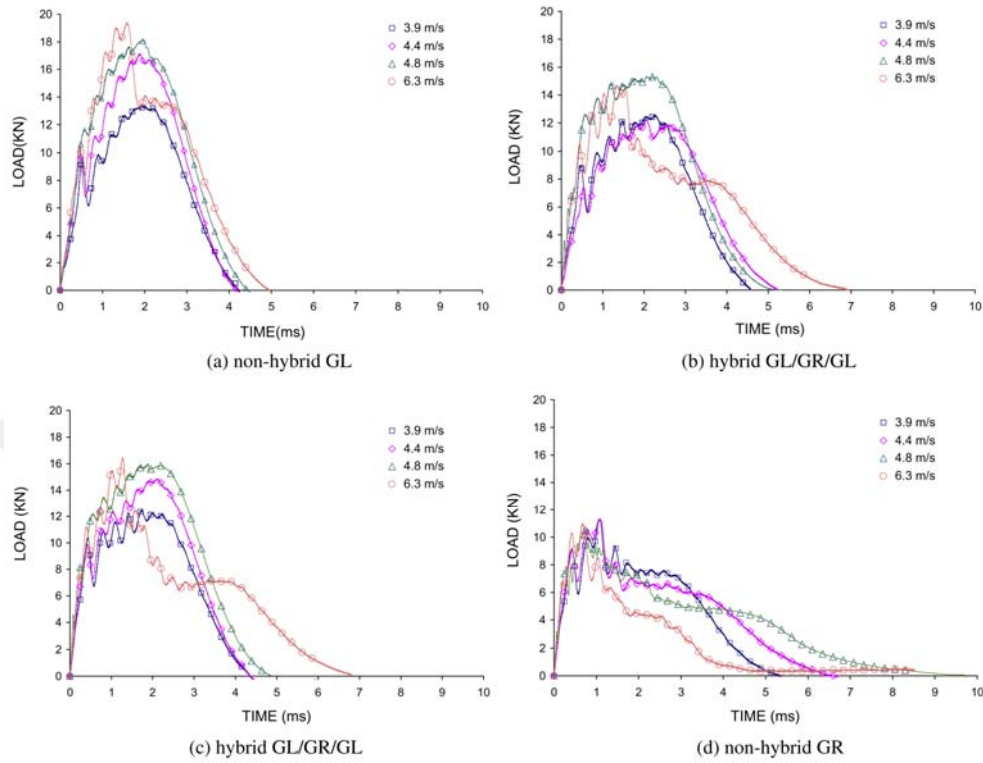
Figure 2.5. Load versus time curves at different impact energy levels (Sevkat et al., 2009b)

Uzay et al. (2018), produced interply and intraply hybrid composite structures with carbon fiber, aramid fiber and carbon/aramid hybrid fabrics. According to Charpy impact test results, the authors found that hybrid composite structures, especially made with hybrid fabric, have significant benefits on impact strength as shown in Figure 2.6
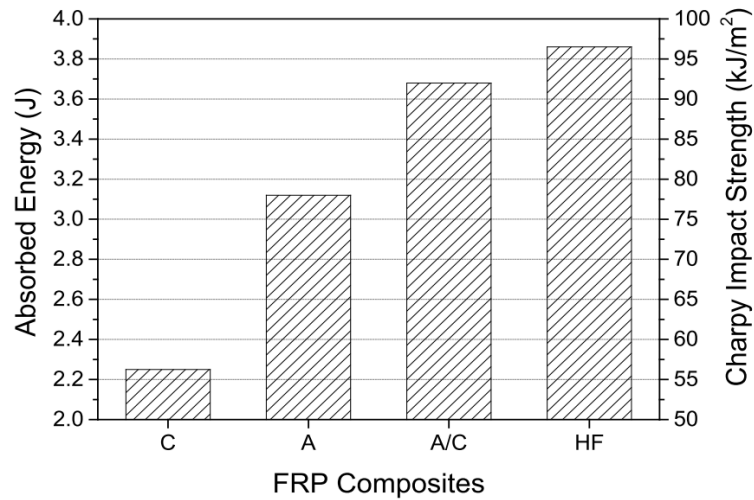
Figure 2.6.   Absorbed energy and Charpy impact strength of composite structures (C: pure carbon, A: pure aramid, A/C: aramid/carbon hybridization, HF: hybrid fiber) (Ç. Uzay et al., 2018)

2.2. Sandwich Composites

The impact behaviour of sandwich structures depends upon a number of variables that affect the testing results. Wang et al. (2013), investigated the effect of both impact variables (impactor diameter and impact energy) and sandwich variables (face sheet thickness, core thickness) on the impact behaviour. Carbon/epoxy face sheets and polyurethane foam core sandwich panels were subjected to drop weight impact test. They investigated the effect of impact energy, impactor size, face sheet thickness and core thickness on the results in terms of contact force, the contact time and impactor displacement. The increase in the face sheet thickness resulted higher contact force lower absorbed energy and damage as shown in Figure 2.7 and Table 2.3.
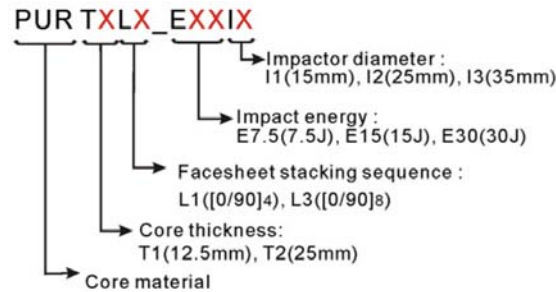
Figure 2.7. Coding for specimens (Wang et al., 2013)

Table 2.3. Drop weight impact test results (Wang et al., 2013)

Test case	Peak load (kN)	Duration (s)	Absorbed energy (J)	Absorbed energy/impact energy ratio	Planar damage diameter (mm)	Residual indentation (mm)
PURT1L1_E30I1	3.91	0.0105	17.58	58.6%	18.2	5.8
PURT1L1_E30I2	5.63	0.0081	15.38	51.3%	27.5	3.0
PURT1L3_E30I2	6.27	0.0075	13.97	46.6%	18.1	1.9
PURT2L1_E30I1	3.84	0.0098	17.36	57.8%	17.9	5.9
PURT2L1_E30I2	6.03	0.0075	15.72	52.4%	26.8	3.0
PURT2L1_E30I3	6.79	0.0070	14.26	47.5%	16.8	2.0
PURT2L3_E7.5I1	3.52	0.0073	3.83	51.1%	4.9	0.8
PURT2L3_E15I1	3.92	0.0078	8.27	55.1%	10.6	1.2
PURT2L3_E30I1	4.95	0.0081	16.90	56.3%	17.3	3.6
PURT2L3_E30I2	6.72	0.0070	14.02	46.7%	17.7	1.9

Besides changing the thickness of face sheets, using different kind of materials have also changed the damage modes. Park et al. (2008), constructed sandwich structures having both carbon/epoxy and glass/epoxy face sheets $[0_2/90_4/0_2]$ with 10 and 20 mm thick Nomex® honeycomb core, and then subjected them to the low velocity impact tests in order to examine the impact behaviour. Especially, as 10 mm thick core sandwich tended to bend more compared to the thicker one, the effect of skin type was observed clearly. But, as 20 mm thick core sandwich had better rigidity than thinner one, the difference in impact forces were found closer. In the case of using 10 mm thick core sandwiches, carbon/epoxy face sheets provided higher impact forces than glass/epoxy face sheets sandwiches as shown in Figure 2.8. On the other hand, carbon/epoxy face sheets sandwiches were more sensitive to impact energy when compared to glass/epoxy face sheets sandwiches as shown in Figure 2.9.
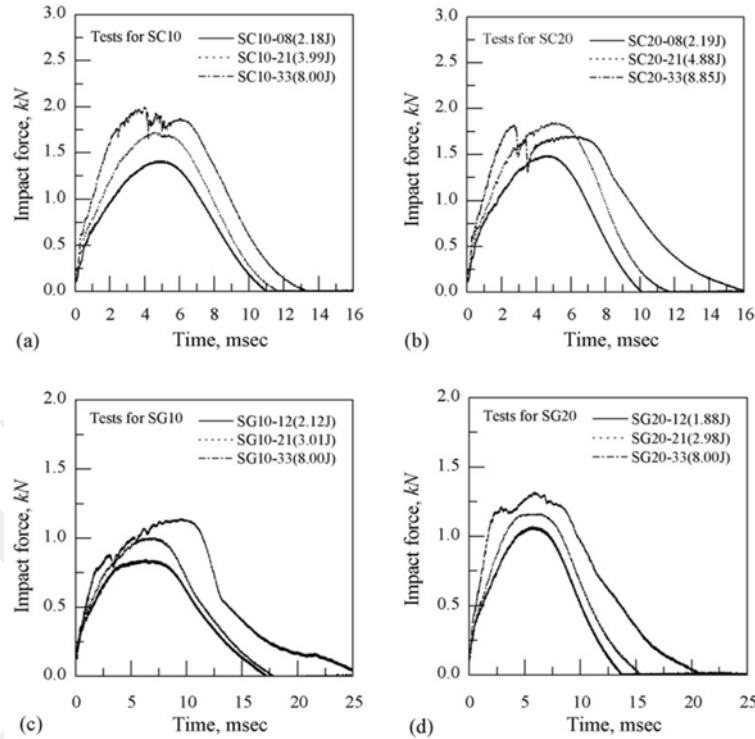
Figure 2.8.   Impact force versus time curves (SC10: carbon/epoxy face sheet with
              10 mm core, SC20: carbon/epoxy face sheet with 20 mm core, SG10:
              glass/epoxy face sheet with 10 mm core, SG20: glass/epoxy face sheet
              with 20 mm core) (Park et al., 2008)
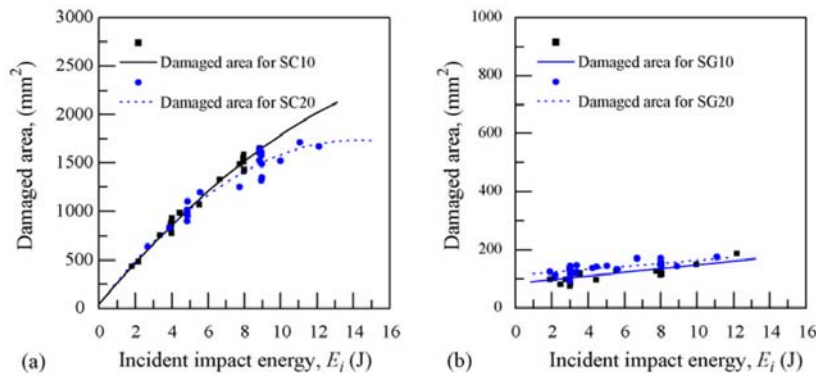
Figure 2.9.   Damaged area versus impact energy (SC10: carbon/epoxy face sheet
              with 10 mm core, SC20: carbon/epoxy face sheet with 20 mm core,
              SG10: glass/epoxy face sheet with 10 mm core, SG20: glass/epoxy
              face sheet with 20 mm core) (Park et al., 2008)

26

Using different type of materials for face sheets has directly affected the impact resistance of the structures. Therefore, in order to improve impact properties of sandwich panels, it is possible to make some modifications in the face sheets instead of using heavy metallic cores. Researchers modified the face sheets by using hybridization method as currently made for laminated fiber reinforced polymer composites. Yang et al. (2015), hybridized woven carbon fiber and glass fiber fabrics with vinyl ester matrix and constructed the sandwich structure by using urethane foam core. Six different sandwich structures were obtained with the aid of hybridization ([C_4/Foam core/C_4], [C_2/G_2/Foam core/G_2/C_2], [G_2/C_2/Foam core/C_2/G_2], [G/C]$_2$/Foam core/[C/G]$_2$, [$G/C_2/G$/Foam core/$G/C_2/G$] and [G_4/Foam core/G_4]). According to the tests under 30 J impact energy, contact surface of the sandwiches with pure carbon fiber face sheets was completely perforated whereas contact surface of the pure glass fiber face sheets-sandwich resisted to perforation. The highest contact force value was obtained from the pure glass fiber face sheets sandwich and the lowest contact force value was corresponded to pure carbon fiber face sheets sandwich. The results of hybrid face sheets sandwiches were in between of both. Sequencing of fiber fabrics for hybridization also affected the impact results. The sandwich configuration which has two carbon fiber plies at the contact surface (Figure 2.10b) showed better dynamic performance than other hybrid face sheets (Figure 2.10c, 2.10d, 2.10e).

(a) [C$_4$/Foam core/C$_4$]

(b) [C$_2$/G$_2$/Foam core/G$_2$/C$_2$]

(c) [G$_2$/C$_2$/Foam core/C$_2$/G$_2$]

(d) [G/C]$_2$/Foam core/[C/G]$_2$

(e) [G/C$_2$/G/Foam core/G/C$_2$/G]

(f) [G$_4$/Foam core/G$_4$]
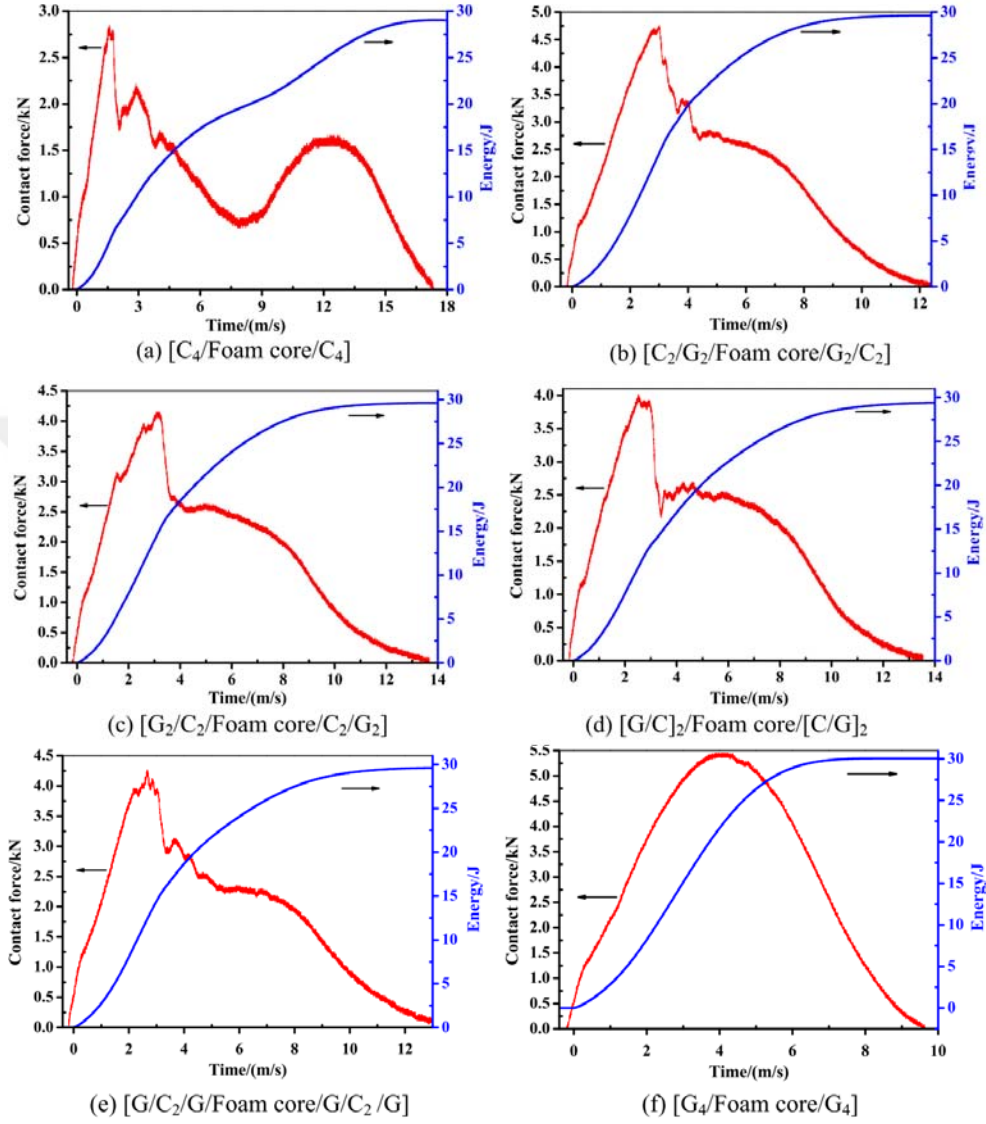
Figure 2.10.   Contact force versus time curves for different stacking sequences
(Yang et al., 2015)

There are very limited researches that aim to increase toughness of sandwich core materials. Hosur et al. (2008), constructed sandwiches with polyurethane foam core that are filled by 0.5% and 1% nano-clay additive, and woven carbon fiber/epoxy face sheets that are filled by 1% and 2% nano-clay,

28

respectively. The sandwich structures were subjected to impact energies of 15, 30 and 45 J, respectively and the results were obtained as given in Table 2.4 (according to the core material). Nano-clay additives provided less damage compared to neat foam core at the same impact energy levels according to deflection levels at the peak load.

Table 2.4. Low velocity impact test results according to different core filling ratio at 15, 30, 45 J impact energy (a: for 1% filled face sheets, b: for 2% filled face sheets) (Hosur et al., 2008)

Type of core	Impact energy (J)	Peak load (kN)	Deflection at peak load (mm)	Energy to max load (J)	Total energy (J)	Impact velocity (m/s)	Total time (ms)	Absorbed energy (J)	Time to max load (ms)
Neat	14.91	1.79	7.74	9.02	13.69	2.12	8.35	4.67	4.13
0.5%	14.97	1.98	6.85	9.02	13.69	2.13	7.22	4.66	3.68
1%	14.72	1.978	6.78	8.73	13.44	2.10	7.03	4.70	3.63
Neat	29.52	2.30	8.89	12.87	20.67	2.98	11.08	7.79	3.25
0.5%	29.46	2.22	8.81	12.45	19.62	2.98	8.80	7.17	3.21
1%	29.54	2.36	8.56	13.63	23.08	2.98	8.76	9.44	3.15
Neat	44.62	2.19	8.73	12.52	19.45	3.67	6.43	6.93	2.51
0.5%	44.57	2.26	7.02	10.09	19.07	3.66	6.53	8.97	1.99
1%	44.60	2.24	7.32	10.37	20.29	3.67	6.55	9.92	2.08

(a)

Type of core	Impact energy (J)	Peak load (kN)	Deflection at peak load (mm)	Energy to max load (J)	Total energy (J)	Impact velocity (m/s)	Total time (ms)	Absorbed energy (J)	Time to max load (ms)
Neat	14.77	2.03	6.46	8.71	13.50	2.11	6.92	4.78	3.44
0.5%	14.79	1.92	6.59	8.78	13.50	2.11	6.97	4.71	3.53
1%	14.92	2.00	6.69	9.09	13.54	2.12	6.79	4.44	3.58
Neat	29.49	1.83	10.26	13.97	21.49	2.98	9.40	7.52	3.82
0.5%	29.44	2.18	8.47	13.29	24.82	2.98	8.35	11.52	3.13
1%	29.51	2.12	8.45	12.58	23.93	2.98	8.45	11.35	3.09
Neat	44.54	1.94	9.10	11.85	20.12	3.66	7.12	8.26	2.62
0.5%	44.59	2.60	8.89	14.98	24.11	3.67	6.85	9.13	2.59
1%	44.46	2.03	7.04	9.01	16.39	3.66	5.91	7.38	1.99

(b)

On the other hand, different type of sandwich structures have been made in order to increase impact resistance. For instance, using dual core (Figure 2.11a) (Ouadday et al., 2018), fiber metal laminate (FML) face sheets and metal foam core (Figure 2.11b) (Liu et al., 2017), polyurethane (PU) foam filled pyramidal lattice core (Figure 2.11c) (G. Zhang et al., 2014).

(a)

(b)

(c)
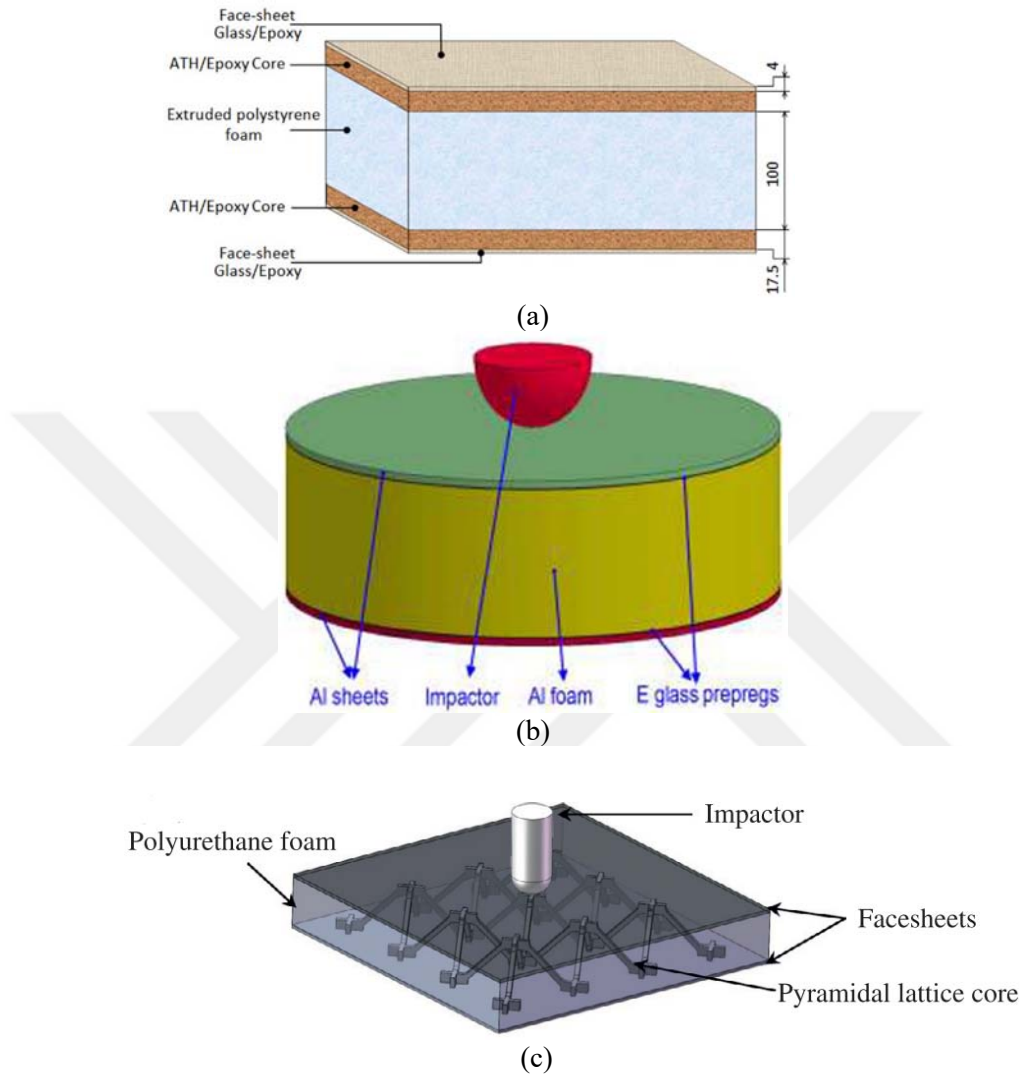
Figure 2.11.   Schematics of other types of sandwich structures: (a) dual core (Ouadday et al., 2018), (b) FML face sheets and metal foam core (Liu et al., 2017), (c) PU foam filled lattice core (G. Zhang et al., 2014)

2.3. Aim of the Study

Sandwich structures with woven carbon/epoxy face sheet and PVC foam core material are widely used in many industries. The main issue of these light

weight structures is poor impact properties because of their brittle nature. In this thesis work, it is aimed to improve the impact properties of polymeric sandwich structures without considerable weight increase. Because weight is crucial especially in transportation industry. For this reason, instead of using the heavier face sheets and core materials, the light weight carbon/epoxy face sheet is toughened by additives. Three different additive materials, graphene, boron carbide and kaolin, are used in different ratios (2%, 5% and 10%) to toughen the face sheet. In this way, a significant increase in impact resistance is expected without a large increase in weight. As a result, the developed sandwich structures may not only have high stiffness and strength but may also have high impact strength.

3. MATERIAL AND METHOD

3.1. The Materials Used In the Study

In this thesis work, carbon fiber fabrics and closed cell polymer foam core together with polymer matrix are used for manufacturing the sandwich panels. In addition to this, additive materials which homogeneously mixed with polymer matrix were used in order to investigate their effects on impact properties as in the scope of this study. On the other hand, besides the constituent materials for sandwich composites, a sonic homogenizer was used to achieve homogeneous mixing of additives within the polymer matrix.

3.1.1. Carbon Fiber Fabrics

Woven plain carbon fiber fabrics, which were used for manufacturing the face sheets of sandwiches, were procured from Kordsa Inc. (2018) in Turkey. Face sheets are the load bearing part of the sandwich panel, and determine the general properties of the sandwiches (Daniel et al., 2002). Figure 3.1(a) shows the pattern of the woven carbon fiber fabric. The physical and mechanical properties of carbon fiber fabrics used in this study are given in Table 3.1.

| (a) | (b) |

Figure 3.1.   Sandwich structure components: (a) woven carbon fiber fabric; (b) closed cell PVC foam

33

Table 3.1. Physical and mechanical properties of carbon fiber fabric used for the fabrication of sandwiches in this study (HS: High strength, 3K: 3000 filaments per tow)

Property	Value
Weave style/pattern	Woven plain
Density (kg/m^3)	1790
Areal weight (g/m^2)	200
Fiber type/model	Warp = 3K HS Carbon fiber Weft = 3K HS Carbon fiber
Filament diameter (micron)	Warp = Weft = 7
Tensile strength (MPa)	Warp = Weft = 3800
Tensile modulus (GPa)	Warp = Weft = 240
Tensile strain (%)	1,6
Carbon assay (%)	95

3.1.2. PVC Foam Core Materials

The core material is located between the face sheets and increases the distance between them to increase the moment of inertia. So, bending stiffness increases with the increase in moment of inertia. It is possible to find core materials in various shapes (foam, honeycomb etc.) and materials (Polyurethane, PVC, metal, wood etc.). In this study, closed cell polyvinylchloride (PVC) foam core material was used as the core material as shown in Figure 3.1(b).

Closed cell, rigid polymer foam core that is commercial industrial PVC foam core, obtained from Dost Kimya (2018), and it was used to construct sandwich panels. The cores with 10 mm thickness was used throughout the whole sandwich configurations. Table 3.2 presents the physical and mechanical properties of the core material.

Table 3.2. Physical and mechanical properties of PVC core used for the fabrication
            of sandwiches in this study

Property	Value
Type	Closed cell foam
Density (kg/m^3)	48
Thickness (mm)	10
Areal weight (g/m^2)	480
Compressive strength perpendicular to the plane (MPa)	0.6
Compressive modulus perpendicular to the plane (MPa)	48
Tensile strength in the plane (MPa)	0.95
Tensile modulus in the plane (GPa)	35
Shear strength (MPa)	0.55
Shear modulus (MPa)	16

3.1.3. Polymer Matrix

The sandwich production was carried out by using epoxy polymer resin and its hardener. Hexion MGS L160 epoxy and Hexion MGS H160 hardener were obtained from Dost Kimya (2018). Their physical and chemical properties are given in Table 3.3. The mixing ratio of epoxy resin to hardener was set to 100:25 by weight. The physical and mechanical properties of mixed compound are given in Table 3.4.

Table 3.3. Physical and chemical properties of epoxy resin and hardener used for the fabrication of sandwiches in this study

Property	Epoxy Resin	Hardener
Type	MGS L160	MGS H160
Density (kg/m^3)	1130-1170	960-1000
Viscosity (mPas)	700-900	10-50
Epoxy equivalent (g/equivalent)	166-182	-
Epoxy value (equivalent/100 gr)	0.55-0.6	-

Table 3.4. Physical and mechanical properties of epoxy and hardener mixture used for the fabrication of sandwiches in this study

Property	Matrix
Mixed products	MGS L160 / MGS H160
Mixing ratio by weight	100:25
Density (kg/m^3)	1180-1200
Flexural strength (MPa)	110-140
Modulus of elasticity (GPa)	3.2-3.5
Tensile strength (MPa)	70-80
Compressive strength (MPa)	80-100
Elongation at break (%)	5 – 6
Impact strength (KJ/m^2)	40 – 50

3.1.4. Additive Materials

As the study aims to investigate the effect of additive materials in micron size on low velocity impact behaviour of sandwich structures, three different additives were obtained from Ege Nanotek Kimya (2018) in Turkey. These are

graphene, boron carbide, and kaolin. The chemical compositions, physical and mechanical properties of the materials are given in Table 3.5 to 3.7.

Table 3.5. Properties of graphene nanoplatelets ([1](Lee et al., 2008), [2](P. Zhang et al., 2014))

Property	Graphene nanoplatelets
Diameter (µm)	24
Thickness (nm)	6
Surface area (m[2]/g)	120
Purity (%)	99.5
Intrinsic strength[1] (GPa)	130 ± 10
Modulus of elasticity[1] (TPa)	1 ± 0.1
Fracture Toughness[2] (MPa(m)[0.5])	4 ± 0.6

Table 3.6. Properties of boron carbide ([1](CES Selector, 2018))

Property	Boron carbide
Particle size (µm)	0 – 50
Purity (%)	99
Density[1] (kg/m^{3})	2490 – 2550
Modulus of elasticity[1] (GPa)	362 – 380
Tensile strength[1] (MPa)	261 – 289
Hardness[1] (Vickers)	3990 – 4410
Fracture toughness[1] (MPa(m)[0.5])	2.8 – 3.4

Table 3.7. Properties of kaolin ([1](CES Selector, 2018))

Property	Kaolin
Particle size (µm)	5.5
Purity (%)	99
Density[1] (kg/m^3)	2500 – 2620
Modulus of elasticity[1] (GPa)	19.6 – 20.4
Tensile strength[1] (MPa)	45.8 – 50.6

3.2. Method

This section provides methods used in this work for composite sandwich production, preparation of test specimens, and performing of the low velocity impact tests. The flow chart provided in Figure 3.2 represents the process and test steps. Specimen dimensions were determined according to ASTM D7136/D7136M – 12. Figure 3.3 shows the dimensions for specimens and sandwich structures that are produced in this work. 10 different sandwich configurations were produced as shown in Table 3.8. These configurations were subjected to low velocity impact test at three energy level of 10 J, 17.50 J, and 25 J. As shown in Figure 3.3, each sandwich configuration is produced in 2 panels in order to obtain more homogeneous samples. Total of 20 panels were produced for the complete investigation.
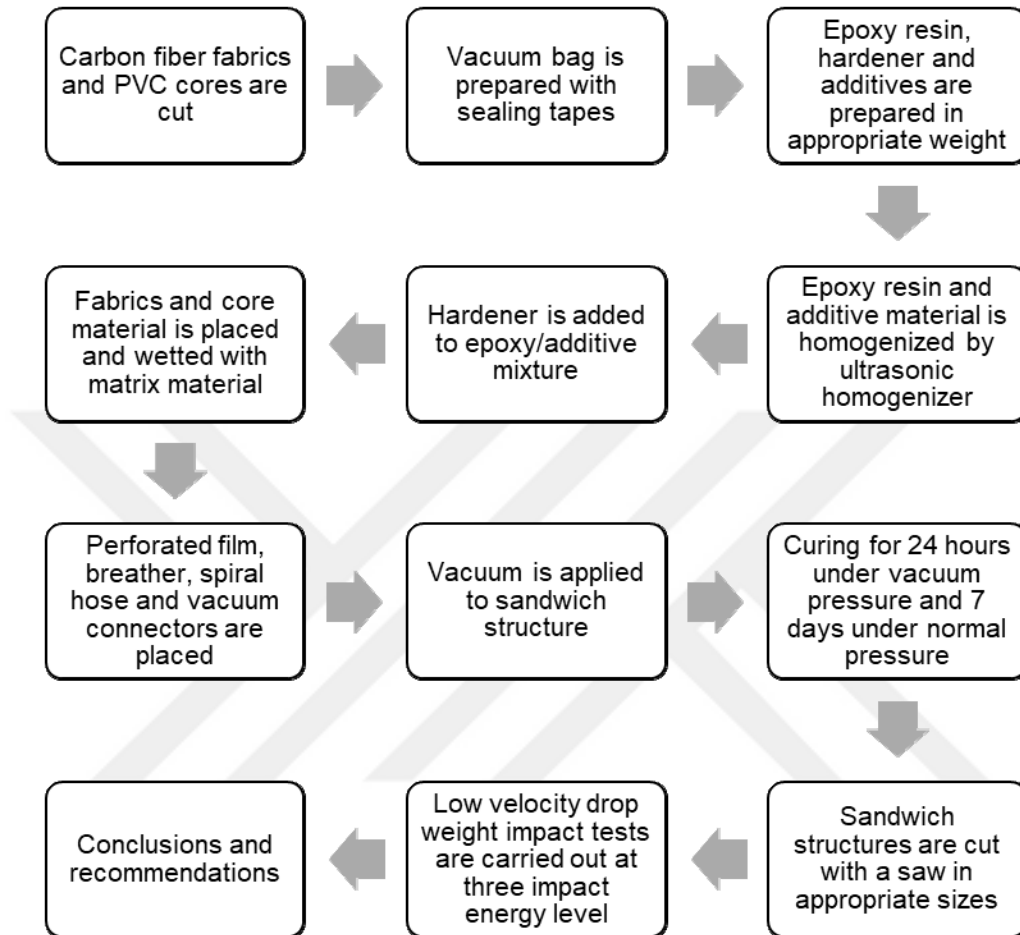
Figure 3.2. Process and test steps
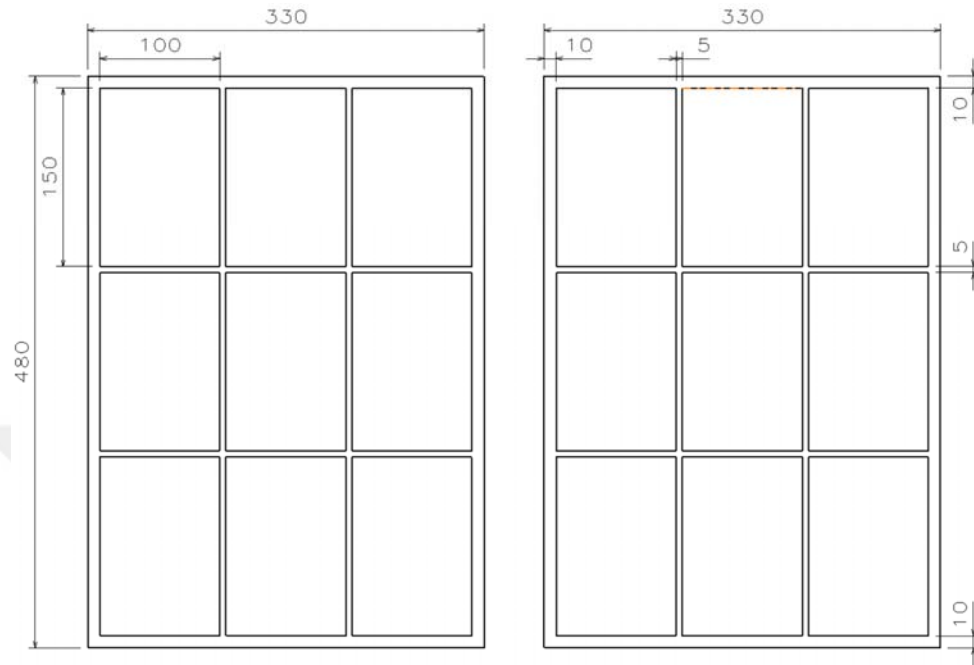
Figure 3.3. Panel and test specimen dimensions

Table 3.8. Sandwich configurations

		Additive Percent			
		0%	2%	5%	10%
Additive Material	Neat (None)	X			
	Graphene		X	X	X
	Boron Carbide		X	X	X
	Kaolin		X	X	X

3.2.1. Manufacturing of Sandwich Panels

The production of the sandwiches used in the test are explained step by step in this section. Sandwich panels were manufactured after the constituent materials had been prepared. Firstly, the number of panels and their sizes were determined considering the variety of additive materials and testing conditions.

According to the sizes shown in Figure 3.3, carbon fiber fabrics and foam core materials were cut adequately as shown in Figure 3.4. The face sheets of the sandwich panels used in this study consist of four layers of carbon fiber fabric. Therefore, one PVC core material and eight sheets of carbon fiber fabrics are required for each panel. In total, 20 panels were produced and 25.344 m^2 carbon fiber fabrics and 3.168 m^2 PVC core materials were used.

Figure 3.4. Cutting of carbon fiber fabrics

The vacuum bag was cut in enough sizes for the vacuum process of the two panels as shown in Figure 3.5(a). Then, the sealing tape was bonded to the one face of the vacuum bag as shown in Figure 3.5(b).

| | (a) | (b) |

Figure 3.5. Preparing of vacuum bag

In the production method of the hand lay-up and vacuum bagging, the mass of the matrix material should be equal to the mass of the carbon fiber fabric. To achieve this, 500 grams epoxy-hardener mixture was prepared for 500 grams fabric mass. The mixing ratio is 400:100 grams according to the information obtained from the manufacturer. As shown in Figure 3.6(a), 400 grams of epoxy was poured into the mixing bowl. The additive materials were weighed according to the configuration (2% = 10 gr, 5% = 25 gr, 10% = 50 gr) to produce. Figure 3.6(b) shows 25 grams of graphene prepared for 5% graphene containing configuration.

(a)   (b)
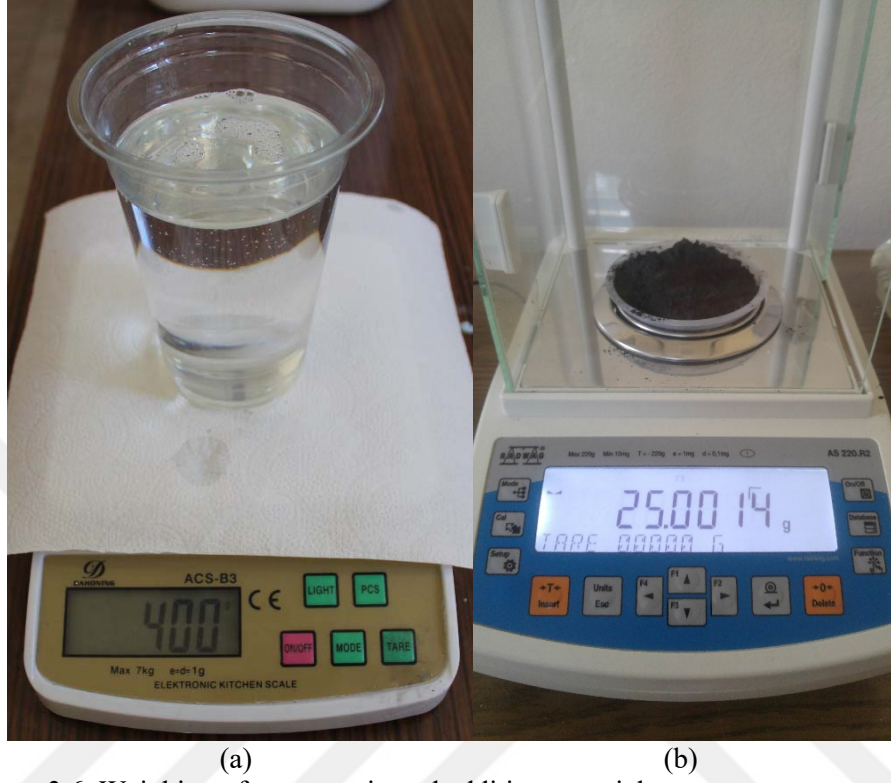
Figure 3.6. Weighing of epoxy resin and additive material

There are important factors to consider when preparing the matrix material. One of these is the MGS L160 epoxy and the MGS H160 hardener offers 1 hour of processing time when mixed with 100:25 by weight at room temperature as recommended by the supplier. Therefore, the epoxy and hardener mixing process must be carried out as the last step of the matrix preparation process. In this thesis work, firstly the additive material and epoxy resin were roughly mixed using a stick. Then the mixture was homogenized with ultrasonic homogenizer machine for one hour as shown in Figure 3.7. During this process, water bath was used to prevent the epoxy resin from overheating. Finally, after 20 minutes of cooling in water bath at room temperature, filled epoxy was mixed with the hardener, and the matrix material was ready for the use.

Figure 3.7. Sonication processes of additives

As shown in Figure 3.8, carbon fiber fabrics and core material were placed in proper stacking sequence, and wetted out with matrix material. In this step, production was carried out by hand lay-up method with four layers of carbon fiber as face sheets, and 10 mm thick PVC foam as core material. In each vacuum bag, two sandwich panels in the same configuration were produced.
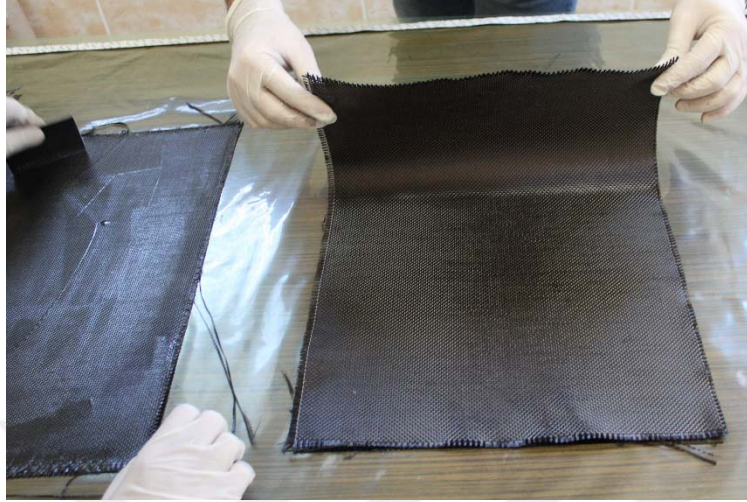
Figure 3.8. Production of sandwich panels with hand lay-up method

After the hand lay-up method, the steps required for the vacuum bagging method were applied. In vacuum bagging method, it is very important to apply the vacuum homogeneously to the entire panel. As shown in Figure 3.10, the panels were covered with breather, which allows air to pass to the vacuum pump. The perforated film was used to prevent the breather and sandwich structures from sticking as shown in Figure 3.9. This film has a perforated structure and does not obstruct the air flow.

Figure 3.9. Cutting and application of perforated film

Figure 3.10. Cutting and application of breather

The vacuum pack was surrounded by a spiral hose so that the vacuum can be effectively carried out from all sides of the vacuum package. The vacuum hose was connected to the spiral hose by a T connection at a suitable edge of the vacuum pack as shown in Figure 3.11.

Figure 3.11. Vacuum hose

The last step before applying the vacuum is to seal the vacuum bag with the sealing tape as shown in Figure 3.12. This step should be done very carefully because the vacuum bag will be left for 24 hours at room temperature for curing. Even small leaks within 24 hours can cause the vacuum to deteriorate.

Figure 3.12. Closing the vacuum bag

In the last step of vacuum bagging method, the package was vacuumed by using a RC-8D vacuum pump as shown in Figure 3.13. After making sure that there was no leakage in the package, the composite panels were left to cure in vacuum atmosphere for 24 hours. This may guaranty that the layers could be brought closer to each other, and allow to suck excess resin and air bubbles out of the sandwich composite structure. As a result, vacuum bagging method allows to obtain a better fiber volume fraction.

Figure 3.13. Application of vacuum

After 24 hours curing of the epoxy under vacuum, the vacuum bags were unpacked. Then the bare sandwich structures were kept for another seven days at room temperature for curing. Then, the composite plates were cut with a saw according to ASTM D7136 Standard (150x100 mm).

3.2.2. Low Velocity Impact Tests

The test samples were subjected to impact test with Ceast Fractovis Plus drop tower impact device available in Mechanical Engineering Department of Erciyes University with the permission of the department as shown in Figure 3.14. The parameters used for the impact test are given in Table 3.9. Equation 1 is used to calculate the impact energy.

$$E = m \times g \times h \qquad (1)$$

Here;

E   : Impact energy (J)

m   : Impactor mass (kg)

48

g   : Gravitational acceleration (m/s^2)

h   : Drop height (m)

Table 3.9. Impact test parameters

Property	Test 1	Test 2	Test 3
Impact Energy (J)	10	17,50	25
Drop Height (m)	0.203	0.355	0.507
Impactor Mass (kg)	5.02		
Specimen Dimensions (mm)	150 x 100		
Impact area dimensions (mm)	125 x 75		
Impactor Tip Shape and Diameter (mm)	Hemispherical, 20		
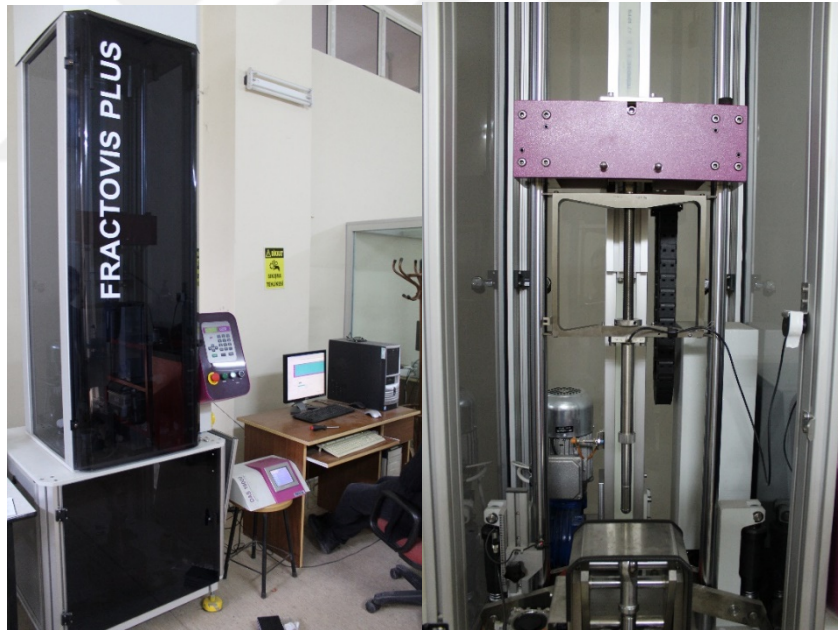
Figure 3.14.   Ceast Fractovis Plus drop tower impact test device used in Mechanical Engineering department of Erciyes University

49

Sandwich specimen was fixed on the plate which has 125x75 mm gap according to ASTM D7136 standard as shown in Figure 3.15. Time, impact force, impactor displacement and energy values were obtained by the test device software. Load-time, energy-time and load-displacement curves were drawn by using raw data in Origin program as shown in Figures 4.1 to 4.3 (Origin, 2018).

Figure 3.15. Support fixture

3.3. Cost

In an engineering material used in industry, the cost of the material is as important as the mechanical properties such as the strength of the material. When calculating the cost, the USD price at the date of purchase of the products was taken into consideration. Table 3.10 lists the material quantities and unit prices required to produce 1 m^2 sandwich structure. Total cost of each sandwich configuration without considering the labour cost and the percent cost increase compared to the configuration without additives are given in next section in Table 4.1.

Table 3.10. Cost of each product

Product	Unit Cost	Quantity	Total Cost of per m^2 sandwich
Carbon Fiber	14.879 $/m^2	8 m^2	119.032 $
PVC Foam Core	31.98 $/m^2	1 m^2	31.98 $
Epoxy	20.79 $/kg	1.28 kg	26.611 $
Hardener	25.58 $/kg	0.32 kg	8.186 $
Graphene	2200.088 $/kg	0.032 kg	70.403 $
		0.08 kg	176.007 $
		0.16 kg	352.014 $
Boron Carbide	752.66 $/kg	0.032 kg	24.085 $
		0.08 kg	60.213 $
		0.16 kg	120.426 $
Kaolin	3.778 $/kg	0.032 kg	0.121 $
		0.08 kg	0.302 $
		0.16 kg	0.604 $

4. RESULTS AND DISCUSSION

In this study, sandwich structures, which are made from carbon fiber reinforced face sheets, PVC foam core material and epoxy matrix with additive material in different proportions from various materials, were subjected to drop weight impact tests. The experimental results of the drop weight impact tests obtained from the sandwich structures presented in this section with figures, tables and images.

The results of each test are plotted in a same figure title containing two separate charts. "Load-time" and "energy-time" test results are depicted together at Figure (a) of each title, while the test results of "load-displacement" curves are plotted separately in Figure (b) of each title. The unit of load is Newton (N), the unit of energy is Joule (J), the unit of displacement is millimetre (mm), and the unit of time is millisecond (ms) in all charts.

When the load-time figures are examined, it is observed that the load firstly rises (first peak, F_1), then reduces a little and then rises again (second peak, F_2). Briefly, two peaks are seen in graphs. The reason for this is that the surface layers of the sandwich structures were produced from rigid carbon fiber, which can carry loads, and the core materials were produced from lightweight PVC foam. The impact force rises quickly from the moment the striker tip touches the top surface layer until the surface layer fails. Then it starts to penetrate into the core material which has a lower impact resistance compared to the surface layer. After the core material is punctured, the striker tip hits the lower surface layer. Similar to top surface layer, the impact force rises and reduces respectively. As an example to represent the behaviour during tests Figure 4.1 shows a simple load-time curve and corresponding peak points.
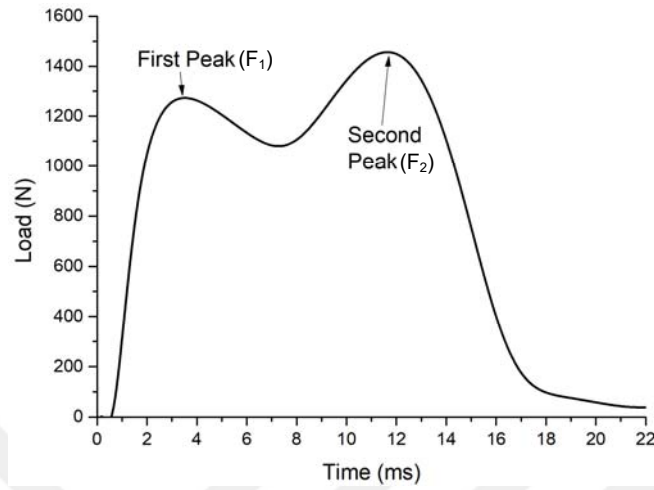
Figure 4.1. Simple load time curve

Figure 4.2 depicts the energy-time relationship as an example to the expected behaviour. The peak in the figure indicates the impact energy applied to test specimens by a striker tip. If the striker tip bounces back after hitting the sample, the energy of striker tip is called as rebound energy. A portion of the energy of the striker tip is absorbed by the sample during impact. Impact energy, rebound energy and absorbed energy are shown in Figure 4.2.
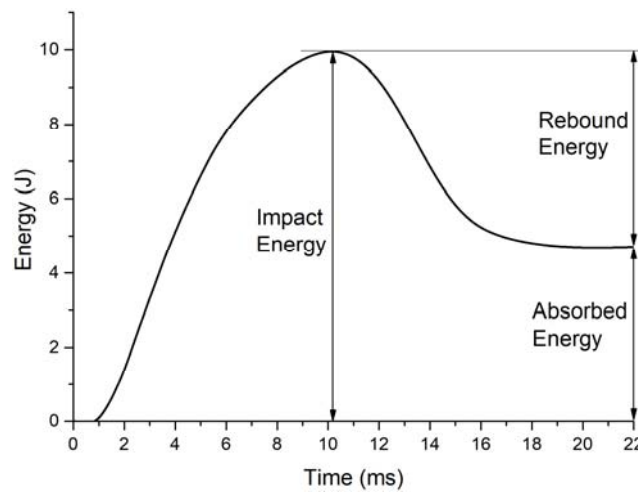
Figure 4.2. Simple energy-time curve

54

The shape of the load-displacement figure is very important to know whether the sample is punctured or not. Figure 4.3 gives examples to both cases. If displacement increases and then decreases until closing the curve as shown in Figure 4.3(a), it indicates that the sample has not been punctured. So the load-displacement curve is a closed curve. If the sample is punctured, the displacement increases until the end of the test as shown in Figure 4.3(b). So the load-displacement curve is an open curve.

| (a) | (b) |
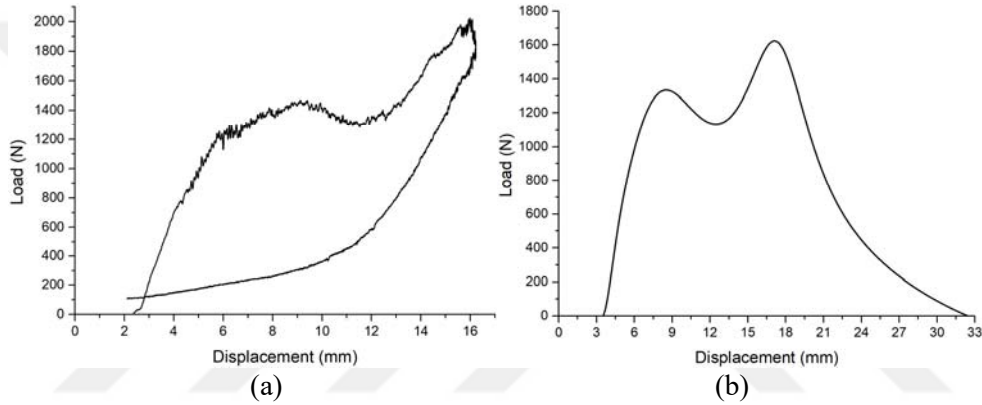
Figure 4.3.   Simple load-displacement curves (a) closed curve representing unpunctured specimen, (b) open curve representing punctured specimen.

The results obtained from experiments are given. When fallowing figures are examined, it is seen that there are five replications for each variable. Section 4.1 provides the test results of the sandwich structures made with epoxy matrix without any additive material (neat epoxy). Sections 4.2 to 4.4 provide test results and comparisons of the results for different additive quantity of the each material. In between sections 4.5 and 4.7, the comparisons were made for the same additive quantity of different materials. All the comparisons were made considering the same impact energy level.

Although there are test results at three different energy levels in the sandwich structure made from neat epoxy and there are also test results at three

different energy levels (10 J, 17.50 J, and 25 J) and three different additive material ratios (2%, 5% and 10%) in the sandwich structures made with filled matrix, only one configuration of the test results are presented for 10 J in the main text. The test results for 17.5 J and 25 J impact energy levels are given in Appendix. The mean curves for load-time, energy-time and load displacement figures were obtained by taking the average of the results obtained from the five replications for each configuration. Diagrams containing the mean curves are given comparatively in this section.

Also the total cost of each sandwich configuration without considering the labour cost and the percent cost increase are compared for each configuration without additives are given in Table 4.1.

Table 4.1. Total cost of sandwich configurations and cost increase in percentage

Configuration	2%	5%	10%
Sandwich with Graphene Additive	256.212 $ (+37.9 %)	361.816 $ (+94.7 %)	537.823 $ (+189.4 %)
Sandwich with Boron Carbide Additive	209.894 $ (+13 %)	246.022 $ (+32.4 %)	306.235 $ (+64.8 %)
Sandwich with Kaolin Additive	185.93 $ (+0.06 %)	186.111 $ (+0.16 %)	186.413 $ (+0.32)

4.1. The Results of Sandwich Structures with Neat Epoxy

The load-time, energy-time and load-displacement figures of sandwich structures without additive at 10 J impact energy level are given in Figures 4.4(a) and 4.4(b). The results at 17.5 J and 25 J impact energy levels are given in Appendix. Numeric results for maximum impact loads, absorbed energy and indentation depth obtained from the mean of five replications for each configuration of sandwiches with neat epoxy are provided in Table 4.2.
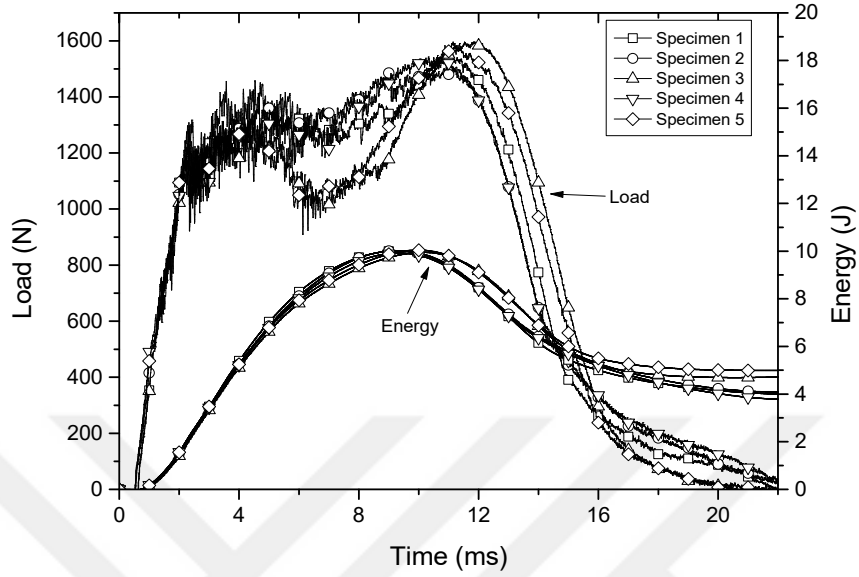
(a)
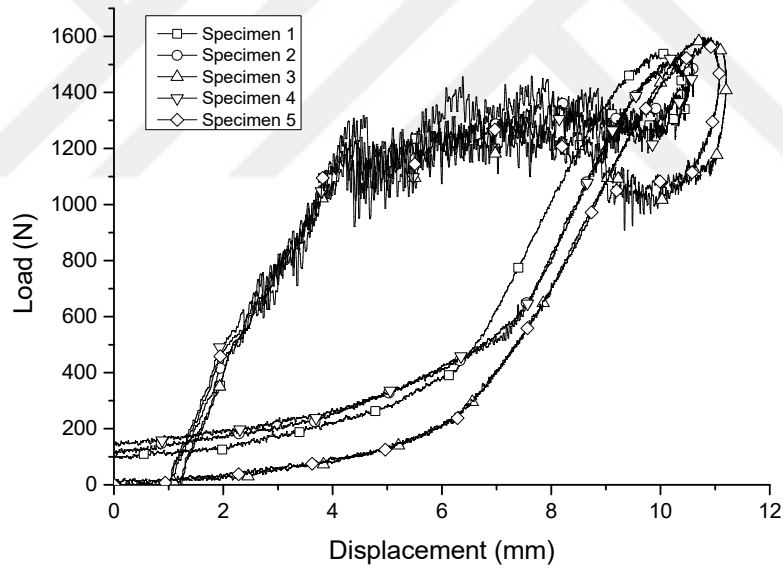
(b)

Figure 4.4.   Impact test curves of sandwiches with neat epoxy at 10 J energy level: (a) load versus time and energy versus time, (b) load versus displacement.

57

Table 4.2. Impact test results of sandwiches with neat epoxy

Property	Impact Energy	Neat Epoxy
F_1 (N) (First Peak)	10 J	1299.4
	17.50 J	1350.7
	25 J	1358.7
F_2 (N) (Second Peak)	10 J	1533.9
	17.50 J	1640.5
	25 J	1552.6
Absorbed Energy (J)	10 J	4.32
	17.50 J	13.8
	25 J	24.73
Indentation Depth (mm)	10 J	9.49
	17.50 J	14.93
	25 J	Punctured

4.2. Effect of Different Percent of Graphene Nano-platelets

The load-time, energy-time and load-displacement figures of sandwich structures contain 10% graphene additive at 10 J impact energy level are given in Figures 4.5(a) and 4.5(b). The results at 17.5 J and 25 J impact energy levels are given in Appendix. Numeric results for maximum impact loads, absorbed energy and indentation depth obtained from the mean of five replications for each configuration of sandwiches with graphene additive are provided in Table 4.3. Also the percent change in the test results of the graphene filled samples compared to the samples with neat epoxy are shown in Table 4.3.
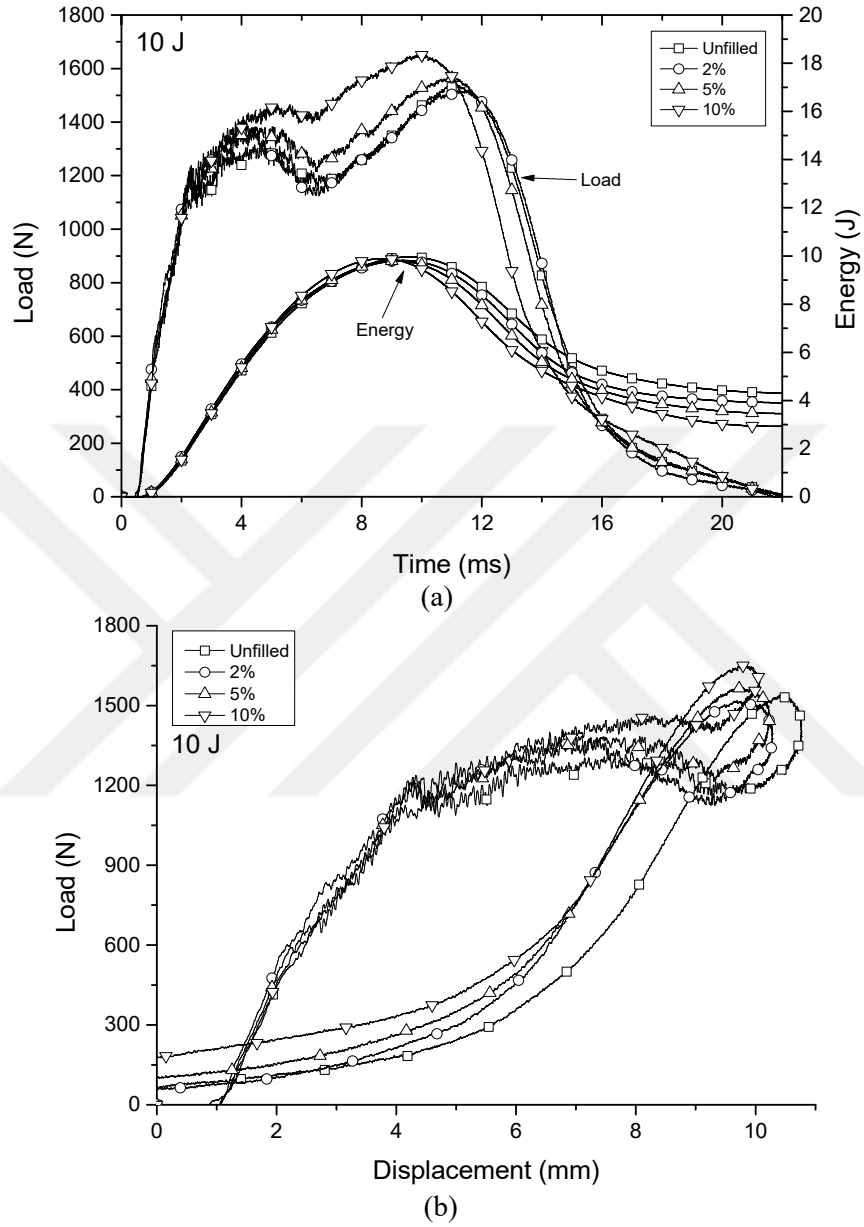
(a)

(b)
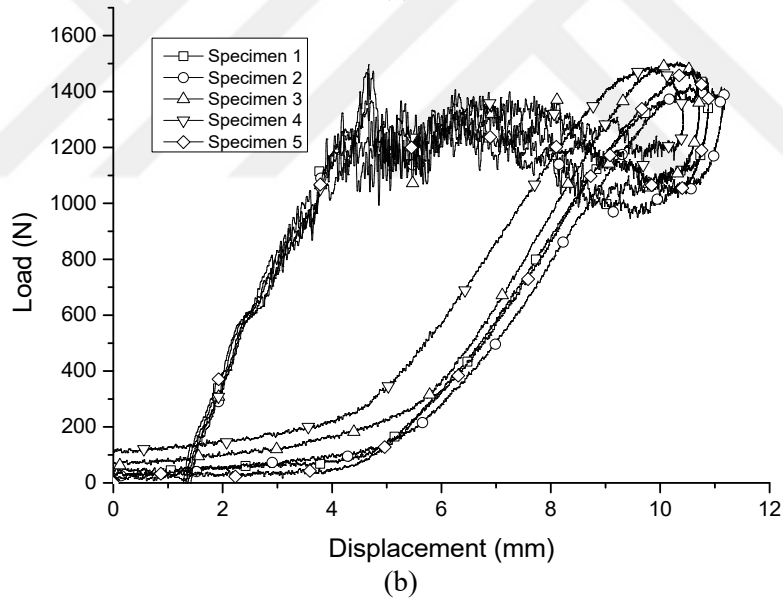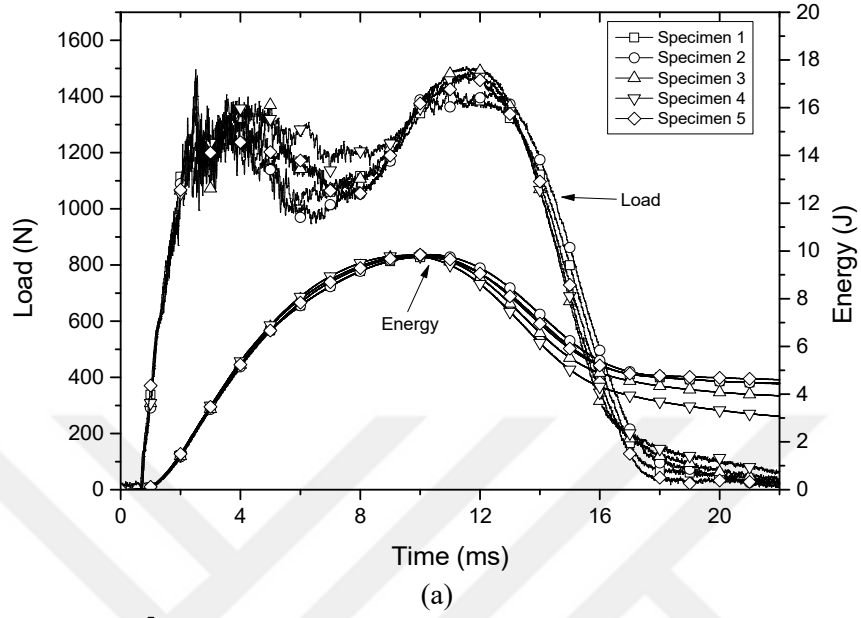
Figure 4.5. Impact test curves of 10% graphene filled sandwich at 10 J energy
            level: (a) load versus time and energy versus time, (b) load versus
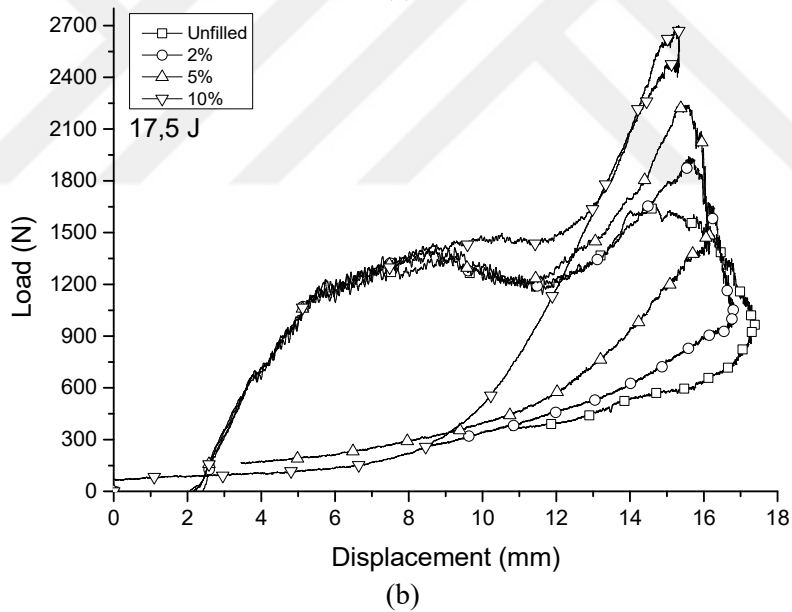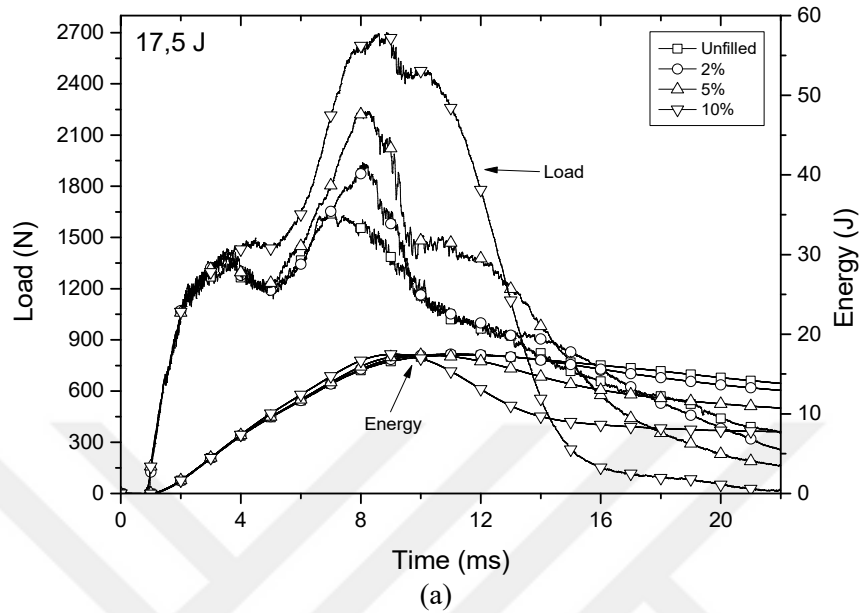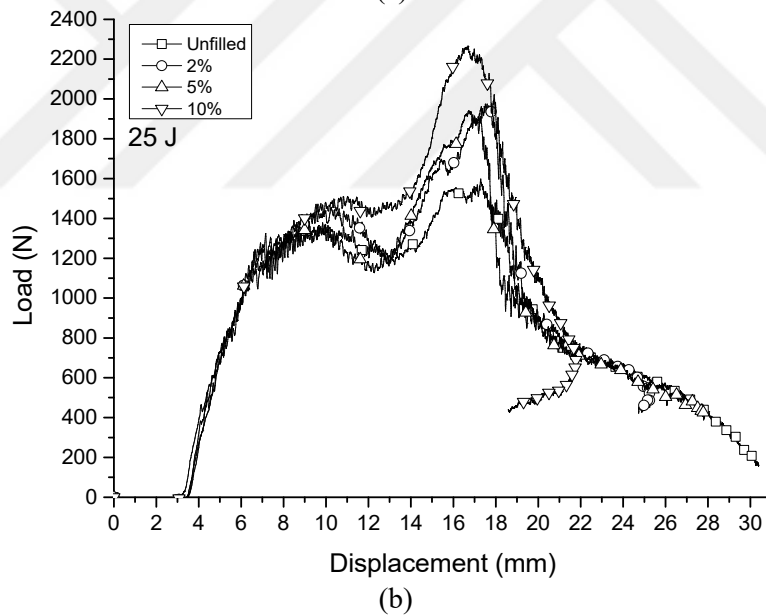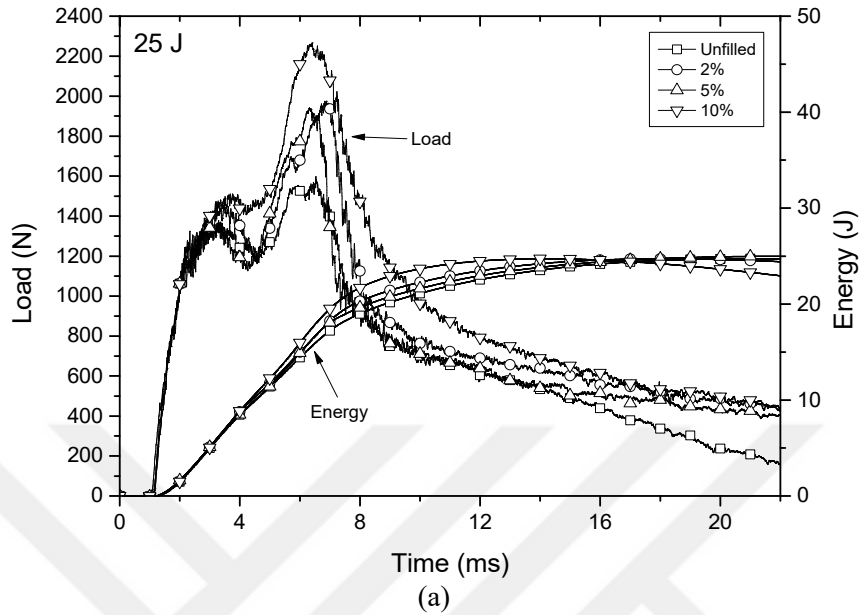   displacement.

Figures 4.6 to 4.8 show the effect of graphene additive in different weight ratio on impact properties of the sandwich structures. The damage conditions of these samples after the drop weight impact test are given in Figure 4.9.

There was no significant increase in the reaction forces (impact forces) due to the absence of penetration at the 10 J impact energy level, but a significant decrease in the amount of indentation depth by up to 8%.

The most significant improvements in sandwich structures containing graphene additive material were observed at 17.50 J energy level. At this energy level, the maximum reaction force of the 5% graphene filled configuration increased by 35.6%. Furthermore, the amount of indentation depth decreased by 12.4% compared to the configuration with neat epoxy. The configuration with 10% additive material showed low impact resistance compared to samples containing 2% and 5% additive material. Figure 4.7 shows that, although there is a significant amount of deformation in the lower face sheets of the sandwiches containing 10% graphene, the lower face sheets of the sandwiches containing 2% and 5% graphene are almost not damaged at 17.50 J impact energy. The energy absorption capacities of sandwich structures are inversely proportional to the size of the damage at the end of the impact. In this case, it can be rated from "high energy absorption level" to low as neat epoxy, 10%, 2%, 5% graphene configurations respectively.

When the results at 25 J energy level are observed, the positive effects of 2% and 5% graphene additives are seen. The structure with neat epoxy and the structure containing 10% graphene were completely punctured at this energy level, although the lower face sheets of the 2% and 5% graphene containing structures were not punctured. This can be seen in Figures 4.8(b) and 4.9. There was also a decrease in the maximum impact forces due to the negative effect of the increase in the amount of additives at this energy level.

When the results at all energy levels are examined, it is seen that the graphene addition in the ratios of 5% and below are found to be very beneficial for the impact strength of the sandwich structure. Low amounts of graphene additive

provides a good dispersion in the epoxy matrix, and make a better fiber-matrix interface. In this way, a better impact resistance is obtained in the structure. As shown in Figure 4.8, samples with 2% and 5% graphene additive were not completely punctured even at 25 J impact energy. On the other hand, samples with 10% graphene additive were punctured at 25 J energy level. The perforation was possibly caused due to the high amount of graphene, poor dispersion in the epoxy matrix and weakening of the fiber-matrix interface. Wang et al. observed agglomerations due to poor dispersion in high amount of graphene additive (5%), and stated that this may cause stress concentration (Wang et al., 2016). It can be said that the sandwich structure with 2% graphene additive is better than 5% and 10%. This is because the high amount of graphene reduces impact properties. Furthermore, it increases cost as it is given in Table 4.3.
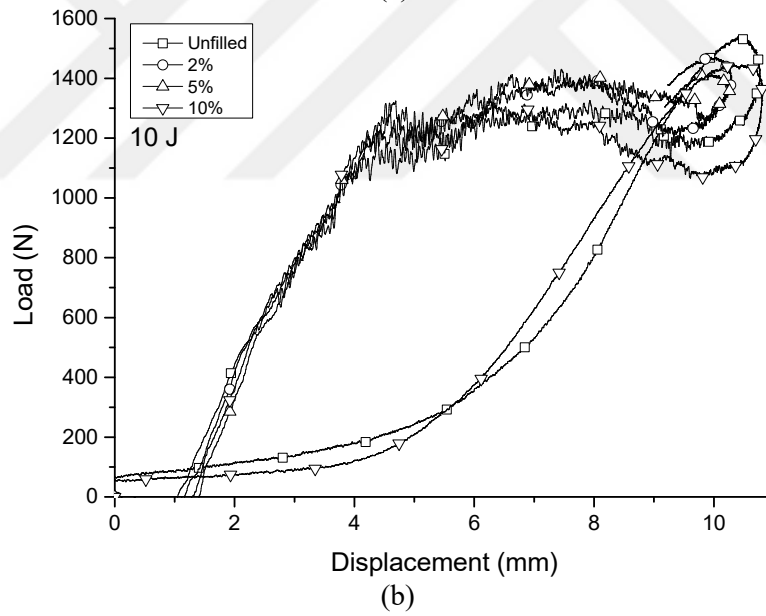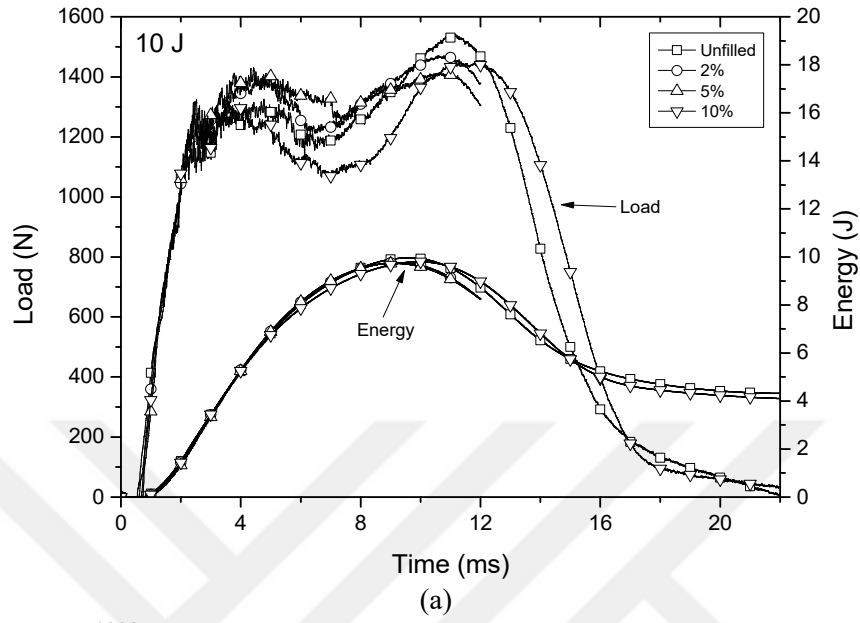
Figure 4.6. Impact test curves of graphene filled sandwiches at 10 J energy: (a) load versus time and energy versus time curves, (b) load versus displacement curves.

62

(a)

(b)
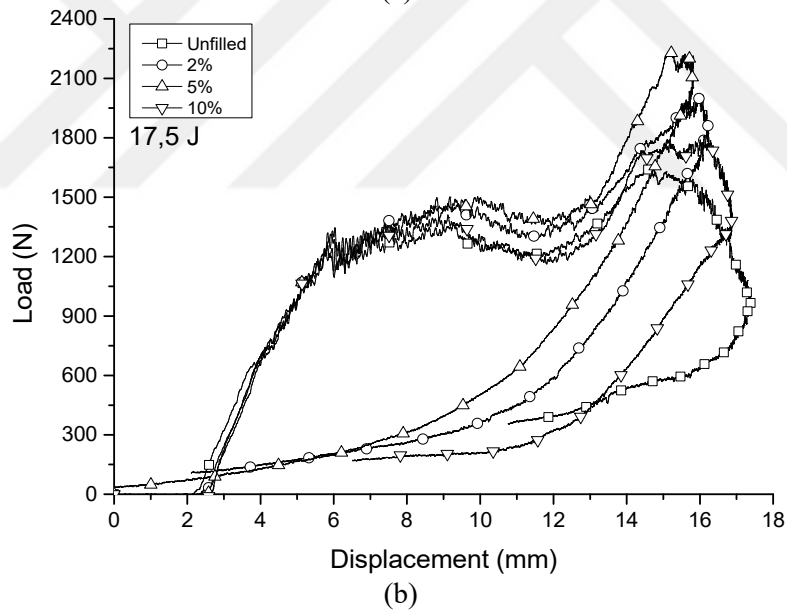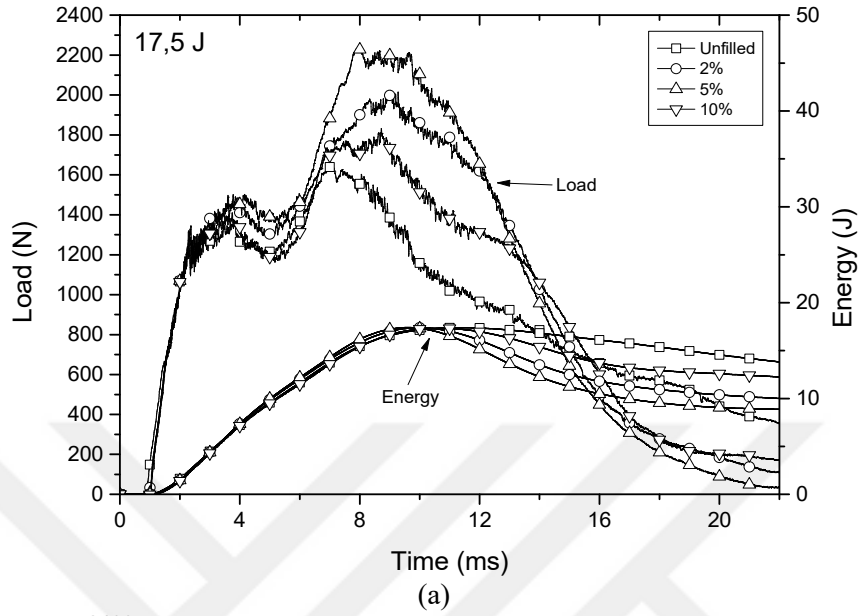
Figure 4.7. Impact test curves of graphene filled sandwiches at 17.50 J energy: (a) load versus time and energy versus time curves, (b) load versus displacement curves.

(a)

(b)
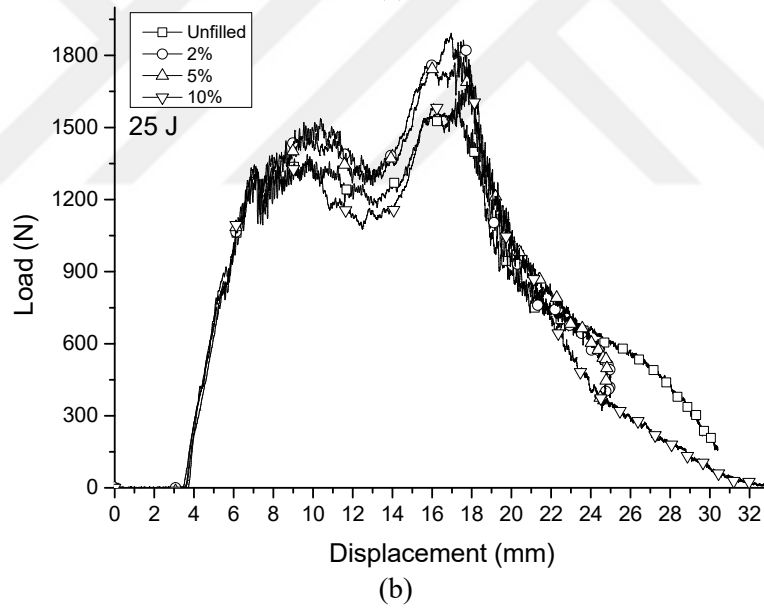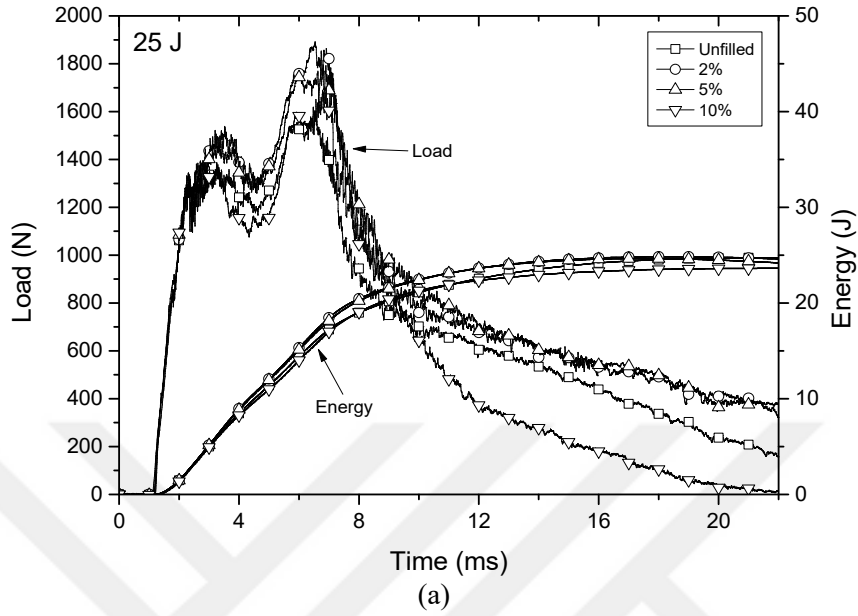
Figure 4.8.   Impact test curves of graphene filled sandwiches at 25 J energy: (a) load versus time and energy versus time curves, (b) load versus displacement curves.

Table 4.3. Comparison of graphene filled sandwiches and percent contribution of graphene content to impact properties and cost of sandwiches

Property	Impact Energy	Neat Epoxy	Graphene Content (±percent contribution)		
			2%	5%	10%
F_1 (N) (First Peak)	10 J	1299.4	1393 (+7.2%)	1421.3 (+9.4%)	1308.5 (+0.7%)
	17.50 J	1350.7	1454.1 (+7.7%)	1488.4 (+10.2%)	1400.4 (+3.7%)
	25 J	1358.7	1537.7 (+13.2%)	1455.3 (+7.1%)	1363.8 (+0.4%)
F_2 (N) (Second Peak)	10 J	1533.9	1467.9 (-4.3%)	1410.2 (-8.1%)	1442.8 (-5.9%)
	17.50 J	1640.5	1998.4 (+21.8%)	2225.2 (+35.6%)	1786.8 (+8.9%)
	25 J	1552.6	1869.6 (+20.4%)	1760.6 (+13.4%)	1667.5 (+7.4%)
Absorbed Energy (J)	10 J	4.32	-	-	4.12 (-4.6%)
	17.50 J	13.8	10.01 (-27.5%)	8.88 (-35.7%)	12.28 (-11%)
	25 J	24.73	24.6 (-0.5%)	24.2 (-2.1%)	23.64 (-4.4%)
Indentation Depth (mm)	10 J	9.49	8.87 (-6.5%)	8.72 (-8.1%)	9.3 (-2%)
	17.50 J	14.93	13.5 (-9.6%)	13.08 (-12.4%)	14.29 (-4.3%)
	25 J	Punctured	21.21	21.1	Punctured
Cost \$/m²		185.809	256.212 (+37.9 %)	361.816 (+94.7 %)	537.823 (+189.4 %)
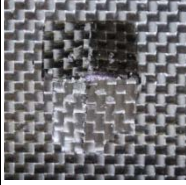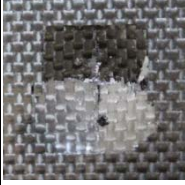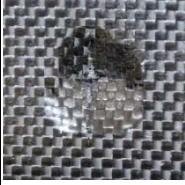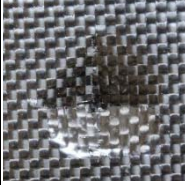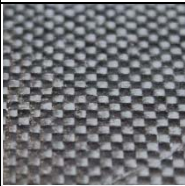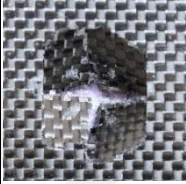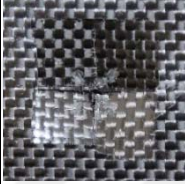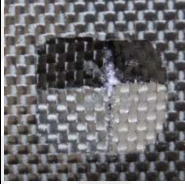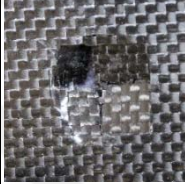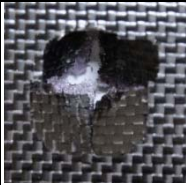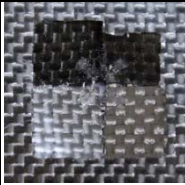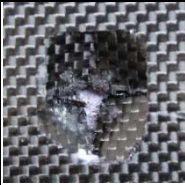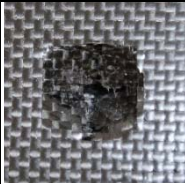
| Impact Energy	Face Sheet	Neat Epoxy	Graphene Content		
			2%	5%	10%
10 J	Top				
	Bottom				
17.50 J	Top				
	Bottom				
25 J	Top				
	Bottom				

Figure 4.9. Post-impact failure images and damage patterns of graphene filled sandwiches after testing

4.3. Effect of Different Percent of Boron Carbide Particles

The load-time, energy-time and load-displacement figures of sandwich structures contain 10% boron carbide additive at 10 J impact energy level are given in Figures 4.10(a) and 4.10(b). The results at 17.5 J and 25 J impact energy levels are given in Appendix. Numeric results for maximum impact loads, absorbed energy and indentation depth results obtained from the mean of five replications for each configuration of sandwiches with boron carbide additive are provided in Table 4.4. Also the percent change in the test results of the boron carbide filled samples compared to the samples with neat epoxy are shown in Table 4.4.
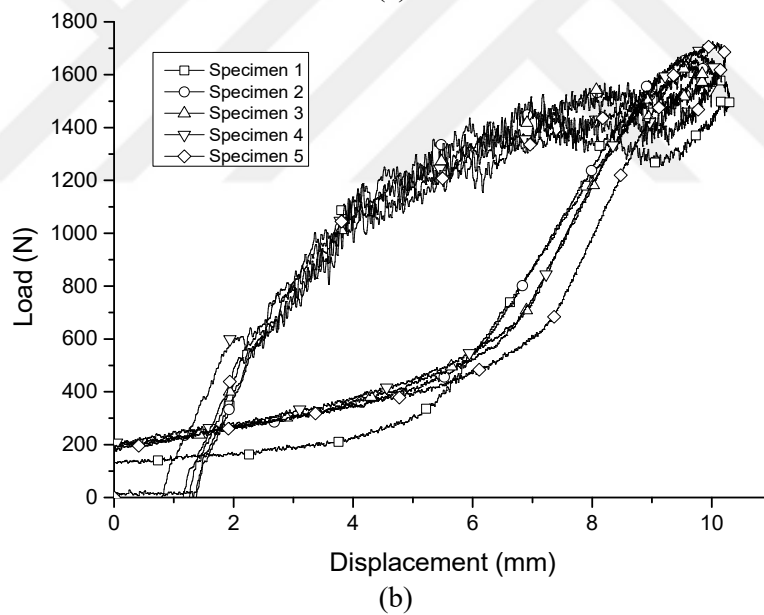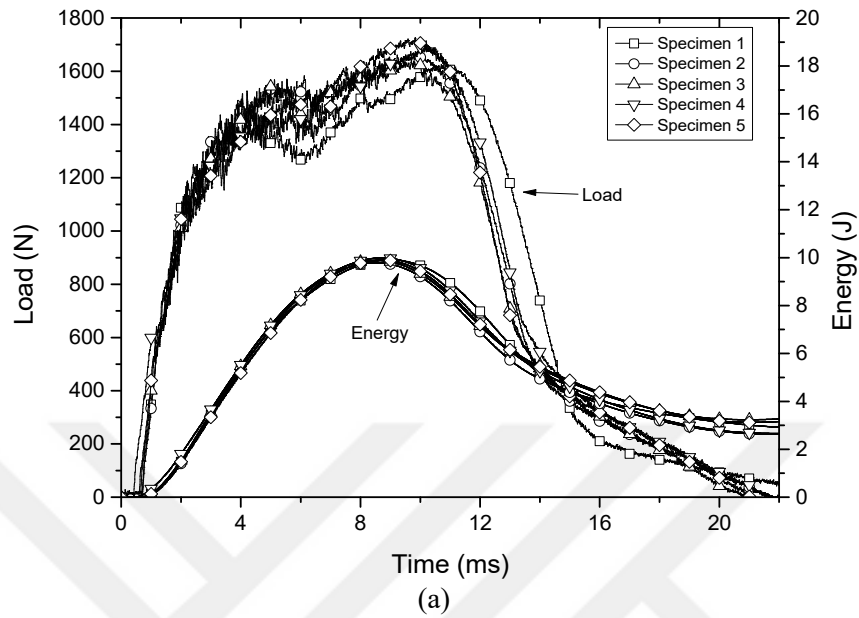
Figure 4.10.   Impact test curves of 10% boron carbide filled sandwich at 10 J energy level: (a) load versus time and energy versus time, (b) load versus displacement.

Figures 4.11 to 4.13 show the effect of boron carbide additive on impact properties of the sandwich structures. The damage conditions of these samples after the drop weight impact test are shown in Figure 4.15.

Although there was no penetration at the 10 J impact energy level, the reaction force increased by 12.5% and the indentation depth decreased by 7.7%. Because of the inverse relationship between the damage size and the amount of energy absorption, the most energy absorbing configuration was structure with neat epoxy, while the least energy absorbing was 10% boron carbide containing structure. The 10% boron carbide containing structure absorbed 2.93 J energy while structure with neat epoxy absorbed 3.91 J at 10 J impact energy, applied by the drop weight of the test rig.

Similar to graphene added samples, the maximum reaction force increase in boron carbide added samples were seen in 17.50 J impact energy. The maximum reaction forces of 2%, 5% and 10% boron carbide filled configurations increased by 17.3%, 36% and 63.8% respectively. The amount of indentation depth decreased up to 13% compared to the configuration with neat epoxy. The amount of energy absorptions of 2%, 5% and 10% boron carbide filled configurations were 12.91 J, 10.76 J and 7.80 J respectively while the configuration with neat epoxy was 13.80 J at 17.50 J impact energy. The amount of boron additive was directly proportional to the reaction forces, and it is inversely proportional to the absorbed energy and the indentation depth. As shown in Figure 4.14, the damage size of the lower face sheets decreased due to the increase in the amount of boron carbide in the sandwich structure.

The effect of boron carbide on the impact resistance of the samples was also positive in 25 J impact energy. The maximum impact force of 10% boron carbide filled configuration increased by 44.6%. Although the lower face sheets of the boron carbide containing structures were not punctured, the structure with neat epoxy was completely punctured at 25 J impact energy.

69

When the results at all energy levels are examined, it is seen that the boron carbide addition in the all ratios are very beneficial for the impact strength of the sandwich structure. As shown in Figure 4.14, none of the samples containing different amounts of boron carbide were punctured even at 25 J impact energy. In addition, when the samples subjected to 17.50 J impact energy are examined, it is seen that the damage in the lower surface layer decreases significantly due to the increase in boron carbide ratio. Boron carbide additive provides a good dispersion in the epoxy matrix and make a better fiber-matrix interface. In this way, a better impact resistance is obtained and seen in the structure. The best impact results in boron carbide added samples were observed at the 10% additive level.

(a)

(b)

Figure 4.11.   Impact test curves of boron carbide filled sandwiches at 10 J energy:
(a) load versus time and energy versus time curves, (b) load versus
displacement curves

71

Figure 4.12.   Impact test curves of boron carbide filled sandwiches at 17.50 J
                energy: (a) load versus time and energy versus time curves, (b) load
                versus displacement curves.

(a)

(b)

Figure 4.13.   Impact test curves of boron carbide filled sandwiches at 25 J energy:
(a) load versus time and energy versus time curves, (b) load versus
displacement curves

73

Table 4.4. Comparison of boron carbide filled sandwiches and percent contribution of boron carbide content to impact properties and cost of sandwiches

Property	Impact Energy	Neat Epoxy	Boron Carbide Content (±percent contribution)		
			2%	5%	10%
F_1 (N) (First Peak)	10 J	1299.4	1398.1 (+7.6%)	1381.2 (+6.3%)	1461.9 (+12.5%)
	17.50 J	1350.7	1400.8 (+3.7%)	1387.9 (+2.8%)	1476.4 (+9.3%)
	25 J	1358.7	1418.8 (+4.4%)	1376.7 (+1.3%)	1496.9 (+10.2%)
F_2 (N) (Second Peak)	10 J	1533.9	1516.5 (-1.1%)	1570.2 (+2.4%)	1653.5 (+7.8%)
	17.50 J	1640.5	1924.7 (+17.3%)	2230.8 (+36%)	2687.7 (+63.8%)
	25 J	1552.6	1966.9 (+26.7%)	1930.9 (+24.4%)	2245.7 (+44.6%)
Absorbed Energy (J)	10 J	4.32	3.91 (-9.5%)	3.46 (-19.9%)	2.93 (-32.2%)
	17.50 J	13.8	12.91 (-6.4%)	10.76 (-22%)	7.8 (-43.5%)
	25 J	24.73	24.41 (-1.3%)	24.98 (+1%)	22.95 (-7.2%)
Indentation Depth (mm)	10 J	9.49	9.04 (-4.7%)	8.96 (-5.6%)	8.76 (-7.7%)
	17.50 J	14.93	14.27 (-4.4%)	13.75 (-7.9%)	12.41 (-16.9%)
	25 J	Punctured	21.51	24.34	17.96
Cost $/m^2		185.809	209.894 (+13%)	246.022 (+32.4%)	306.235 (+64.8%)

74
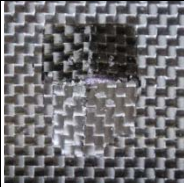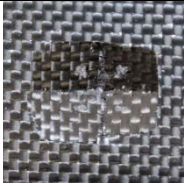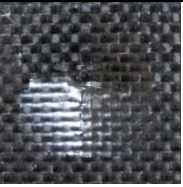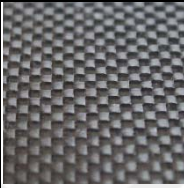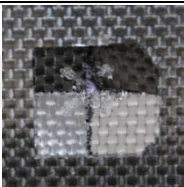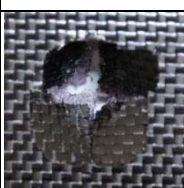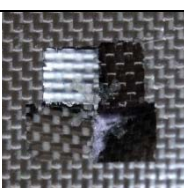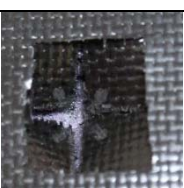
Impact Energy	Face Sheet	Neat Epoxy	Boron Carbide Content		
			2%	5%	10%
10 J	Top				
	Bottom				
17.50 J	Top				
	Bottom				
25 J	Top				
	Bottom				

Figure 4.14. Post-impact failure images and damage patterns of boron carbide filled sandwiches after testing

4.4. Effect of Different Percent of Kaolin Particles

The load-time, energy-time and load-displacement figures of sandwich structures contain 10% kaolin additive at 10 J impact energy level are given in Figures 4.15(a) and 4.15(b). The results at 17.5 J and 25 J impact energy levels are given in Appendix. Numeric results for maximum impact loads, absorbed energy and indentation depth results obtained from the mean of five replications for each configuration of sandwiches with kaolin additive are provided in Table 4.5. Also the percent change in the test results of the kaolin filled samples compared to the samples with neat epoxy are shown in Table 4.5.

(a)

(b)
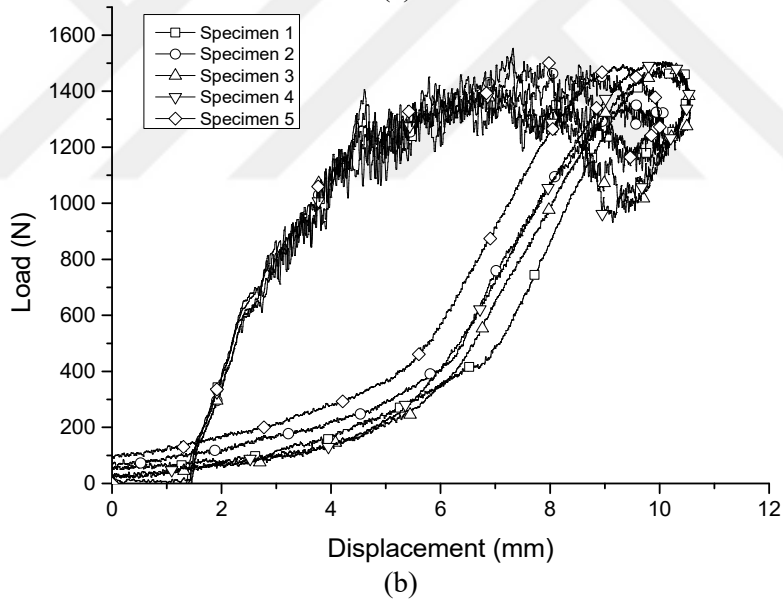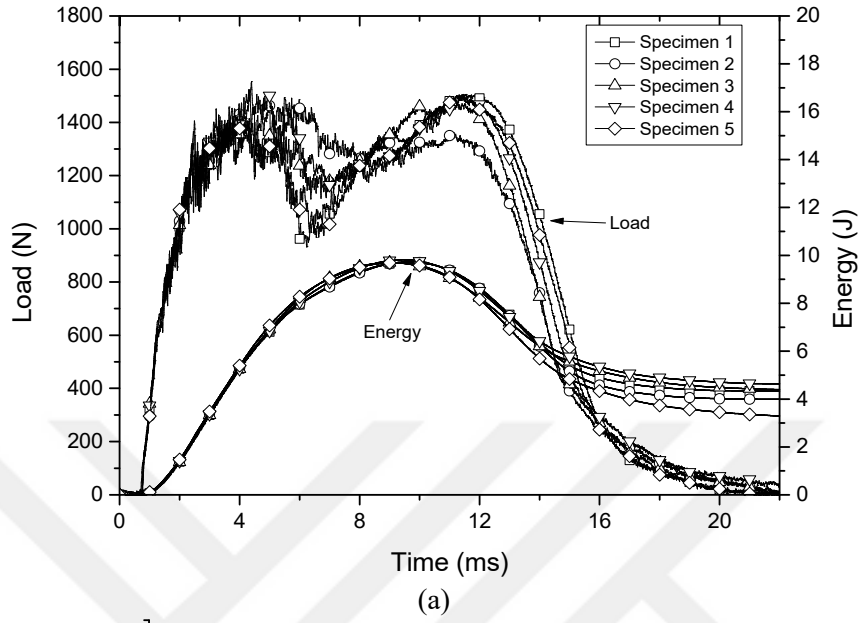
Figure 4.15.   Impact test curves of 10% kaolin filled sandwich at 10 J energy level: (a) load versus time and energy versus time, (b) load versus displacement.

Figures 4.16 to 4.18 show the effect of kaolin additive on impact properties of the sandwich structures. The damage conditions of these samples after the drop weight impact test are also given in Figure 4.19.

In general, kaolin additive does not have a significant effect on the impact properties of sandwich structures. This is clearly seen from the test results of kaolin given in Figures 4.16 to 4.19. The specimens showed similar results with configurations with neat epoxy at all impact energy levels.
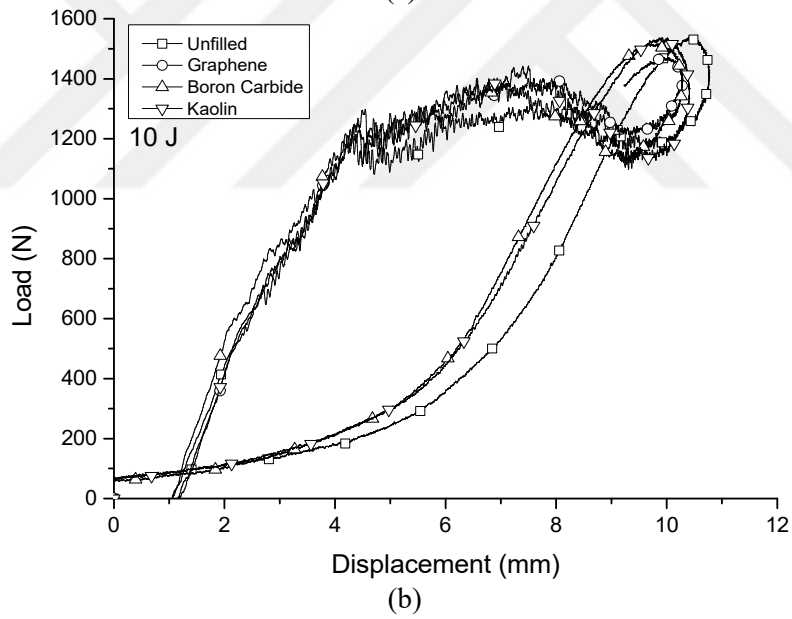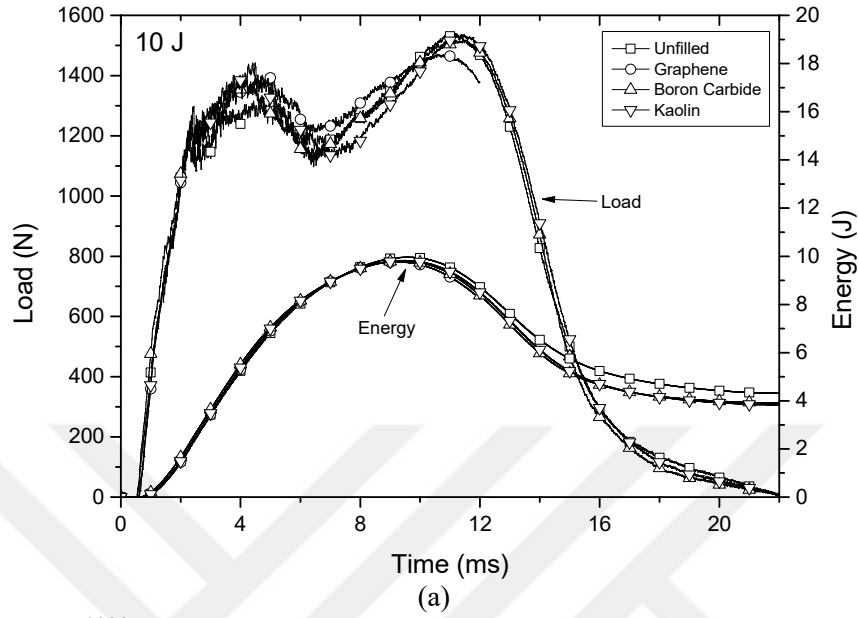
(a)

(b)
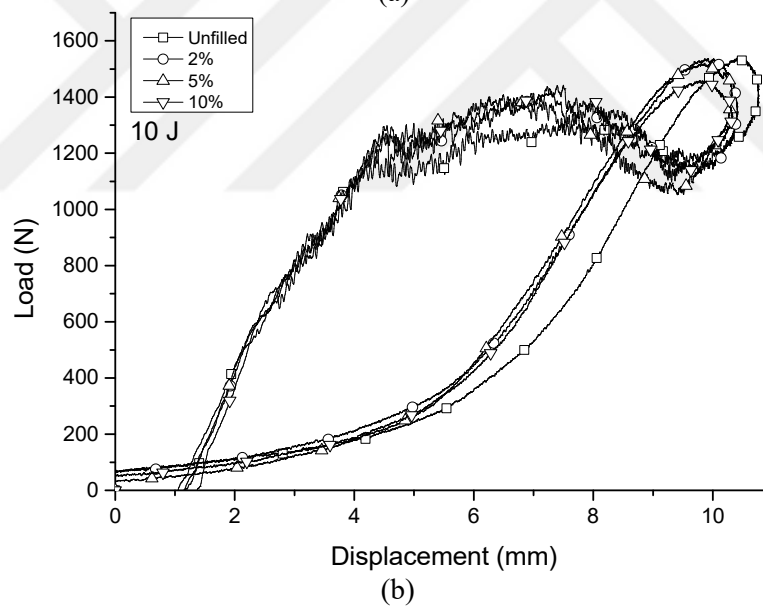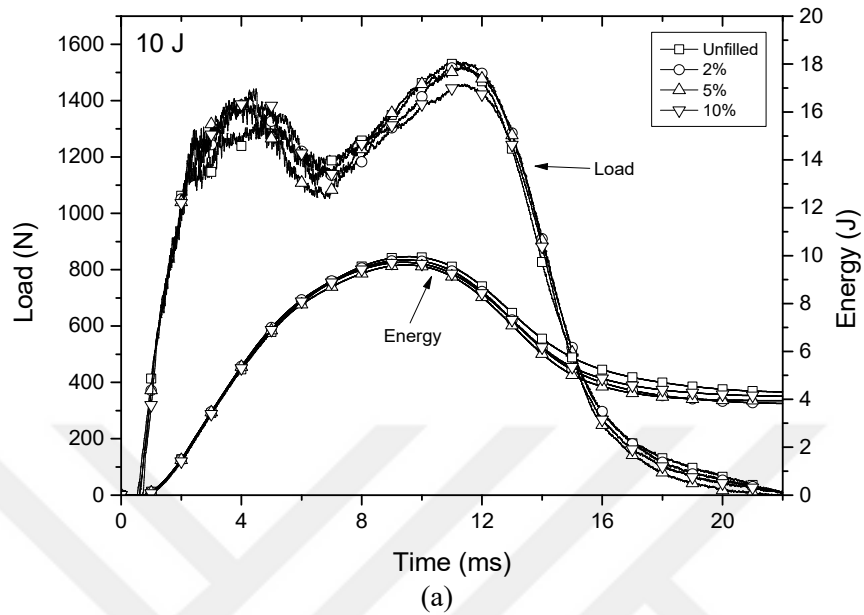
Figure 4.16. Impact test curves of kaolin filled sandwiches at 10 J energy: (a) load versus time and energy versus time curves, (b) load versus displacement curves
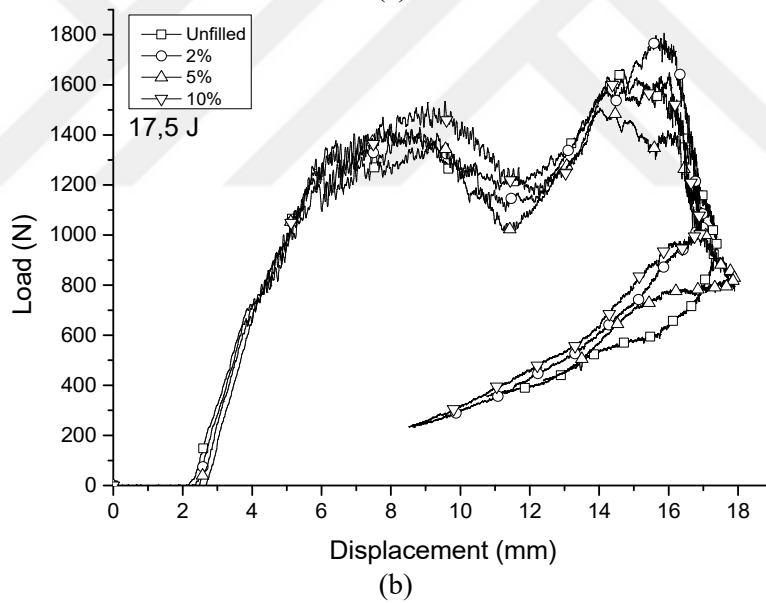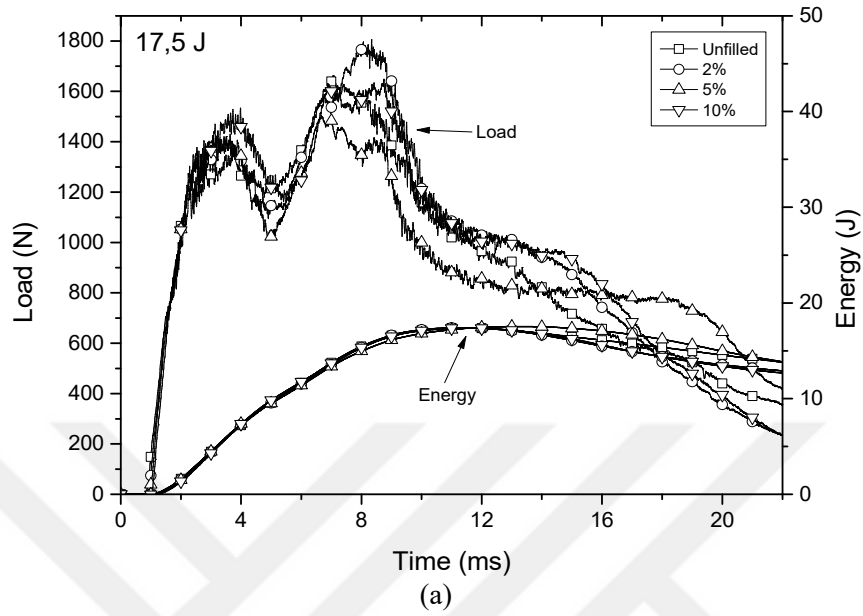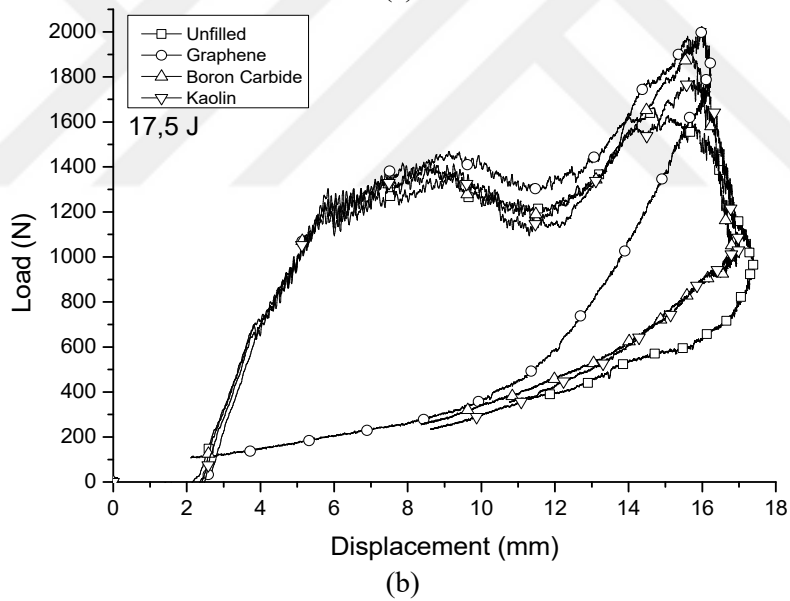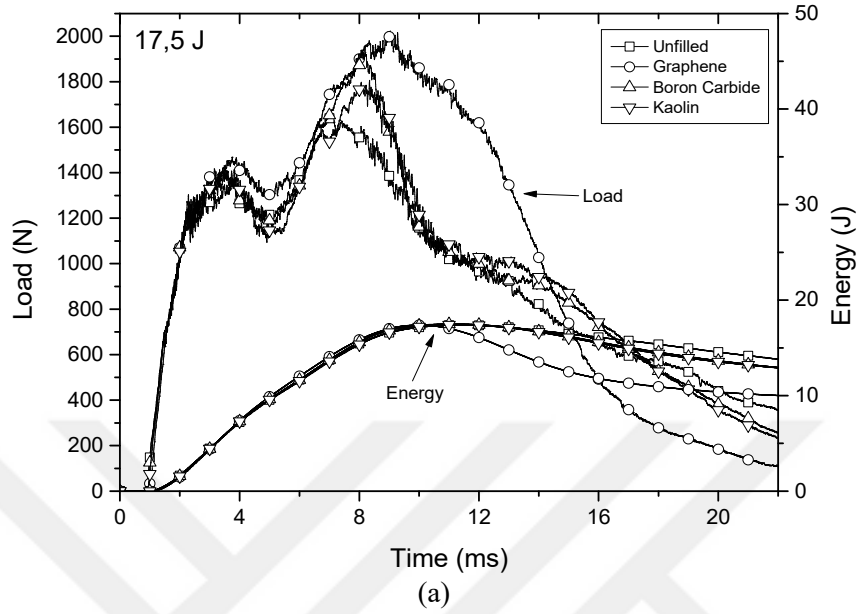
Figure 4.17.   Impact test curves of kaolin filled sandwiches at 17.50 J energy: (a) load versus time and energy versus time curves, (b) load versus displacement curves
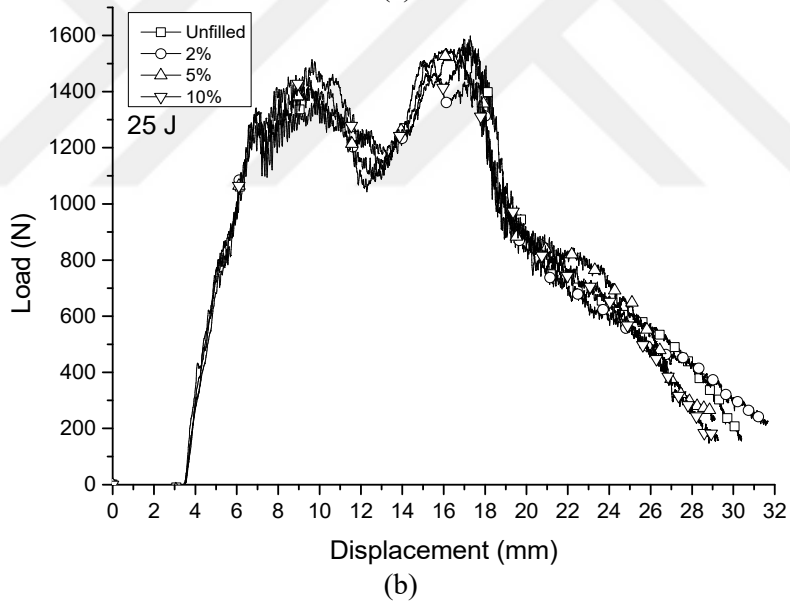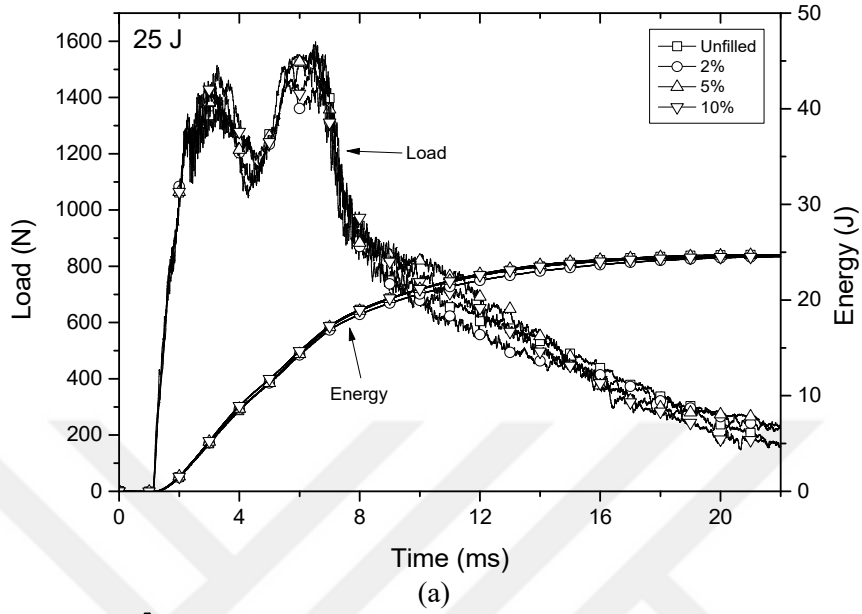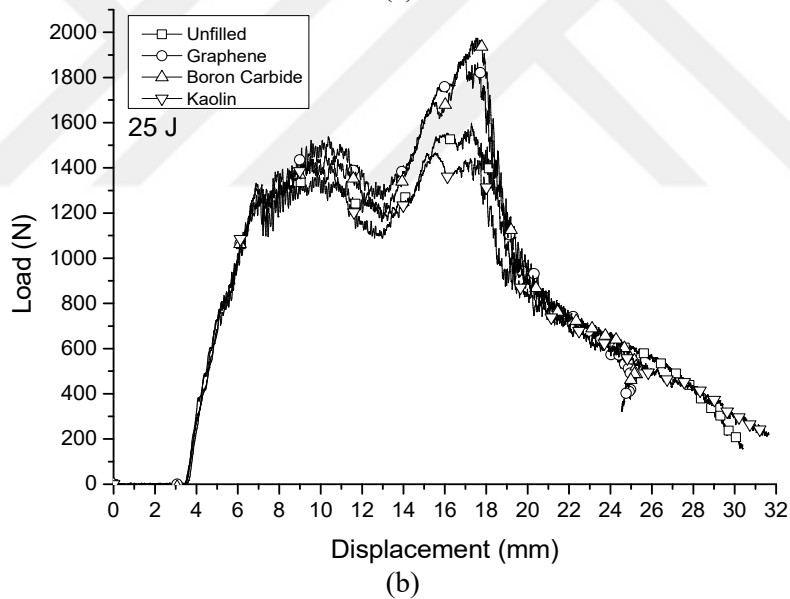
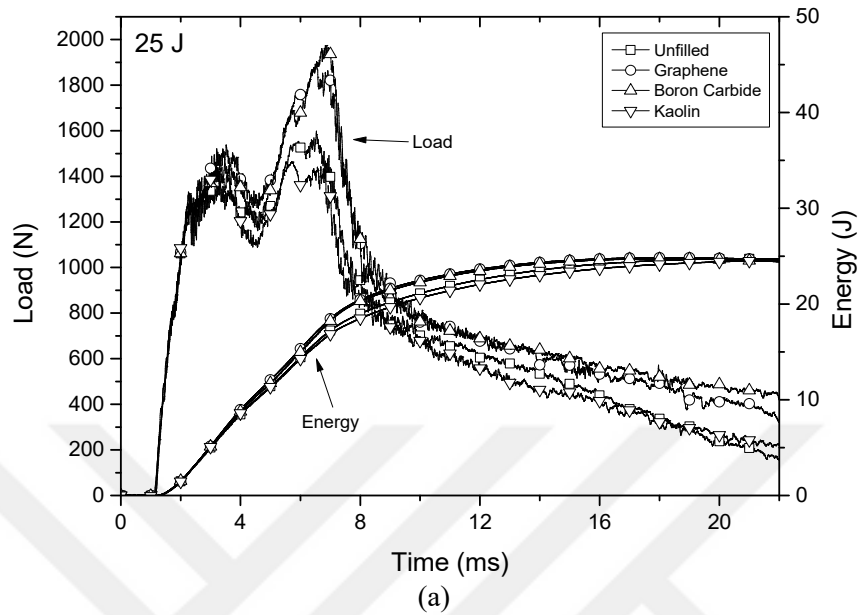Figure 4.18. Impact test curves of kaolin filled sandwiches at 25 J energy: (a) load s time and energy versus time curves, (b) load versus displacement curves

Table 4.5.   Comparison of kaolin filled sandwiches and percent contribution of
kaolin content to impact properties and cost of sandwiches

Property	Impact Energy	Neat Epoxy	Kaolin Content (±percent contribution)		
			2%	5%	10%
F_1 (N) (First Peak)	10 J	1299.4	1435.8 (+10.5%)	1392.2 (+7.1%)	1405.6 (+8.2%)
	17.50 J	1350.7	1392.2 (+3.1%)	1424.7 (+5.5%)	1489.6 (+10.3%)
	25 J	1358.7	1449.1 (+6.7%)	1374.8 (+1.2%)	1501.9 (+10.5%)
F_2 (N) (Second Peak)	10 J	1533.9	1533.9 (0%)	1516 (-1.2%)	1456 (-5.1%)
	17.50 J	1640.5	1771.8 (+8%)	1497.6 (-8.7%)	1629.1 (-0.7%)
	25 J	1552.6	1464.6 (-5.7%)	1573.6 (+1.4%)	1508.2 (-2.9%)
Absorbed Energy (J)	10 J	4.32	3.83 (-11.3%)	3.95 (-8.6%)	4.13 (-4.4%)
	17.50 J	13.8	12.95 (-6.2%)	13.87 (+0.5%)	12.69 (-8%)
	25 J	24.73	24.56 (-0.7%)	24.74 (0%)	24.65 (-0.3%)
Indentation Depth (mm)	10 J	9.49	9.01 (-5.1%)	8.93 (-5.9%)	8.82 (-7.1%)
	17.50 J	14.93	14.38 (-3.7%)	15.2 (+1.8%)	14 (-6.2%)
	25 J	Punctured	Punctured	Punctured	Punctured
Cost $/m^2$		185.809	185.93 (+0.06%)	186.111 (+0.16%)	186.413 (+0.32%)
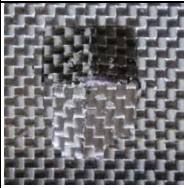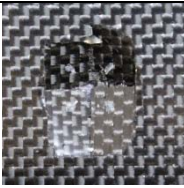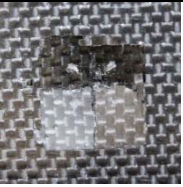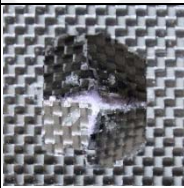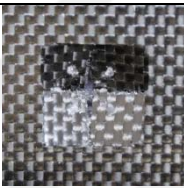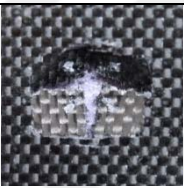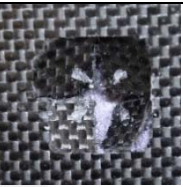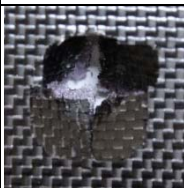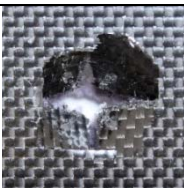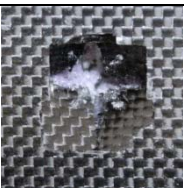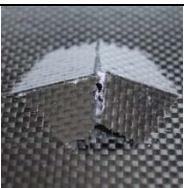
Impact Energy	Face Sheet	Neat Epoxy	Kaolin Content		
			2%	5%	10%
10 J	Top				
	Bottom				
17,50 J	Top				
	Bottom				
25 J	Top				
	Bottom				

Figure 4.19.   Post-impact failure images and damage patterns of kaolin filled sandwiches after testing

83

4.5. Effect of Filling Materials with Content of 2%

Figures 4.20 to 4.22 show the effect of different filling materials containing 2% additive on impact properties of the sandwich structures. Table 4.6 shows the percent change in the test results of the 2% filled configurations compared to the samples with neat epoxy. The damage conditions of these samples after the drop weight impact test are shown in Figure 4.23.

No significant difference was observed in the samples containing 2% additive material in the tests performed at 10 J impact energy. This is because 10 J impact energy is not sufficient for penetration. At this energy level, the striker tip bounces back after hitting the upper face sheet of the sandwich structure for all configurations.

The 17.50 J impact energy level results were more pronounced comparing to the 10 J energy level. The maximum reaction forces of graphene, boron carbide and kaolin filled configurations increased by 21.8%, 17.3% and 8% respectively. So in this impact level, 2% graphene filled sandwiches showed the best results. The amount of indentation depth of graphene filled structure decreased 9.6%, 5.4% and 6.1% compared to the neat epoxy, boron carbide and graphene filled configurations respectively. The amount of energy absorptions of graphene, boron carbide and kaolin filled configurations were 10.01 J, 12.91 J and 12.95 J respectively while the configuration with neat epoxy was 13.80 J when 17.50 J impact energy was applied during the test. As seen in Figure 4.23, the lower face sheets of neat epoxy, boron carbide and kaolin containing samples were significantly damaged but graphene containing sample was slightly damaged. No samples were completely punctured.

When the results at 25 J energy level were examined, the positive effects of graphene and boron carbide additives were observed. Although the neat epoxy and kaolin containing structures were completely punctured at this energy level, the lower face sheets of the graphene and boron carbide containing structures were not punctured. This can be seen from the Figures 4.22(b) and 4.23. This is due to the better fiber-matrix interface of graphene and boron carbide particles. The

maximum impact forces of graphene and boron carbide filled configurations increased by 20.4% and 26.7% respectively. The maximum impact force of kaolin additive decreased by 5.7%. So at 25 J impact energy level, 2% boron carbide filled sandwiches showed the best results.

Cost estimates of graphene, boron carbide and kaolin filled configurations shown that the cost was increased by 37.9%, 13% and 0.06% respectively. It can be concluded that the sandwich structure with boron carbide additive is better than graphene and kaolin in 2% filled sandwiches due to the better impact properties. Also cost of boron carbide filled configuration is 82% lower than graphene filled configuration.

Figure 4.20. Impact test curves of 2% filled sandwiches at 10 J energy: (a) load versus time and energy versus time curves, (b) load versus displacement curves

(a)

(b)

Figure 4.21. Impact test curves of 2% filled sandwiches at 17.50 J energy: (a) load versus time and energy versus time curves, (b) load versus displacement curves

87

(a)

(b)

Figure 4.22. Impact test curves of 2% filled sandwiches at 25 J energy: (a) load versus time and energy versus time curves, (b) load versus displacement curves

Table 4.6.   Comparison of 2% filled sandwiches and percent contribution of additive content to impact properties and cost of sandwiches

Property	Impact Energy	Neat Epoxy	Graphene	Boron Carbide	Kaolin
			(±percent contribution)		
F_1 (N) (First Peak)	10 J	1299.4	1393 (+7.2%)	1398.1 (+7.6%)	1435.8 (+10.5%)
	17.50 J	1350.7	1454.1 (+7.7%)	1400.8 (+3.7%)	1392.2 (+3.1%)
	25 J	1358.7	1537.7 (+13.2%)	1418.8 (+4.4%)	1449.1 (+6.7%)
F_2 (N) (Second Peak)	10 J	1533.9	1467.9 (-4.3%)	1516.5 (-1.1%)	1533.9 (0%)
	17.50 J	1640.5	1998.4 (+21.8%)	1924.7 (+17.3%)	1771.8 (+8%)
	25 J	1552.6	1869.6 (+20.4%)	1966.9 (+26.7%)	1464.6 (-5.7%)
Absorbed Energy (J)	10 J	4.32	-	3.91 (-9.5%)	3.83 (-11.3%)
	17.50 J	13.8	10.01 (-27.5%)	12.91 (-6.4%)	12.95 (-6.2%)
	25 J	24.73	24.6 (-0.5%)	24.41 (-1.3%)	24.56 (-0.7%)
Indentation Depth (mm)	10 J	9.49	8.87 (-6.5%)	9.04 (-4.7%)	9.01 (-5.1%)
	17.50 J	14.93	13.5 (-9.6%)	14.27 (-4.4%)	14.38 (-3.7%)
	25 J	Punctured	21.21	21.51	Punctured
Cost $/m^2$		185.809	256.212 (+37.9%)	209.894 (+13%)	185.93 (+0.06%)
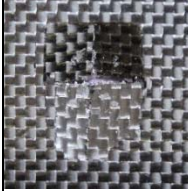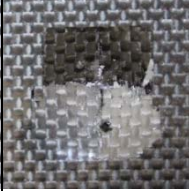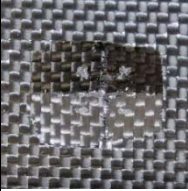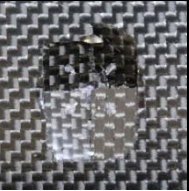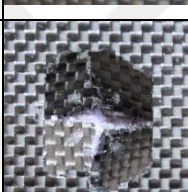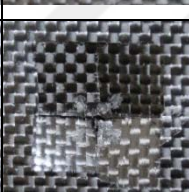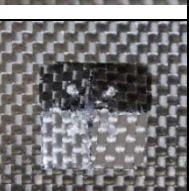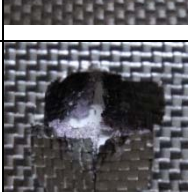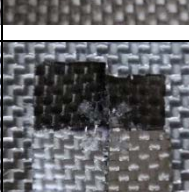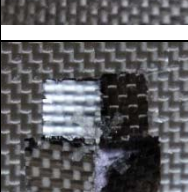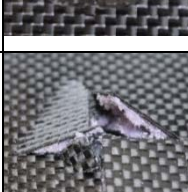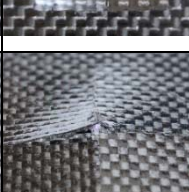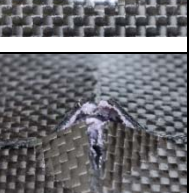
Impact Energy	Face Sheet	Neat Epoxy	Graphene	Boron Carbide	Kaolin
10 J	Top				
	Bottom				
17.50 J	Top				
	Bottom				
25 J	Top				
	Bottom				

Figure 4.23.   Post-impact failure images and damage patterns of 2% filled sandwiches after testing

4.6. Effect of Filling Materials with Content of 5%

Figures 4.24 to 4.26 show the effect of different filling materials in the samples containing 5% additive on impact properties of the sandwich structures. Table 4.7 gives the percent change in the test results of the samples containing 5% filling additive materials compared to the samples with neat epoxy. The damage conditions of these samples after the drop weight impact test are also shown in Figure 4.27.

Similar to 2% filled configurations, no significant difference was observed in the samples containing 5% additive material in the tests performed at 10 J impact energy. This is because 10 J impact energy is not sufficient for penetration. At this energy level, the striker tip bounces back after hitting the upper face sheet of the sandwich structure for all configurations.

When the results at 17.50 J energy level were examined, the positive effects of graphene and boron carbide additives were observed. The maximum impact forces of graphene and boron carbide filled configurations increased by 35.6% and 36% respectively. The maximum impact force of kaolin additive decreased by 8.7%. So in this impact level, 5% boron carbide filled sandwiches showed the best results but graphene containing configuration gave close results to them. The amount of indentation depth of graphene and boron carbide filled structures decreased by 12.4% and 7.9% respectively whilst kaolin filled structures increased by 2% compared to the configurations with neat epoxy. The amount of energy absorptions of graphene, boron carbide and kaolin filled configurations were 8.88 J, 10.76 J and 13.87 J respectively while the configuration with neat epoxy was 13.80 J when 17.50 J impact energy is applied by the striker. As seen in Figure 4.27, the lower face sheets of neat epoxy and kaolin containing samples were significantly damaged whilst graphene and boron carbide containing samples was slightly damaged. No samples were completely punctured.

When the results at 25 J energy level were examined, the positive effects of graphene and boron carbide additives were observed similar to 17.50 J energy

level. Although the neat epoxy and kaolin containing structures were completely punctured at this energy level, the lower face sheets of the graphene and boron carbide containing structures were not punctured. This can be seen from the Figures 4.26(b) and 4.27. This is due to the better fiber-matrix interface of graphene and boron carbide particles. The maximum impact forces of graphene, boron carbide and kaolin filled configurations increased by 13.4%, 24.4% and 1.4% respectively. So 25 J impact energy level, 5% boron carbide filled sandwiches showed the best results.

Cost estimates of graphene, boron carbide and kaolin filled configurations shown that the cost was increased by 94.7%, 32.4% and 0.16% respectively. It can be concluded that the sandwich structure with boron carbide additive is better than graphene and kaolin sandwiches filled with 5% additives due to the better impact properties. Also cost of boron carbide filled configuration is 32% lower than graphene filled configuration.
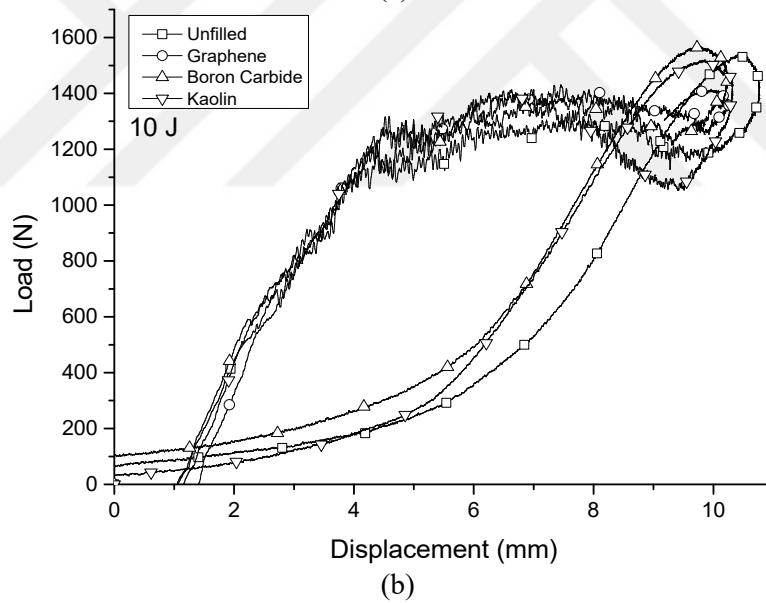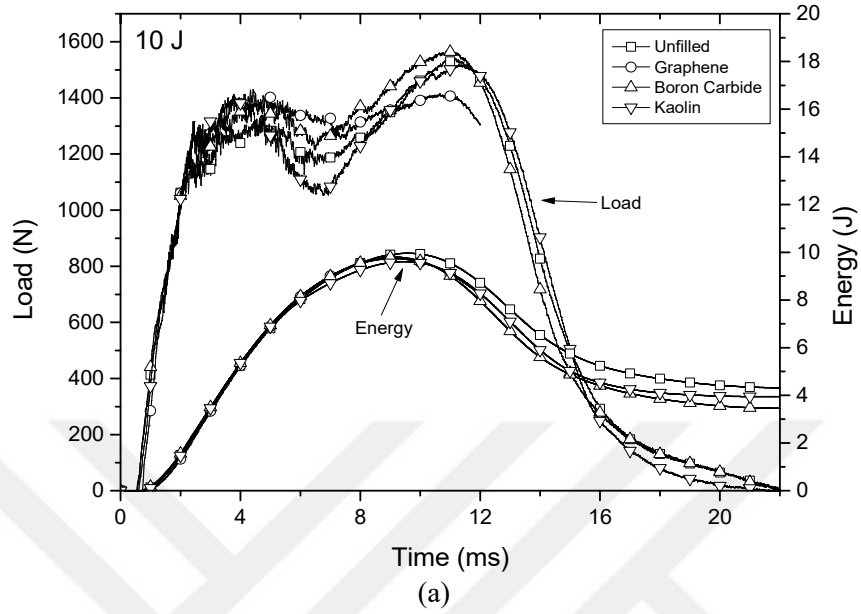
Figure 4.24.   Impact test curves of 5% filled sandwiches at 10 J energy: (a) load versus time and energy versus time curves, (b) load versus displacement curves

(a)

(b)
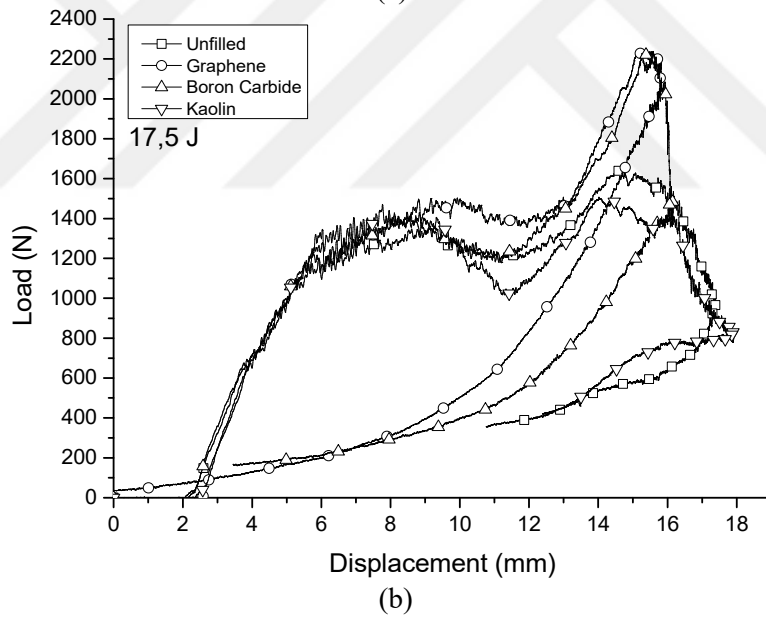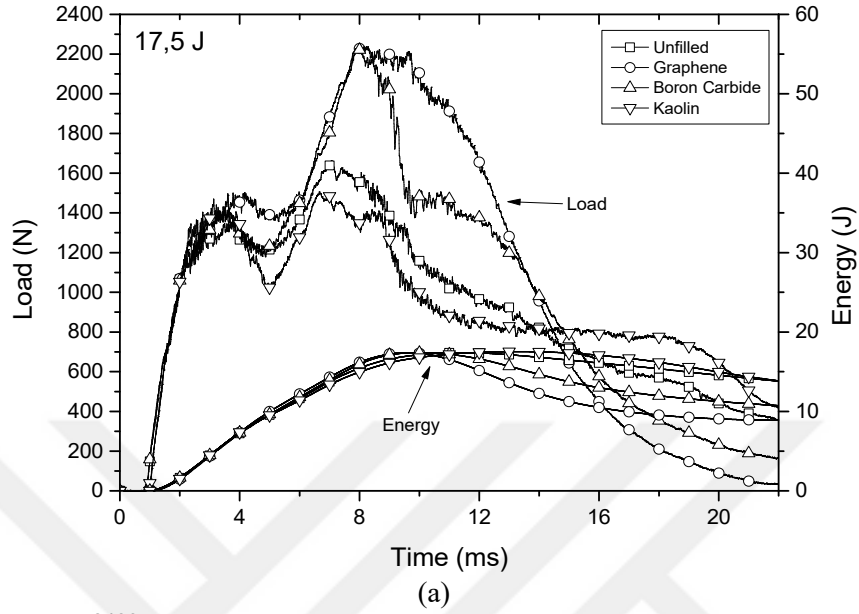
Figure 4.25. Impact test curves of 5% filled sandwiches at 17.50 J energy: (a) load versus time and energy versus time curves, (b) load versus displacement curves
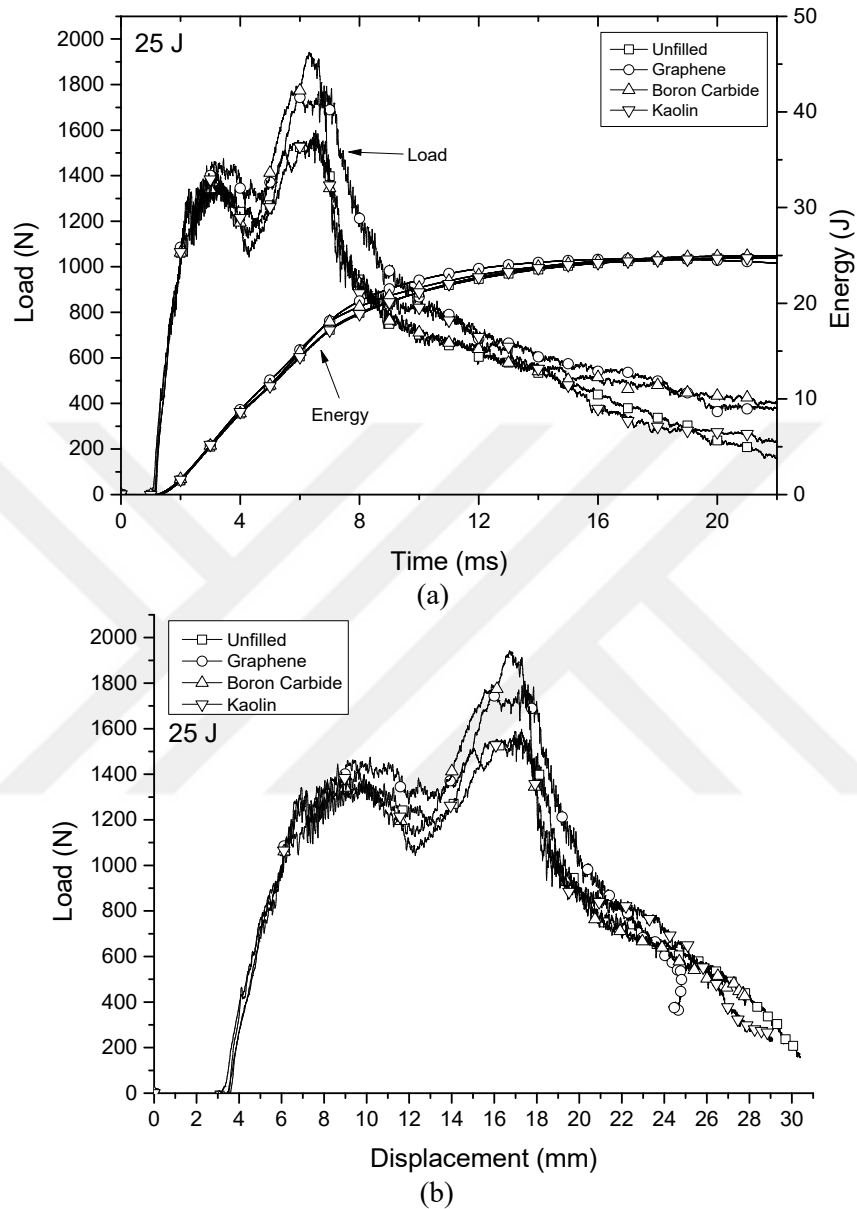
Figure 4.26.   Impact test curves of 5% filled sandwiches at 25 J energy: (a) load versus time and energy versus time curves, (b) load versus displacement curves

Table 4.7.   Comparison of 5% filled sandwiches and percent contribution of additive content to impact properties and cost of sandwiches

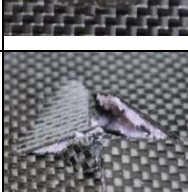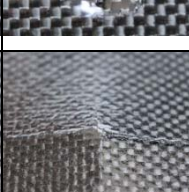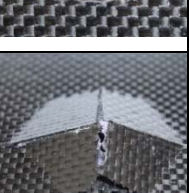| Property	Impact Energy	Neat Epoxy	Graphene	Boron Carbide	Kaolin
			(±percent contribution)		
F_1 (N) (First Peak)	10 J	1299.4	1421.3 (+9.4%)	1381.2 (+6.3%)	1392.2 (+7.1%)
	17.50 J	1350.7	1488.4 (+10.2%)	1387.9 (+2.8%)	1424.7 (+5.5%)
	25 J	1358.7	1455.3 (+7.1%)	1376.7 (+1.3%)	1374.8 (+1.2%)
F_2 (N) (Second Peak)	10 J	1533.9	1410.2 (-8.1%)	1570.2 (+2.4%)	1516 (-1.2%)
	17.50 J	1640.5	2225.2 (+35.6%)	2230.8 (+36%)	1497.6 (-8.7%)
	25 J	1552.6	1760.6 (+13.4%)	1930.9 (+24.4%)	1573.6 (+1.4%)
Absorbed Energy	10 J	4.32	-	3.46 (-19.9%)	3.95 (-8.6%)
	17.50 J	13.8	8.88 (-35.7%)	10.76 (-22%)	13.87 (+0.5%)
	25 J	24.73	24.2 (-2.1%)	24.98 (+1%)	24.74 (+0.1%)
Indentation Depth (mm)	10 J	9.49	8.72 (-8.1%)	8.96 (-5.6%)	8.93 (-5.9%)
	17.50 J	14.93	13.08 (-12.4%)	13.75 (-7.9%)	15.2 (+1.8%)
	25 J	Punctured	21.1	24.34	Punctured
Cost $/m^2		185.809	361.816 (+94.7%)	246.022 (+32.4%)	18.,111 (+0.16%)
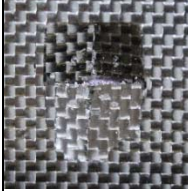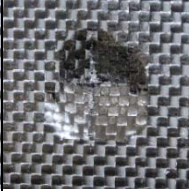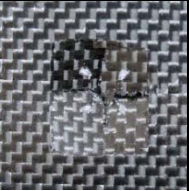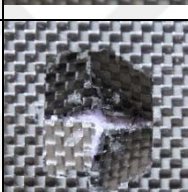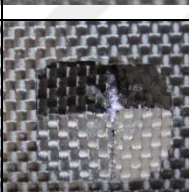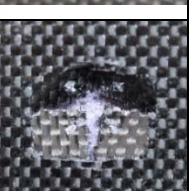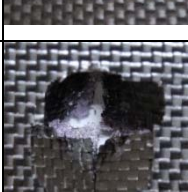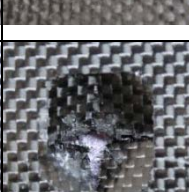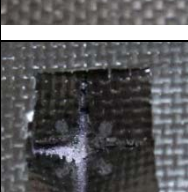
Impact Energy	Face Sheet	Neat Epoxy	Graphene	Boron Carbide	Kaolin
10 J	Top				
	Bottom				
17.50 J	Top				
	Bottom				
25 J	Top				
	Bottom				

Figure 4.27. Post-impact failure images and damage patterns of 5% filled sandwiches after testing

97

4.7. Effect of Filling Materials with Content of 10%

Figures 4.28 to 4.30 show the effect of different filling materials in the samples containing 10% additive on impact properties of the sandwich structures. Table 4.8 gives the percent change for the test results of the samples containing 10% filling additive materials compared to the samples with neat epoxy. The damage conditions of these samples after the drop weight impact test are also shown in Figure 4.31.

Similar to 2% and 5% filled configurations, no significant difference was observed in the samples containing 10% additive material performed at 10 J impact energy. This is because 10 J impact energy is not sufficient for penetration. At this energy level, the striker tip bounces back after hitting the upper face sheet of the sandwich structure for all configurations.

When the results at 17.50 J energy level were examined, there was no significant difference again, except boron carbide added configuration. The maximum impact forces of graphene and boron carbide filled configurations increased by 8.9% and 63.8% respectively. The maximum impact force of kaolin additive decreased by 0.7%. Hence, 10% boron carbide filled sandwiches showed the best results in this impact level. The amount of indentation depth of graphene, boron carbide and kaolin filled structures decreased by 4.3%, 16.9% and 6.2% respectively compared to the configurations with neat epoxy. The amount of energy absorptions of graphene, boron carbide and kaolin filled configurations were 12.28 J, 7.80 J and 12.69 J respectively whilst the configuration with neat epoxy was 13.80 J when 17.50 J impact energy is applied by the striker. As seen in Figure 4.31, the lower face sheets of neat epoxy, graphene and kaolin containing samples were significantly damaged but boron carbide containing samples were slightly damaged. No samples were completely punctured.

When the results at 25 J energy level were examined, the positive effects of boron carbide additives were observed. Although the neat epoxy, graphene and kaolin containing structures were completely punctured at this energy level, the

lower face sheets of the boron carbide containing structures were not punctured. This is seen in Figures 4.30(b) and 4.31. This is due to better fiber-matrix interface of boron carbide. On the other hand, graphene Nano-platelets caused poor dispersion in the epoxy matrix. This weakened the fiber-matrix interface, and caused the structure to be punctured under less energy. The maximum impact forces of graphene and boron carbide filled configurations increased by 7.4% and 44.6% respectively. The maximum impact force of kaolin additive decreased by 2.9%. So at 25 J impact energy level, 10% boron carbide filled sandwiches showed the best results.

Cost estimates of graphene, boron carbide and kaolin filled configurations shown that the cost was increased by 189.4%, 64.8% and 0.32% respectively. It can be concluded that the sandwich structure with boron carbide additive is better than graphene and kaolin sandwiches filled with 10% additives due to the better impact properties. Also, cost of boron carbide filled configuration is 43% lower than graphene filled configuration.

(a)

(b)
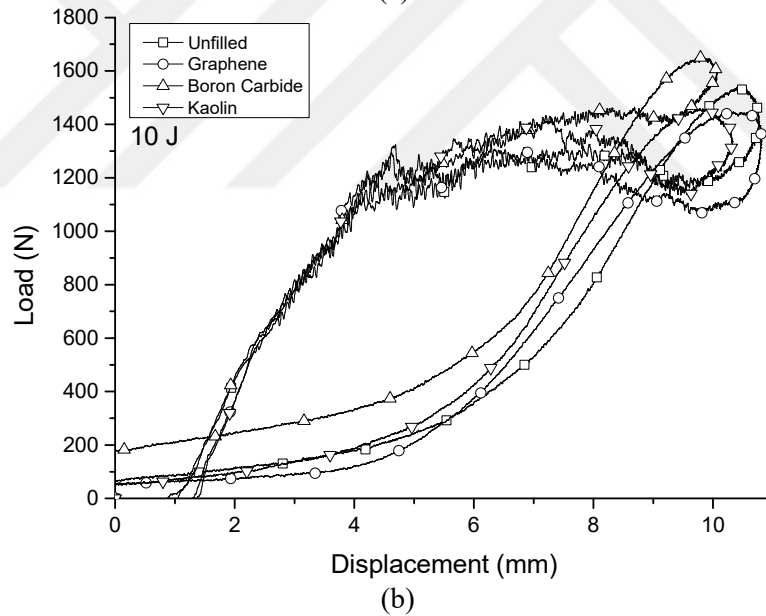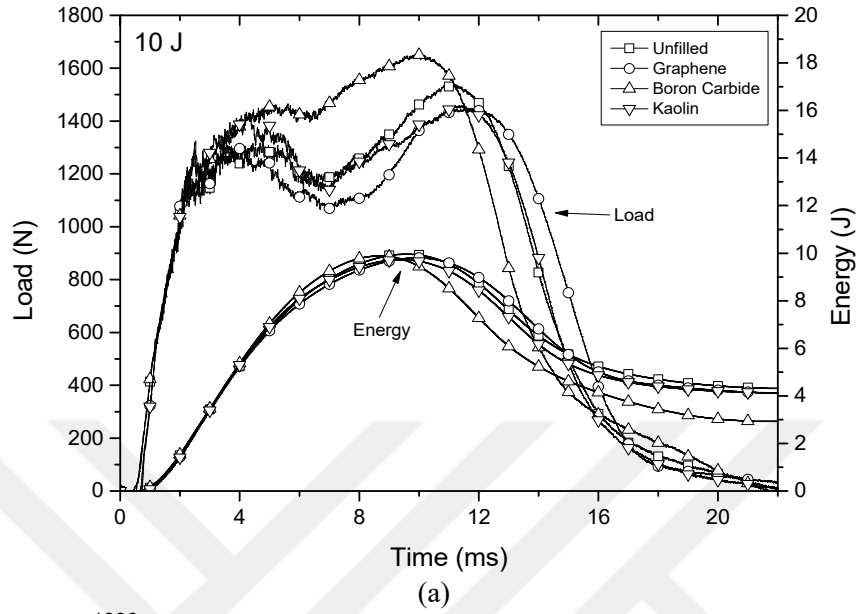
Figure 4.28. Impact test curves of 10% filled sandwiches at 10 J energy: (a) load versus time and energy versus time curves, (b) load versus displacement curves
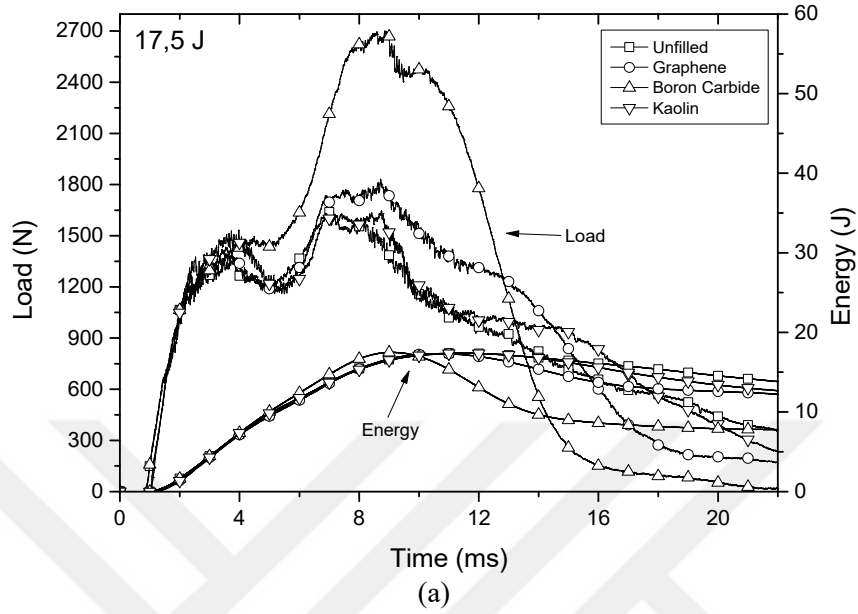
100

(a)

(b)
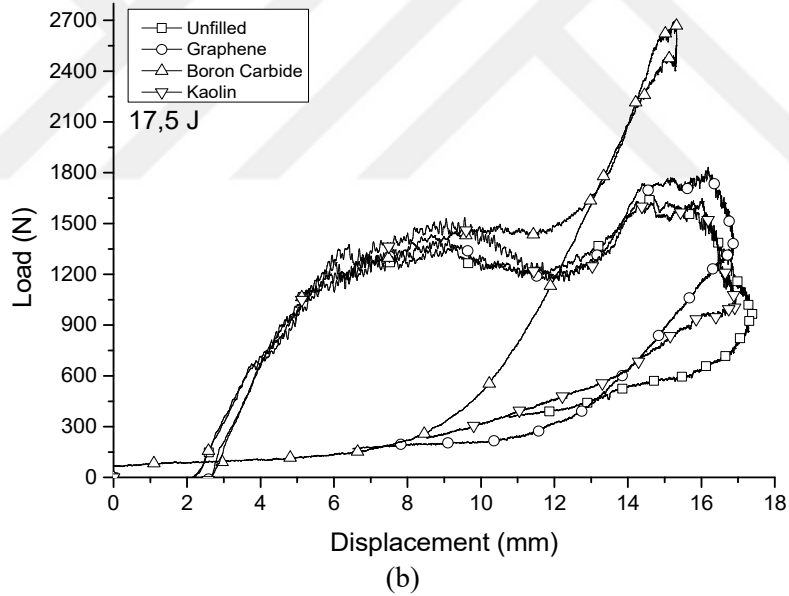
Figure 4.29. Impact test curves of 10% filled sandwiches at 17.50 J energy: (a) load versus time and energy versus time curves, (b) load versus displacement curves
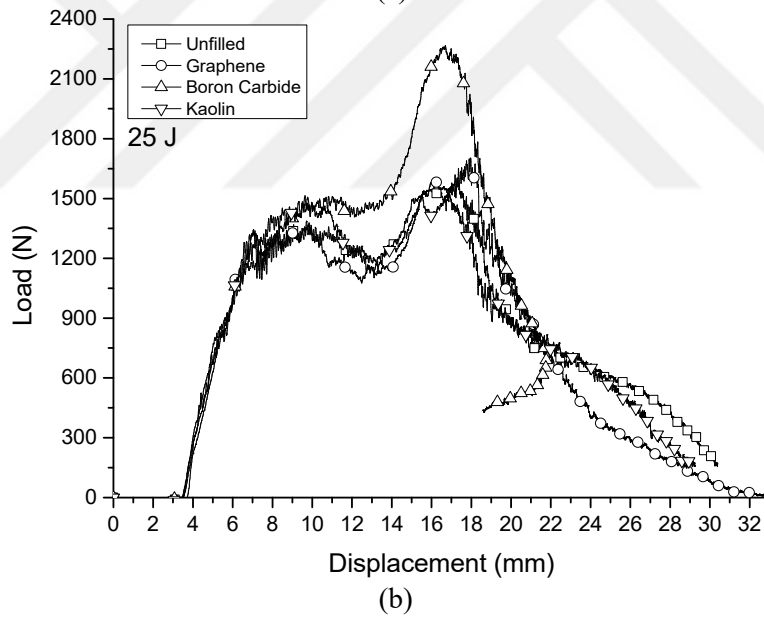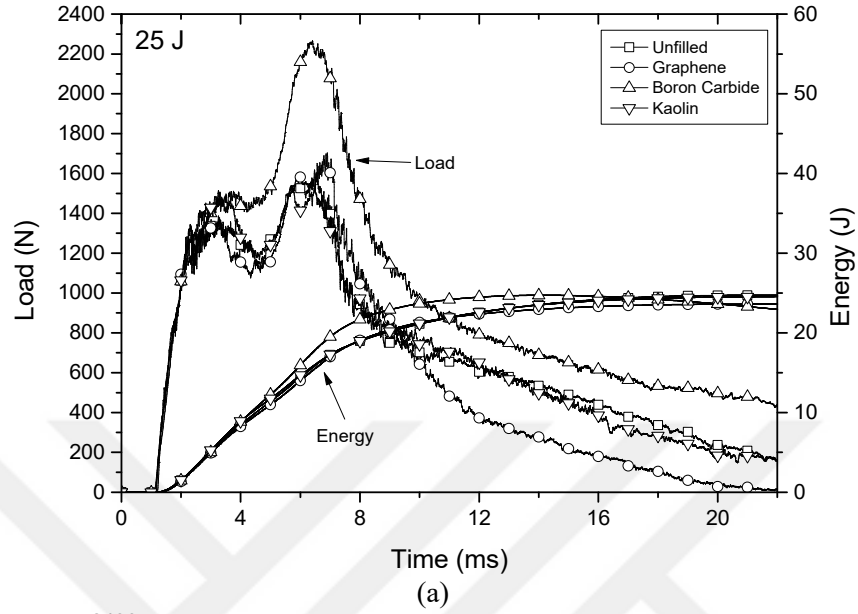
101

(a)

(b)

Figure 4.30.   Impact test curves of 10% filled sandwiches at 25 J energy: (a) load versus time and energy versus time curves, (b) load versus displacement curves

Table 4.8.   Comparison of 10% filled sandwiches and percent contribution of additive content to impact properties and cost of sandwiches

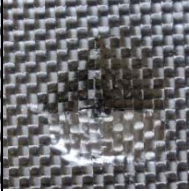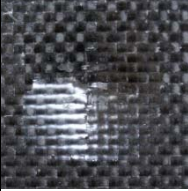| Property	Impact Energy	Neat Epoxy	Graphene	Boron Carbide	Kaolin
			(±percent contribution)		
F_1 (N) (First Peak)	10 J	1299.4	1308.5 (+0.7%)	1461.9 (+12.5%)	1405.6 (+8.2%)
	17.50 J	1350.7	1400.4 (+3.7%)	1476.4 (+9.3%)	1489.6 (+10.3%)
	25 J	1358.7	1363.8 (+0.4%)	1496.9 (+10.2%)	1501.9 (+10.5%)
F_2 (N) (Second Peak)	10 J	1533.9	1442.8 (-5.9%)	1653.5 (+7.8%)	1456 (-5.1%)
	17.50 J	1640.5	1786.8 (+8.9%)	2687.7 (+63.8%)	1629.1 (-0.7%)
	25 J	1552.6	1667.5 (+7.4%)	2245.7 (+44.6%)	1508.2 (-2.9%)
Absorbed Energy (J)	10 J	4.32	4.12 (-4.6%)	2.93 (-32.2%)	4.13 (-4.4%)
	17.50 J	13.8	12.28 (-11%)	7.8 (-43.5%)	12.69 (-8%)
	25 J	24.73	23.64 (-4.4%)	22.95 (-7.2%)	24.65 (-0.3%)
Indentation Depth (mm)	10 J	9.49	9.3 (-2%)	8.76 (-7.7%)	8.82 (-7.1%)
	17.50 J	14.93	14.29 (-4.3%)	12.41 (-16.9%)	14 (-6.2%)
	25 J	Punctured	Punctured	17.96	Punctured
Cost \$/m^2		185.809	537.823 (+189.4%)	306.235 (+64.8%)	186.413 (+0.32%)
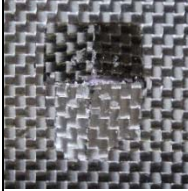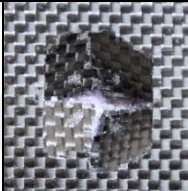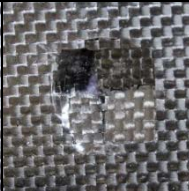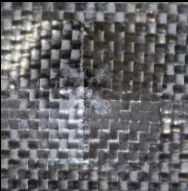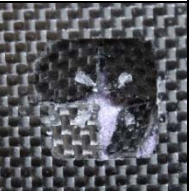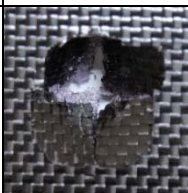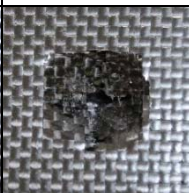
Impact Energy	Face Sheet	Neat Epoxy	Graphene	Boron Carbide	Kaolin
10 J	Top				
	Bottom				
17.50 J	Top				
	Bottom				
25 J	Top				
	Bottom				

Figure 4.31. Post-impact failure images and damage patterns of 10% filled sandwiches after testing

5. CONCLUSIONS

In this study, sandwich structures containing carbon fiber reinforced epoxy resin matrix face sheets and PVC foam core were produced. Graphene, boron carbide and kaolin additives in powder form were mixed into epoxy resin and they are used as matrix material in sandwich structures in three different ratios (2%, 5% and 10%) according to matrix weight. Sandwich structure production was also made with neat epoxy as a reference. The effect of these additives on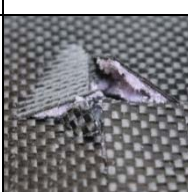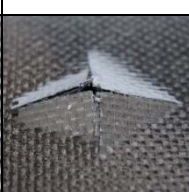 the impact properties of the sandwich structure was investigated by low velocity drop weight impact test. The experiments were carried out at three different energy levels (10 J, 17.5 J and 25 J). When the previous studies were explored it has not been encountered any related studies which investigated the effect of such additives on the results of low velocity drop weight impact of carbon fiber/epoxy facings, and polymer foam core sandwich structure yet. However, the effect of graphene and kaolin additives on the impact properties of the fiber reinforce laminated composites and polymer matrix materials have been studied.

The following conclusions were obtained from the results of the experiments. Experiments performed at 10 J impact energy level yielded similar results in all configurations due to insufficient penetration. 17.5 J and 25 J impact energy levels exhibited more significant differences. In areas that may be subject to higher impact energy levels, such as 17.5 J and 25 J, the use of additives will be beneficial.

When the configurations using graphene additive are examined, it is seen that the impact properties of the sandwich structure are improved especially in the mixing ratios of 2% and 5%. In the tests carried out at 25 J energy level, samples with neat epoxy and 10% graphene were completely punctured, but 2% and 5% graphene filled samples were not punctured. In the literature agglomerations due to poor dispersion were observed especially in high amount of graphene content in matrix (Kalaitzidou et al., 2007; Shen et al., 2012; Wang et al., 2016). Similarly, in

this study, experiments showed that the configuration with low amounts of graphene (2%) contributes higher reaction force than configurations with high amounts of graphene (5% and 10%) at the 25 J impact energy level. As a result of this, the finding matches to the findings of the literature.

Boron carbide additive has exhibited significant improvement on the impact properties of the sandwich structure. In the experiments, it was observed that although the sandwich structure made with neat epoxy was completely punctured, sandwich structures containing different amounts of boron carbide additive were not punctured at 25 J impact energy. The tests performed under 17.50 J impact energy showed an increase in reaction forces and a decrease both in absorbed energy and indentation depth depending on increasing amount of boron carbide.

According to the test results, kaolin additive does not have a significant effect on the impact properties of sandwich structures. In the literature, there are studies claiming that laminated composite structures with clay additive show better impact properties compared to composite structures made with neat epoxy (Fellahi et al., 2001; Bakar et al., 2012; Pekbey et al., 2017). Contrary to the literature, experiments made with kaolin additive, which is a clay variety, did not exhibited any significant effect of kaolin on the impact properties of sandwich structures in this study. This is because kaolin additive is added to the sandwich structure with thin carbon fiber/epoxy face sheets unlike the literature. It is thought that a thickness of 0.8 mm surface layer is so thin as a result of this the specimens fails. Due to very thin face sheets, the effect of kaolin has not been revealed. Using thicker face sheets may reveal the effect of kaolin additive as discussed in the literature.

When all the configurations are examined in terms of cost, graphene additive found to be the most expensive one. Boron carbide additive is medium and kaolin additive is a cheap option. It will be unnecessary to use additives in sandwich structures in areas that may be subject to low impact energy level such as

10 J. The best option for 10 J impact energy is sandwich structure with 10% boron carbide additive according to impact load results. But in this case there will be a 64.8% cost increase for only 7.8% impact load increase. For 17.50 J and 25 J impact energy, the best option is sandwich structure with 10% boron carbide additive according to impact load results similar to 10 J impact energy level. There was 63.8% and 44.6% impact load increase in 17.50 J and 25 J respectively. When the benefit-cost ratio was examined, it was observed that the boron carbide additive overcomes the other options.

Future Studies

One of the most important parameters for sandwich structures is bending stiffness. In future studies, changes in the bending stiffness of sandwich structures produced with matrix containing graphene, boron carbide and kaolin additive materials should be investigated by three or four point bending tests. In this way, the effect of filled matrix material on bending stiffness of sandwich structures can be found out.

It is known that fiber reinforced sandwich structures can be made with a wide variety of face sheets and core materials. The effect of additive particles in sandwich structures, which are made with commonly used face sheet reinforcing materials such as glass fiber and aramid fiber and core materials such as various foams and honeycombs, can be examined.

As seen in the results, 2% graphene containing configuration provides better impact resistance compared to 5% and 10% graphene containing configurations. However, graphene additive ratios between 0% and 2% were not included in this study. It is appropriate to test the graphene additive ratios below 2%. In addition, the effect of boron carbide addition on the mixing ratios above 10% should be investigated in the future.

REFERENCES

Adams, D., 2012. Impact Testing of Composite Materials. Retrieved 24.06.2019, from https://www.compositesworld.com/articles/impact-testing-of-composite-materials

Ahn, B. W., Kim, J. H., Hamad, K., and Jung, S. B., 2017. Microstructure and Mechanical Properties of a B 4 C Particle-Reinforced Cu Matrix Composite Fabricated by Friction Stir Welding. Journal of Alloys and Compounds, 693:688-691.

Altenbach, H., Altenbach, J., and Kissing, W., 2004. Mechanics of Composite Structural Elements. Springer, Germany, 468.

Argüelles, A., Viña, J., Canteli, A. F., and Lopez, A., 2011. Influence of the Matrix Type on the Mode I Fracture of Carbon-Epoxy Composites Under Dynamic Delamination. Experimental Mechanics, 51(3):293–301.

Barbero, E. J., 2017. Introduction to Composite Materials Design (third). CRC, Boca Raton, 535.

Boztepe, M. H., Bayramoglu, M., Uzay, C., Dagsuyu, C., Kokangul, A., and Geren, N., 2019. Characterization of boronized AISI 1050 steel and optimization of process parameters. Materialpruefung/Materials Testing, 61(6):549–553.

Bulut, M., 2017. Mechanical characterization of Basalt/epoxy composite laminates containing graphene nanopellets. Composites Part B: Engineering, 122:71–78.

Campo, E. A., 2008. Selection of Polymeric Materials : How to Select Design Properties from Different Standards. William Andrew, USA, 350.

CES Selector., 2018. Retrieved from http://www.grantadesign.com/products/ces/

Damanpack, A. R., Shakeri, M., and Aghdam, M. M., 2013. A New Finite Element Model for Low-Velocity Impact Analysis of Sandwich Beams Subjected to Multiple Projectiles. Composite Structures, 104:21–33.

Daniel, I. M., Gdoutos, E. E., Wang, K. A., and Abot, J. L., 2002. Failure Modes of Composite Sandwich Beams. International Journal of Damage Mechanics, 11(4):309–334.

Di Sante, R., 2015. Fibre Optic Sensors for Structural Health Monitoring of Aircraft Composite Structures: Recent Advances and Applications. Sensors, 15:18666–18713.

Dost Kimya., 2018. Retrieved 26.06.2019, from https://www.dostkimya.com/tr

Ege Nanotek Kimya., 2018. Retrieved 26.06.2019, from http://egenanotek.com/

Feli, S., Khodadadian, S., and Safari, M., 2016. A Modified New Analytical Model for Low-Velocity Impact Response of Circular Composite Sandwich Panels. Journal of Sandwich Structures and Materials, 18:552–578.

Fellahi, S., Chikhi, N., and Bakar, M., 2001. Modification of Epoxy Resin with Kaolin as a Toughening Agent. Journal of Applied Polymer Science, 82:861–878.

Ghasemnejad, H., Furquan, A. S. M., and Mason, P. J., 2010. Charpy Impact Damage Behaviour of Single and Multi-Delaminated Hybrid Composite Beam Structures. Materials and Design, 31:3653–3660.

Ha, S. K., Kim, S. J., Nasir, S. U., and Han, S. C., 2012. Design Optimization and Fabrication of a Hybrid Composite Flywheel Rotor. Composite Structures, 94:3290–3299.

Hogg, P. J., and Bibo, G. A., 2000. Impact and Damage Tolerance. (J. M. Hodgkinson Editor). Mechanical Testing of Advanced Fibre Composites. Woodhead Publishing Limited, England, pp. 211–247.

Hosur, M. V., Mohammed, A. A., Zainuddin, S., and Jeelani, S., 2008. Processing of Nanoclay Filled Sandwich Composites and Their Response to Low-Velocity Impact Loading. Composite Structures, 82:101–116.

Huang, Y., Zhang, W., Liang, L., Xu, J., and Chen, Z., 2013. A " Sandwich" Type of Neutron Shielding Composite Filled with Boron Carbide Reinforced by Carbon Fiber. Chemical Engineering Journal, 220:143–150.

Kalaitzidou, K., Fukushima, H., and Drzal, L. T., 2007. Mechanical Properties and Morphological Characterization of Exfoliated Graphite-Polypropylene Nanocomposites. Composites Part A: Applied Science and Manufacturing, 38:1675–1682.

Karlsson, K. F., and Åström, B. T., 1997. Manufacturing and Applications of Structural Sandwich Components. Composites Part A: Applied Science and Manufacturing, 28:97–111.

Kelly, A., 2000. Comprehensive Composite Materials.

Kordsa Inc. (2018). Retrieved June 26, 2019, from https://www.kordsa.com/tr

Lee, C., Wei, X., Kysar, J. W., & Hone, J. (2008). Measurement of the elastic properties and intrinsic strength of monolayer graphene. *Science*, *321*(5887), 385–388. https://doi.org/10.1126/science.1157996

Li, W., Sun, F., Wang, P., Fan, H., & Fang, D. (2016). A novel carbon fiber reinforced lattice truss sandwich cylinder: Fabrication and experiments. *Composites Part A: Applied Science and Manufacturing*, *81*, 313–322. https://doi.org/10.1016/j.compositesa.2015.11.034

Liu, C., Zhang, Y. X., & Li, J. (2017). Impact responses of sandwich panels with fibre metal laminate skins and aluminium foam core. *Composite Structures*, *182*, 183–190. https://doi.org/10.1016/j.compstruct.2017.09.015

Mallick, P. K. (2007). *Fiber-Reinforced Composites*. CRC Press. https://doi.org/10.1201/9781420005981

Matadi Boumbimba, R., Froustey, C., Viot, P., & Gerard, P. (2015). Low velocity impact response and damage of laminate composite glass fibre/epoxy based tri-block copolymer. *Composites Part B: Engineering*, *76*, 332–342. https://doi.org/10.1016/j.compositesb.2015.02.007

Navaranjan, N., & Neitzert, T. (2017). Impact Strength of Natural Fibre Composites Measured by Different Test Methods: A Review. *MATEC Web of Conferences*, *109*(01003). https://doi.org/10.1051/matecconf/201710901003

Origin. (2018). Retrieved from https://www.originlab.com/

Ouadday, R., Marouene, A., Morada, G., Kaabi, A., Boukhili, R., & Vadean, A. (2018, February). Experimental and numerical investigation on the impact behavior of dual-core composite sandwich panels designed for hydraulic turbine applications. *Composite Structures*. https://doi.org/10.1016/j.compstruct.2017.11.007

Park, J. H., Ha, S. K., Kang, K. W., Kim, C. W., & Kim, H. S. (2008). Impact damage resistance of sandwich structure subjected to low velocity impact. *Journal of Materials Processing Technology*, *201*(1–3), 425–430. https://doi.org/10.1016/j.jmatprotec.2007.11.196

Pekbey, Y., Aslantaş, K., & Yumak, N. (2017). Ballistic impact response of Kevlar Composites with filled epoxy matrix. *Steel and Composite Structures*, *24*(2), 191–200. https://doi.org/10.12989/scs.2017.24.2.191

Rallini, M., Natali, M., Kenny, J. M., & Torre, L. (2013). Effect of boron carbide nanoparticles on the fire reaction and fire resistance of carbon fiber/epoxy composites. *Polymer*, *54*(19), 5154–5165. https://doi.org/10.1016/j.polymer.2013.07.038

Razali, N., Sultan, M. T. H., Safri, S. N. A., Basri, S., Yidris, N., & Mustapha, F. (2014). High Velocity Impact Test on Glass Fibre Reinforced Polymer (GFRP) Using a Single Stage Gas Gun (SSGG) - An Experimental Based Approach. *Applied Mechanics and Materials*, *564*, 376–381. https://doi.org/10.4028/www.scientific.net/amm.564.376

Richardson, M. O. W., & Wisheart, M. J. (1996). Review of low-velocity impact properties of composite materials. *Composites Part A: Applied Science and Manufacturing*. https://doi.org/10.1016/1359-835X(96)00074-7

Safri, S. N. A., Sultan, M. T. H., Yidris, N., & Mustapha, F. (2014). Low velocity and high velocity impact test on composite materials – A review. *The International Journal of Engineering and Science (IJES)*, *3*(9), 50–60.

Saghafi, H., Fotouhi, M., & Minak, G. (2018). Improvement of the Impact Properties of Composite Laminates by Means of Nano-Modification of the Matrix—A Review. *Applied Sciences*, *8*(12), 2406. https://doi.org/10.3390/app8122406

Sevkat, E., Liaw, B., Delale, F., & Raju, B. B. (2009a). A combined experimental and numerical approach to study ballistic impact response of S2-glass fiber/toughened epoxy composite beams. *Composites Science and Technology*, *69*(7–8), 965–982. https://doi.org/10.1016/j.compscitech.2009.01.001

Sevkat, E., Liaw, B., Delale, F., & Raju, B. B. (2009b). Drop-weight impact of plain-woven hybrid glass-graphite/toughened epoxy composites. *Composites Part A: Applied Science and Manufacturing*, *40*(8), 1090–1110. https://doi.org/10.1016/j.compositesa.2009.04.028

Shen, X. J., Liu, Y., Xiao, H. M., Feng, Q. P., Yu, Z. Z., & Fu, S. Y. (2012). The reinforcing effect of graphene nanosheets on the cryogenic mechanical properties of epoxy resins. *Composites Science and Technology*, *72*(13), 1581–1587. https://doi.org/10.1016/j.compscitech.2012.06.021

Shirvanimoghaddam, K., Khayyam, H., Abdizadeh, H., Akbari, M. K., Pakseresht, A. H., Ghasali, E., & Naebe, M. (2016). Boron carbide reinforced aluminium matrix composite: Physical, mechanical characterization and mathematical modelling. https://doi.org/10.1016/j.msea.2016.01.114

Shokrieh, M. N., & Fakhar, M. N. (2012). EXPERIMENTAL, ANALYTICAL, AND NUMERICAL STUDIES OF COMPOSITE SANDWICH PANELS UNDER LOW-VELOCITY IMPACT LOADINGS M. M. Shokrieh * and M. N. Fakhar. *Mechanics of Materials*, *47*(6), 643–658. Retrieved from https://link.springer.com/content/pdf/10.1007%2Fs11029-011-9244-4.pdf

Swift, K. G., & Booker, J. D. (2013). Plastics and Composites Processing. In *Manufacturing Process Selection Handbook* (pp. 141–174). Elsevier. https://doi.org/10.1016/B978-0-08-099360-7.00005-7

Tuttle, M. E. (2004). *Structural Analysis of Polymeric Composite Materials*. Retrieved from http://books.google.com/books?hl=es&lr=&id=uvrMzybfbiAC&pgis=1

Udupi, S. R., & Rodrigues, L. L. R. (2016). Detecting Safety Zone Drill Process Parameters for Uncoated HSS Twist Drill in Machining GFRP Composites by Integrating Wear Rate and Wear Transition Mapping. *Indian Journal of Materials Science*, *2016*, 1–8. https://doi.org/10.1155/2016/9380583

Uzay, Ç., Acer, D. C., & Geren, N. (2018). Impact Strength of Interply and Intraply Hybrid Laminates Based on Carbon-Aramid / Epoxy Composites. *EUROPEAN MECHANICAL SCIENCE*, *3*(1), 1–5. https://doi.org/10.26701/ems.384440

Uzay, Ç., Boztepe, M. H., Bayramoğlu, M., & Geren, N. (2016). Effect of Post-Curing Heat Treatment on Mechanical Properties of Fiber Reinforced Polymer (FRP) Composites. *Materialpruefung/Materials Testing*, *59*, 366–372.

Uzay, C., Geren, N., Boztepe, M. H., & Bayramoglu, M. (2019). Bending behavior of sandwich structures with different fiber facing types and extremely low-density foam cores. *Materialpruefung/Materials Testing*, *61*(3), 220–230. https://doi.org/10.3139/120.111311

Vacmobiles. (2019). Retrieved June 2, 2019, from https://www.vacmobiles.com/resin_infusion.html

Vasiliev, V. V., & Morozov, E. V. (2007). *Advanced Mechanics of Composite Materials*. *Advanced Mechanics of Composite Materials* (Third). https://doi.org/10.1016/B978-0-08-045372-9.X5000-3

Villanueva, G. R., & Cantwell, W. J. (2004). The high velocity impact response of composite and FML-reinforced sandwich structures. *Composites Science and Technology*, *64*(1), 35–54. https://doi.org/10.1016/S0266-3538(03)00197-0

Wang, F., Drzal, L. T., Qin, Y., & Huang, Z. (2016). Size effect of graphene nanoplatelets on the morphology and mechanical behavior of glass fiber/epoxy composites. *Journal of Materials Science*, *51*(7), 3337–3348. https://doi.org/10.1007/s10853-015-9649-x

Wang, J., Waas, A. M., & Wang, H. (2013). Experimental and numerical study on the low-velocity impact behavior of foam-core sandwich panels. *Composite Structures*, *96*, 298–311. https://doi.org/10.1016/j.compstruct.2012.09.002

Xinyu, F., Yubin, L., Juan, L., Chun, Y., & Ke, L. (2009). Modeling of Heat Conduction in Thermoplastic Honeycomb Core/Face Sheet Fusion Bonding. *Chinese Journal of Aeronautics*, *22*(6), 685–690. https://doi.org/10.1016/S1000-9361(08)60159-4

Yang, B., Wang, Z., Zhou, L., Zhang, J., Tong, L., & Liang, W. (2015). Study on the low-velocity impact response and CAI behavior of foam-filled sandwich panels with hybrid facesheet. *Composite Structures*, *132*, 1129–1140. https://doi.org/10.1016/j.compstruct.2015.07.058

Yashiro, S., Ogi, K., Nakamura, T., & Yoshimura, A. (2013). Characterization of high-velocity impact damage in CFRP laminates: Part i - Experiment. *Composites Part A: Applied Science and Manufacturing*, *48*(1), 93–100. https://doi.org/10.1016/j.compositesa.2012.12.015

Zaman, I., Phan, T. T., Kuan, H. C., Meng, Q., Bao La, L. T., Luong, L., … Ma, J. (2011). Epoxy/graphene platelets nanocomposites with two levels of interface strength. *Polymer*, *52*(7), 1603–1611. https://doi.org/10.1016/j.polymer.2011.02.003

Zhang, G., Wang, B., Ma, L., Wu, L., Pan, S., & Yang, J. (2014). Energy absorption and low velocity impact response of polyurethane foam filled pyramidal lattice core sandwich panels. *Composite Structures*, *108*(1), 304–310. https://doi.org/10.1016/j.compstruct.2013.09.040

Zhang, P., Ma, L., Fan, F., Zeng, Z., Peng, C., Loya, P. E., … Lou, J. (2014). Fracture toughness of graphene. *Nature Communications*, *5*, 1–7. https://doi.org/10.1038/ncomms4782

CURRICCULUM VIATE

Durmuş Can ACER was born in Adana on 04.02.1992. He graduated from 75th Year Anatolian High School (Yüreğir/Adana) in 2010. After graduation from high school, he continued his education in Çukurova University and graduated as Automotive Engineer in 2016.

He began his M.Sc. education at the Mechanical Engineering Department of Çukurova University in 2016. In 2017, he started to work as Research Assistant in the Mechanical Engineering Department of Çukurova University (Adana). He is still working in Mechanical Engineering Department of Çukurova University in the position of Research Assistant.

APPENDIX

1. The Results of Sandwich Structures with Neat Epoxy

(a)

(b)
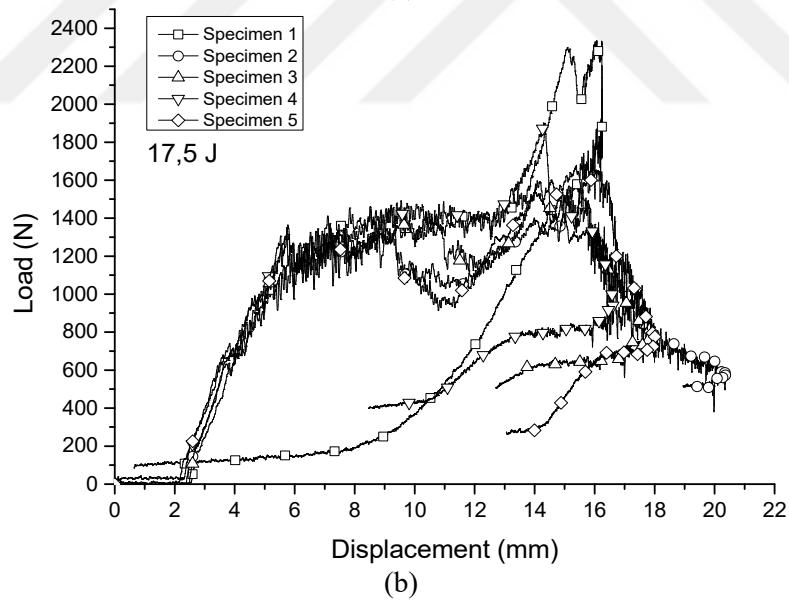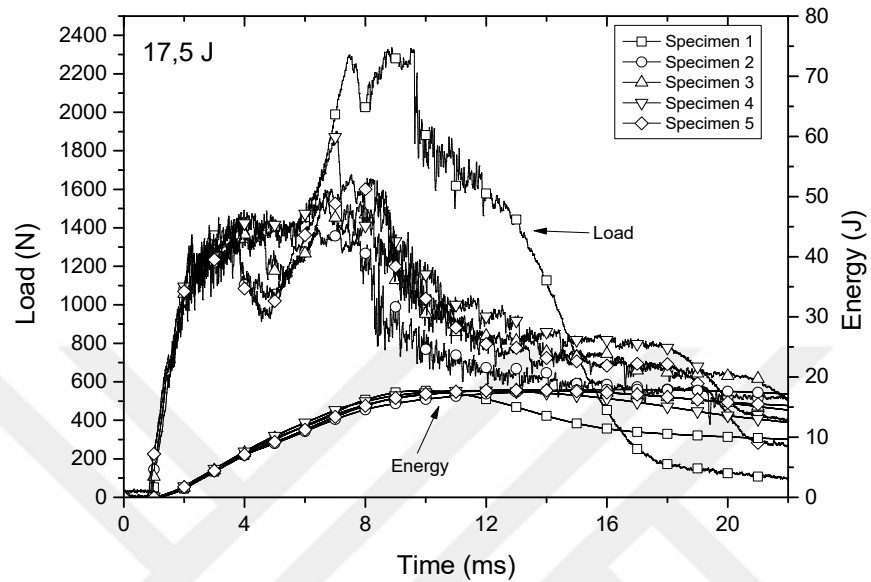
Figure 1. Impact test curves of sandwiches with neat epoxy at 17.5 J energy level: (a) load versus time and energy versus time, (b) load versus displacement
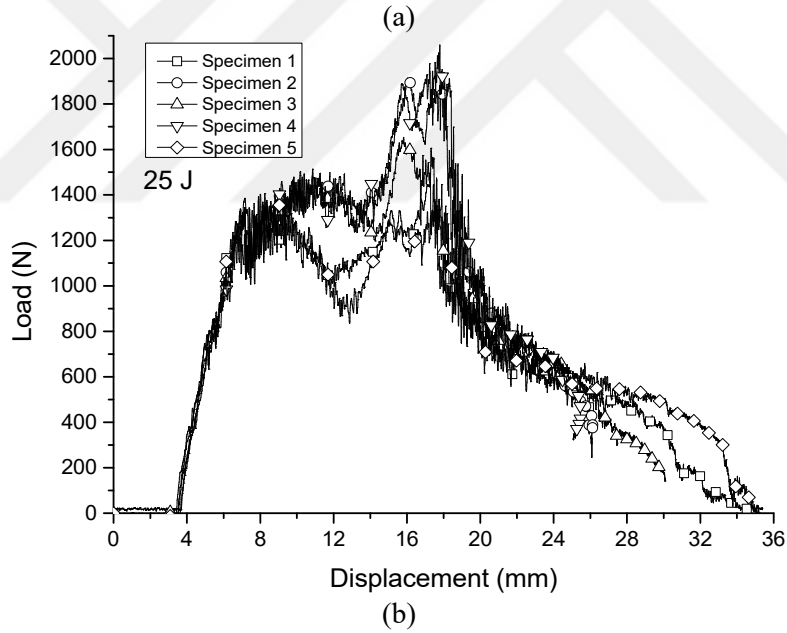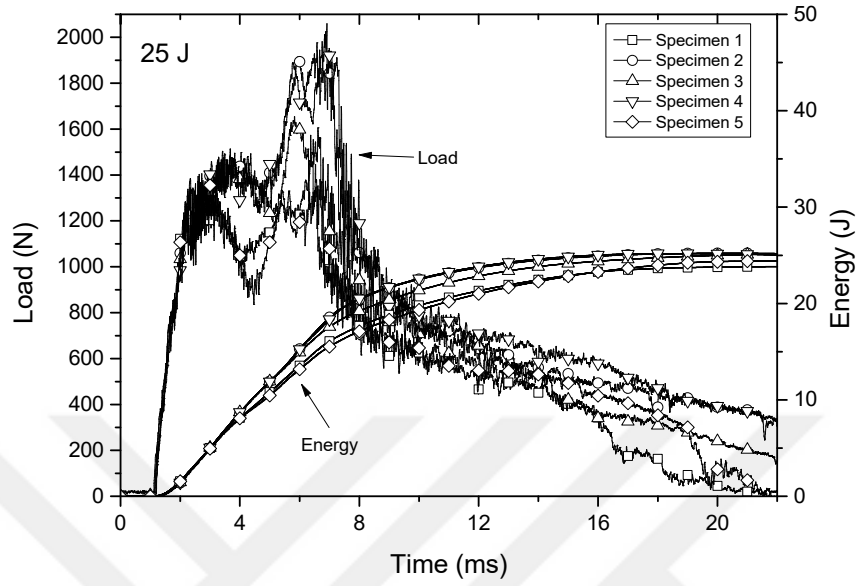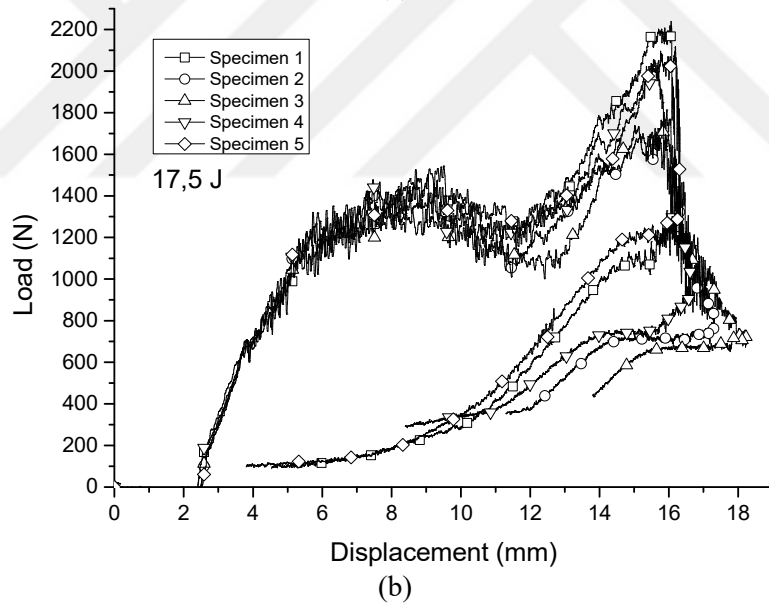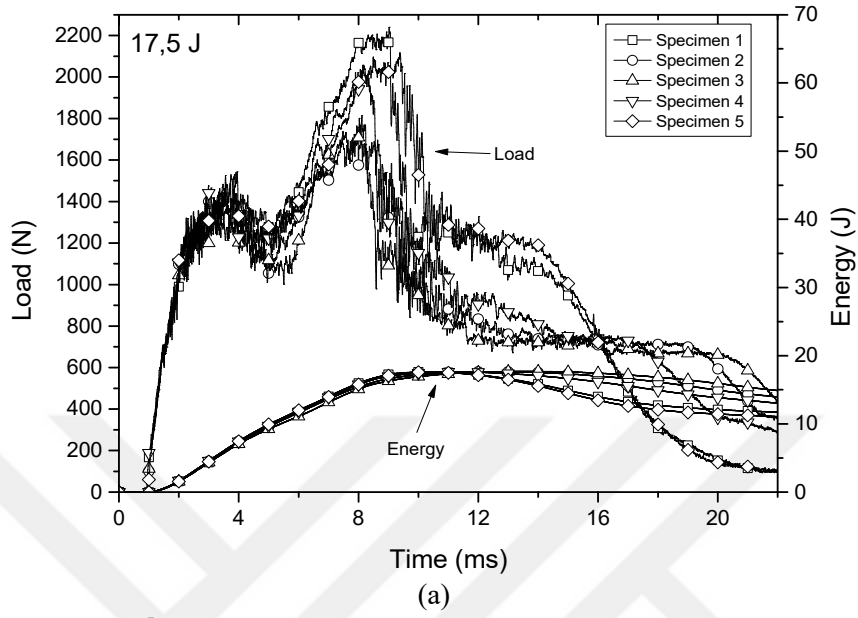
Figure 2. Impact test curves of sandwiches with neat epoxy at 25 J energy level: (a) load versus time and energy versus time, (b) load versus displacement

121

2. Effect of Graphene Nanoplatelets

(a)

(b)
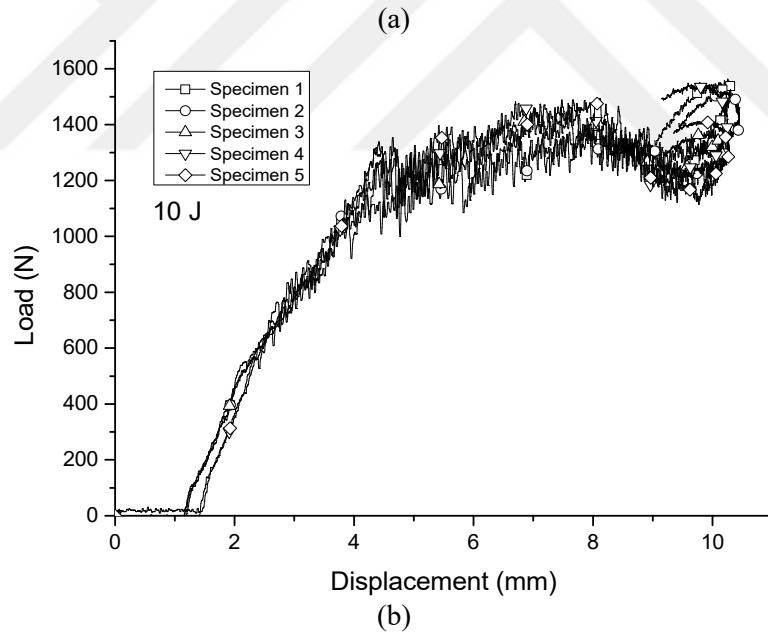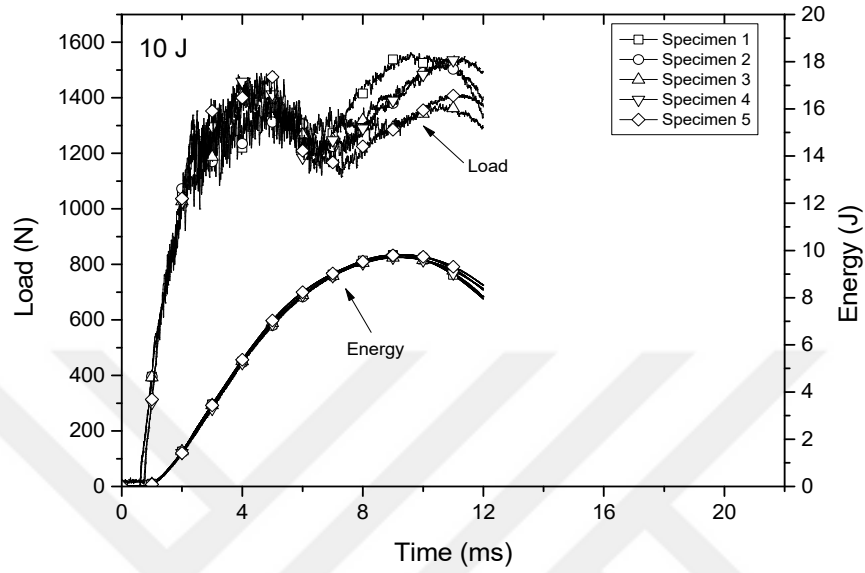
Figure 3. Impact test curves of 2% graphene filled sandwich at 10 J energy level:
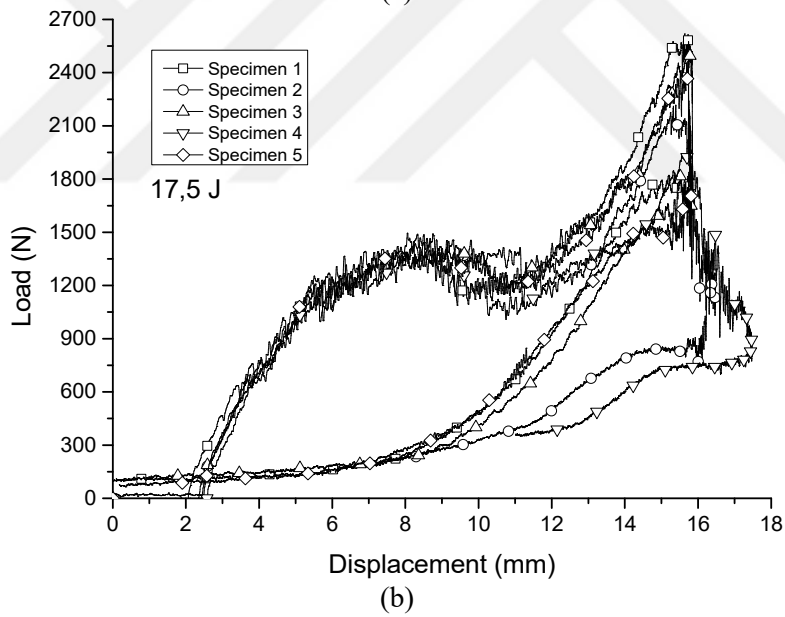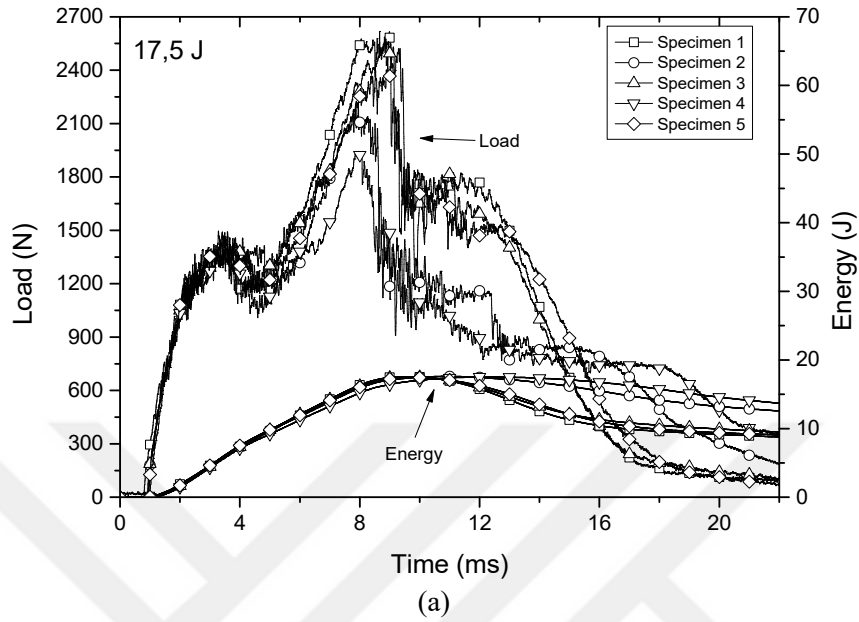(a) load versus time and energy versus time, (b) load versus displacement
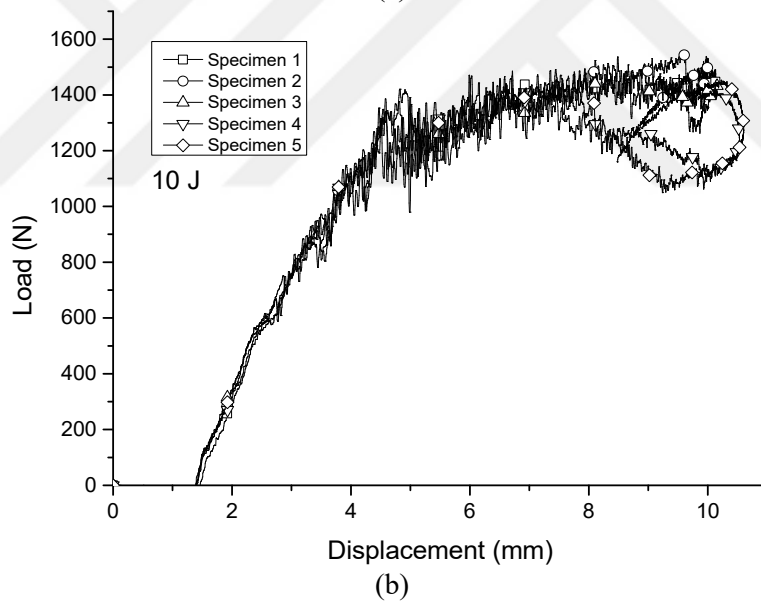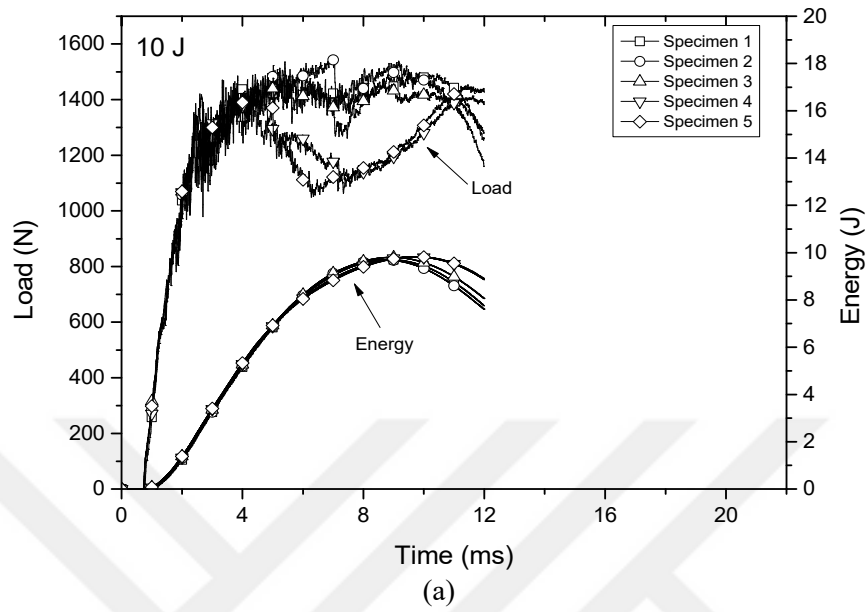
Figure 4.   Impact test curves of 5% graphene filled sandwich at 10 J energy level: (a) load versus time and energy versus time, (b) load versus displacement
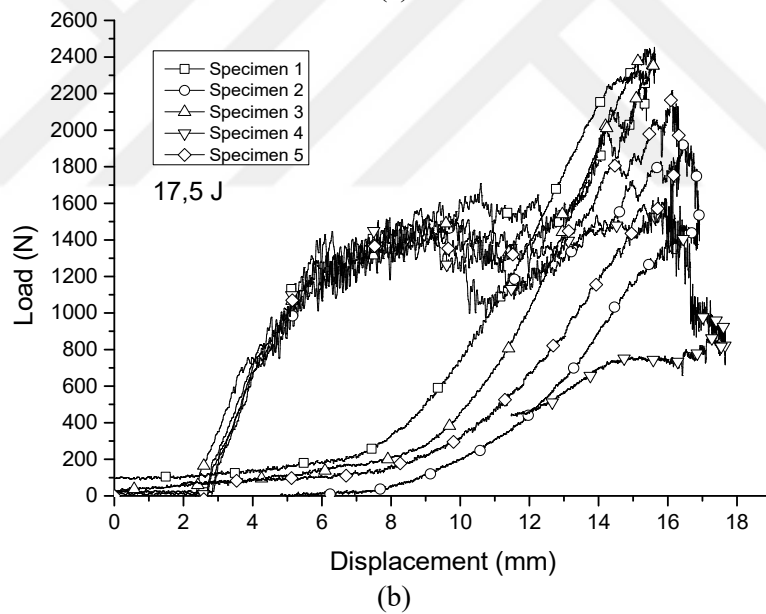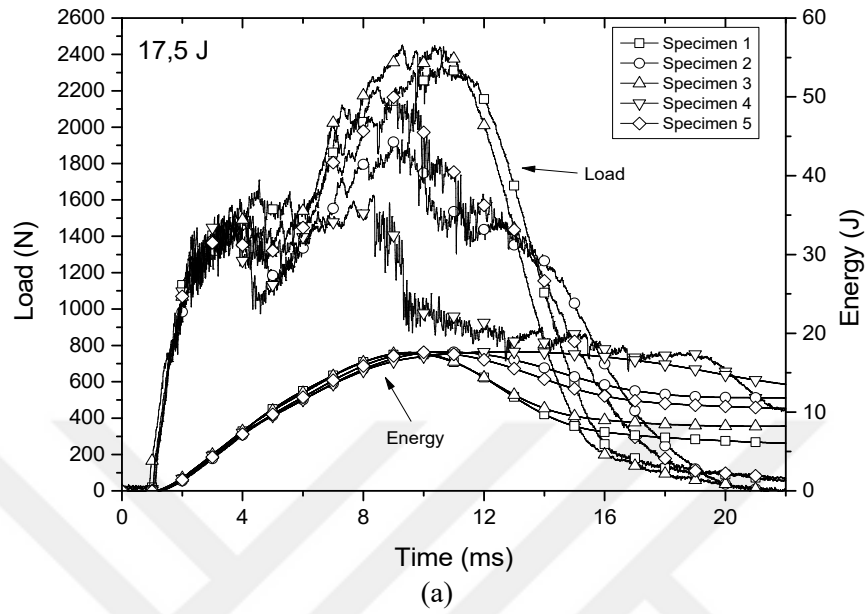
Figure 5. Impact test curves of 2% graphene filled sandwich at 17.5 J energy level: (a) load versus time and energy versus time, (b) load versus displacement
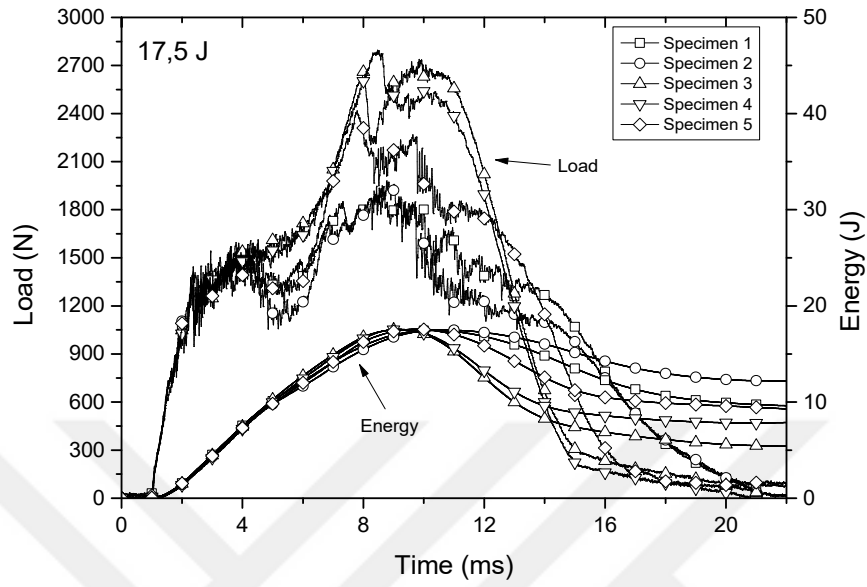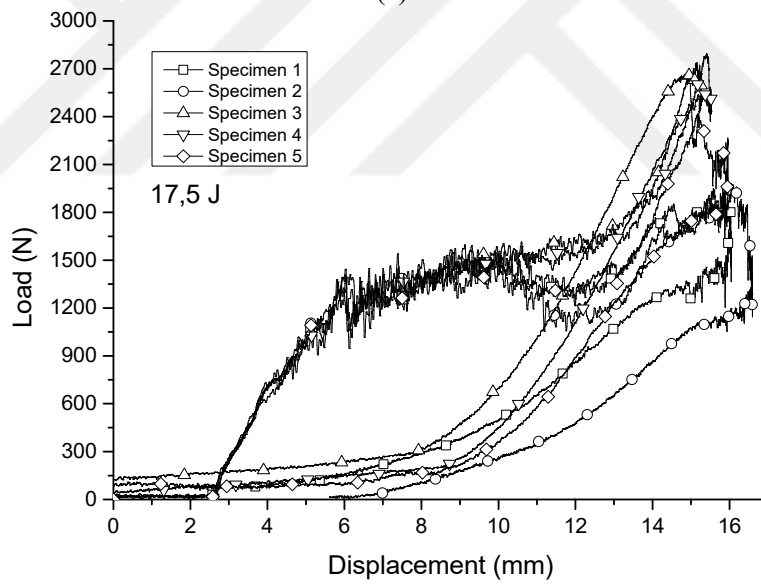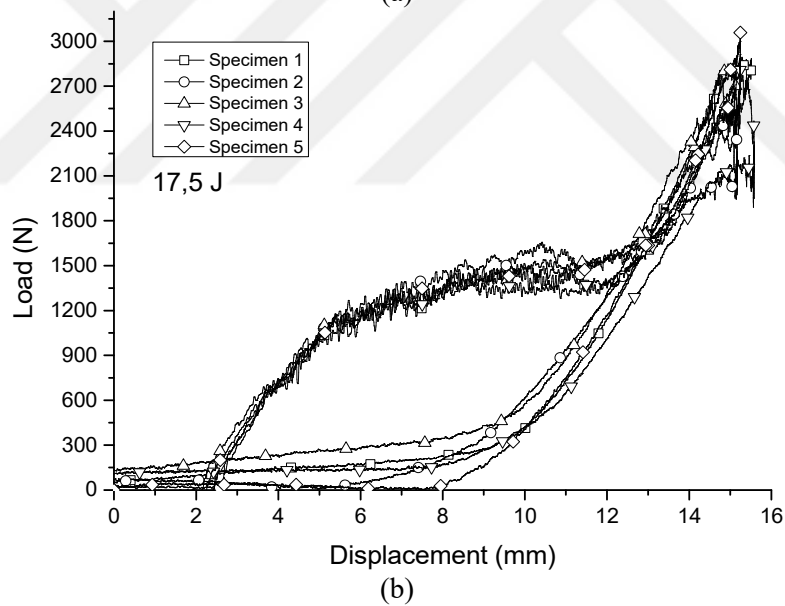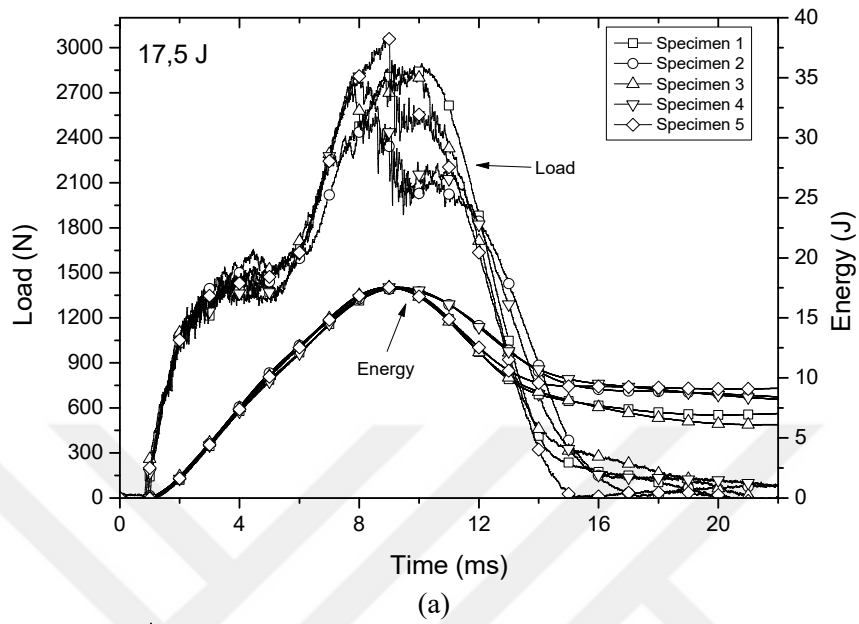
Figure 6. Impact test curves of 5% graphene filled sandwich at 17.5 J energy level:
(a) load versus time and energy versus time, (b) load versus displacement

125
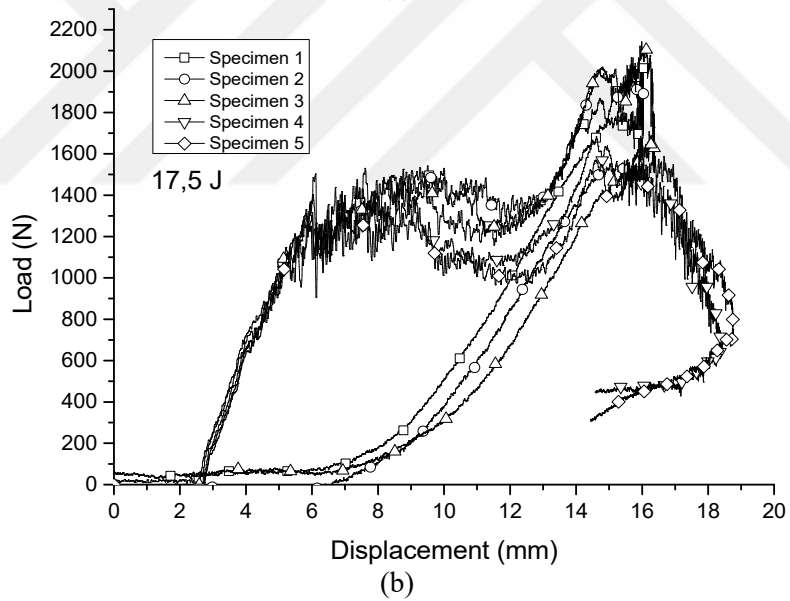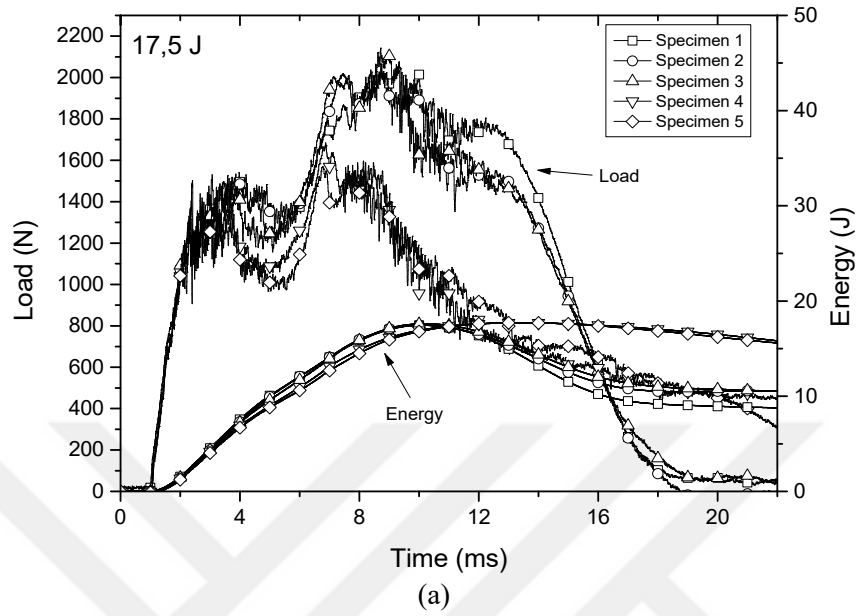
Figure 7.   Impact test curves of 10% graphene filled sandwich at 17.5 J energy
            level: (a) load versus time and energy versus time, (b) load versus
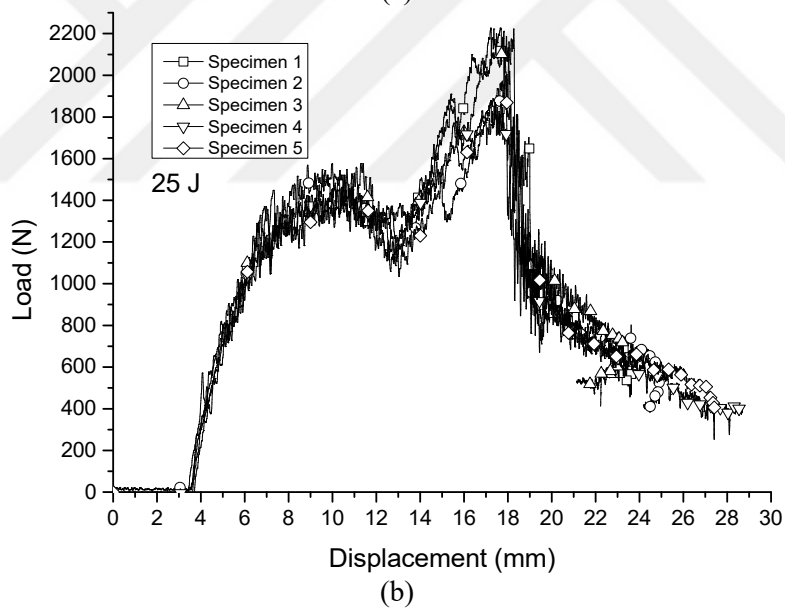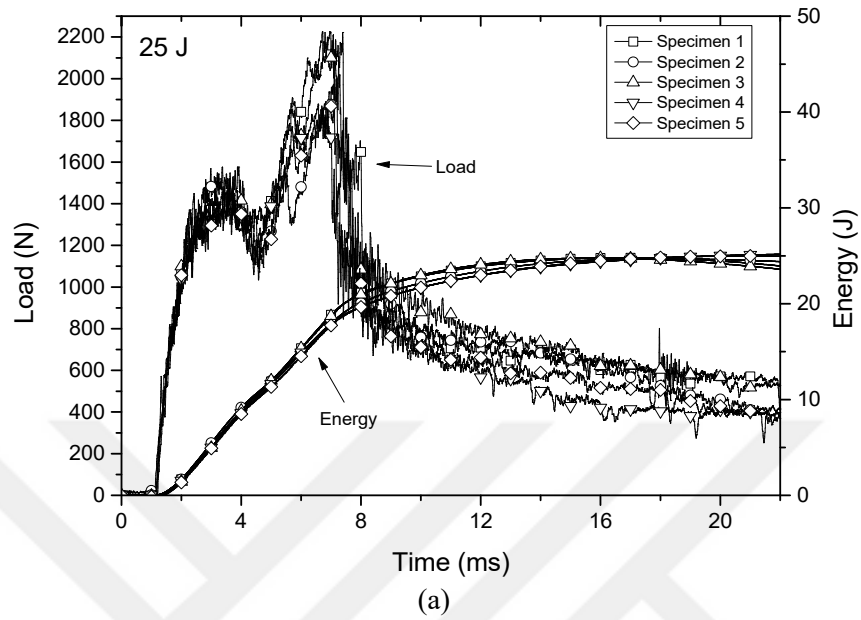   displacement
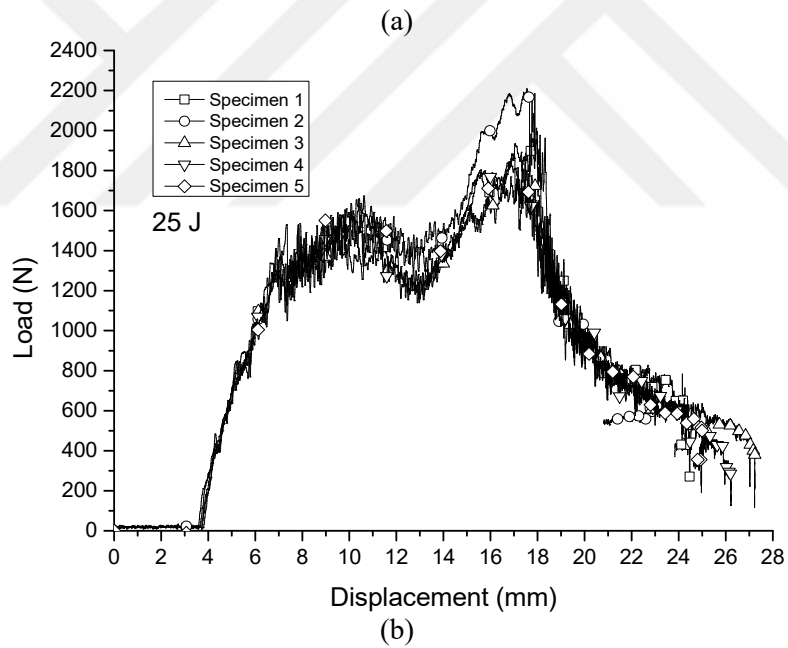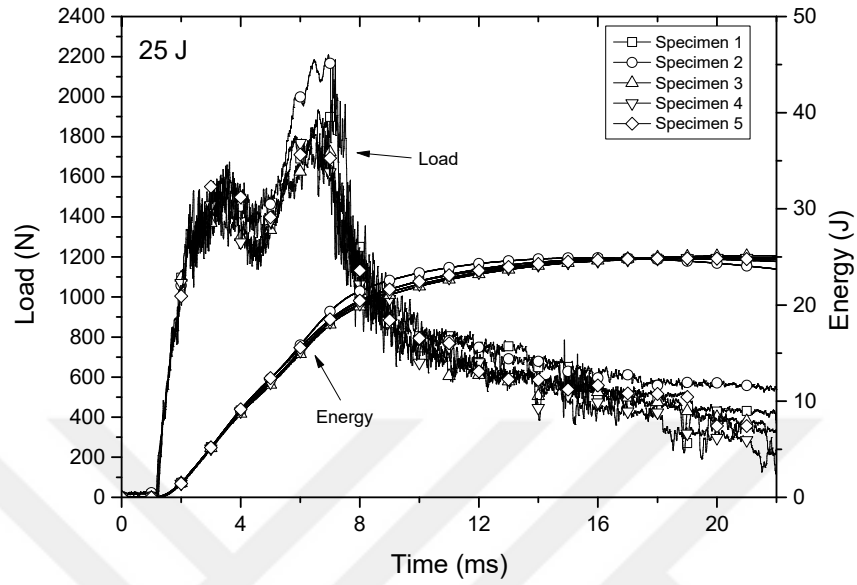
Figure 8. Impact test curves of 2% graphene filled sandwich at 25 J energy level:
(a) load versus time and energy versus time, (b) load versus displacement

127
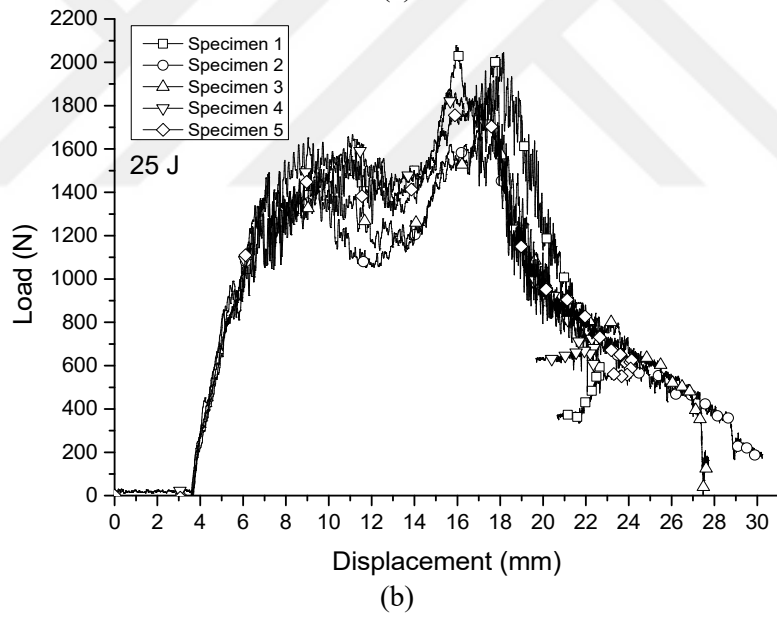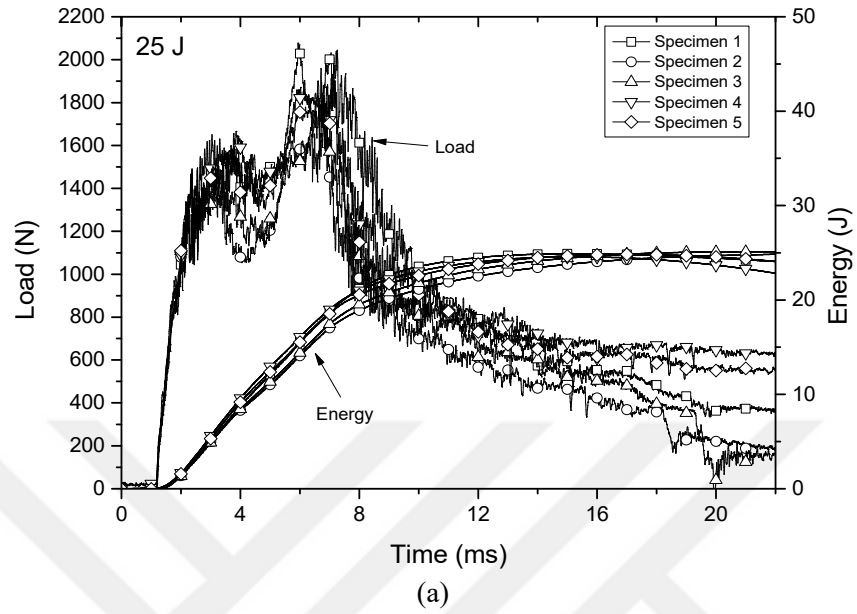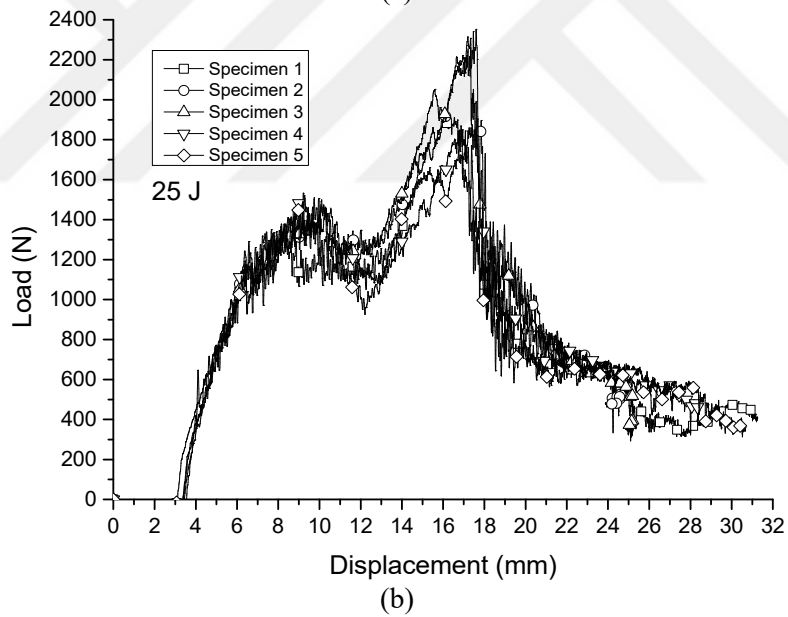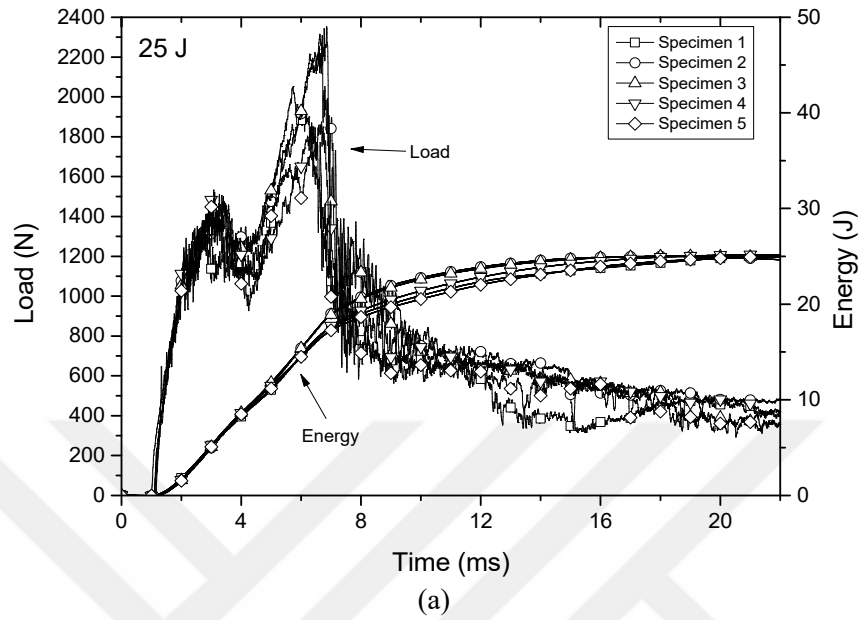
Figure 9. Impact test curves of 5% graphene filled sandwich at 25 J energy level: (a) load versus time and energy versus time, (b) load versus displacement
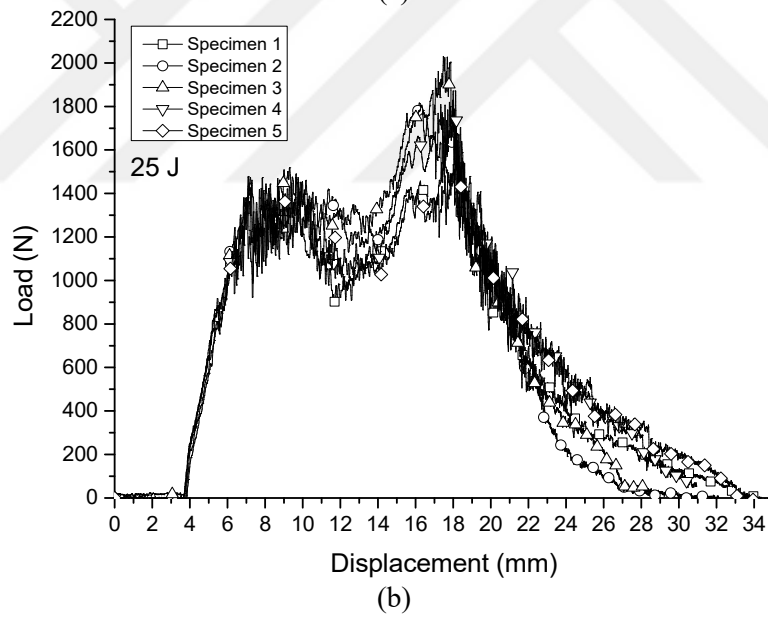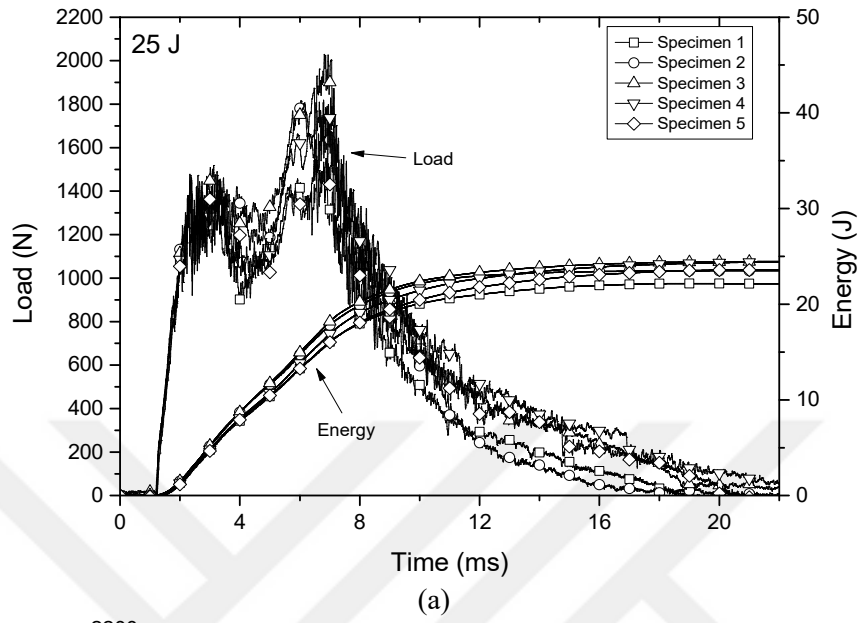
Figure 10. Impact test curves of 10% graphene filled sandwich at 25 J energy level: (a) load versus time and energy versus time, (b) load versus displacement

129

3. Effect of Boron Carbide Particles

(a)

(b)
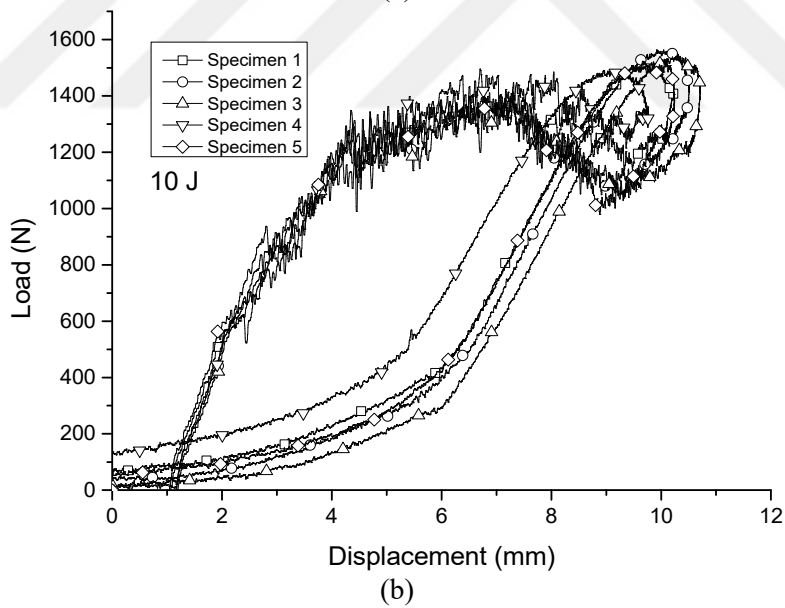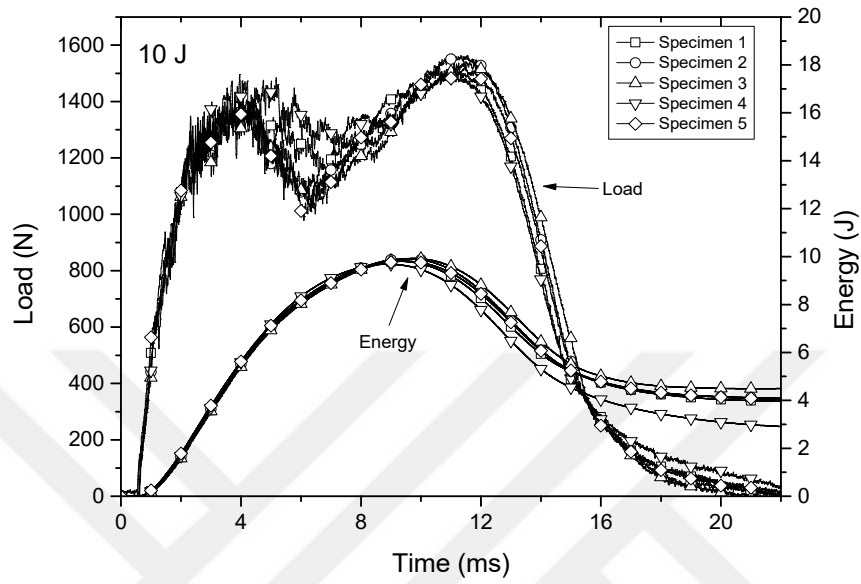
Figure 11. Impact test curves of 2% boron carbide filled sandwich at 10 J energy level: (a) load versus time and energy versus time, (b) load versus displacement
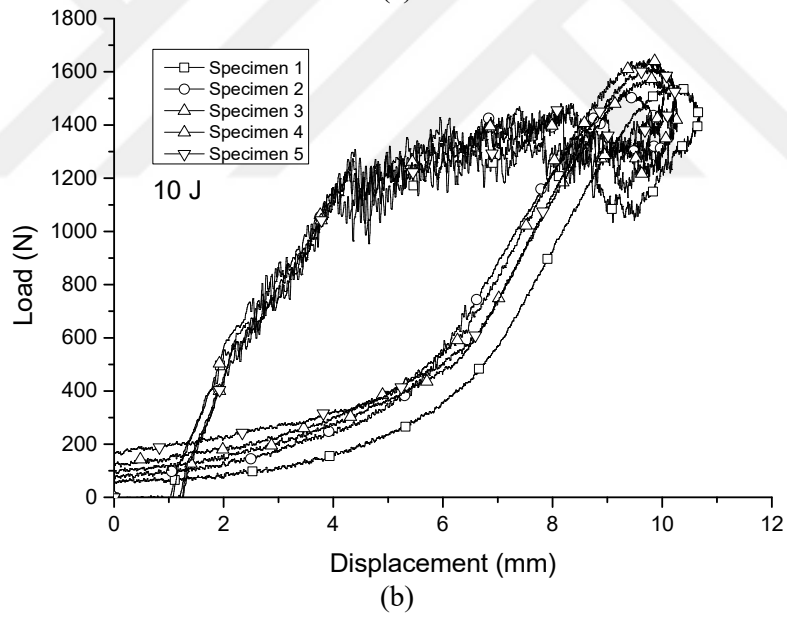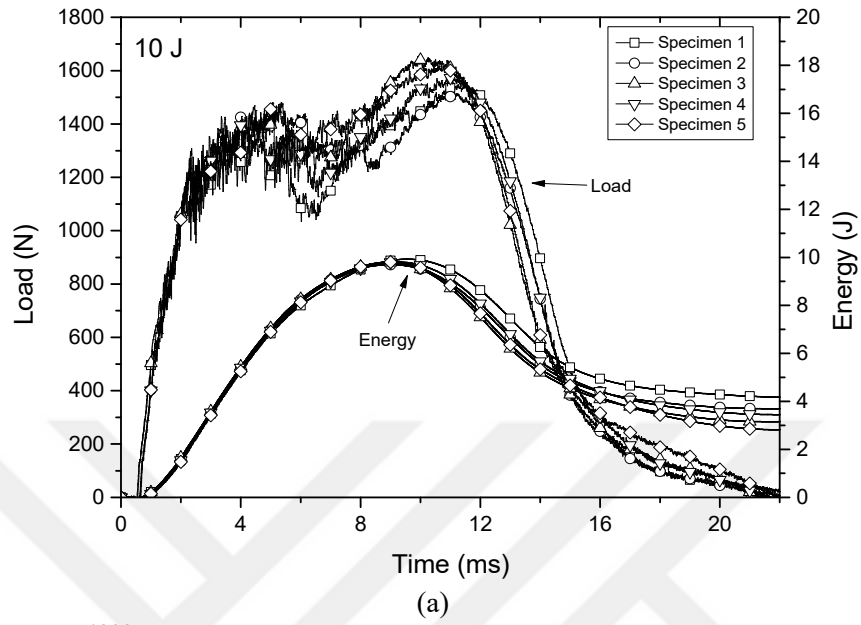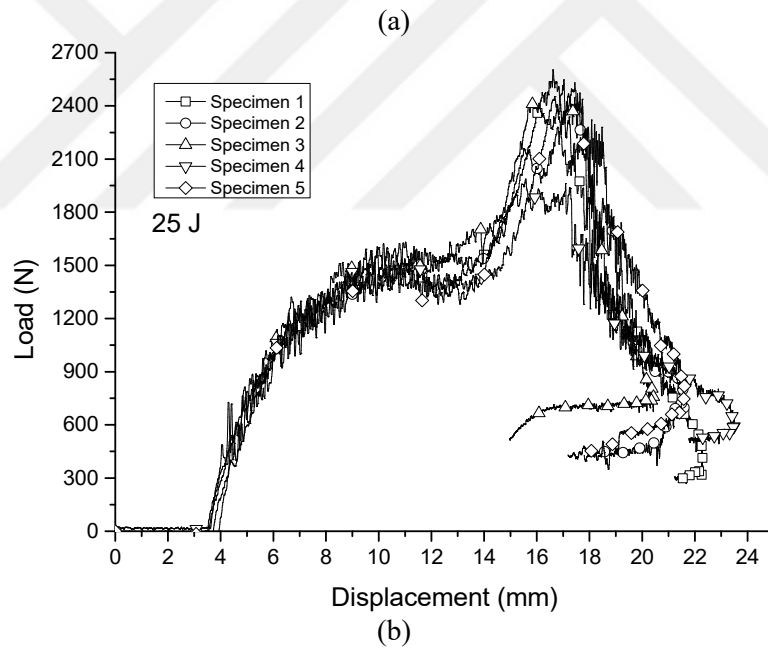
Figure 12. Impact test curves of 5% boron carbide filled sandwich at 10 J energy level: (a) load versus time and energy versus time, (b) load versus displacement
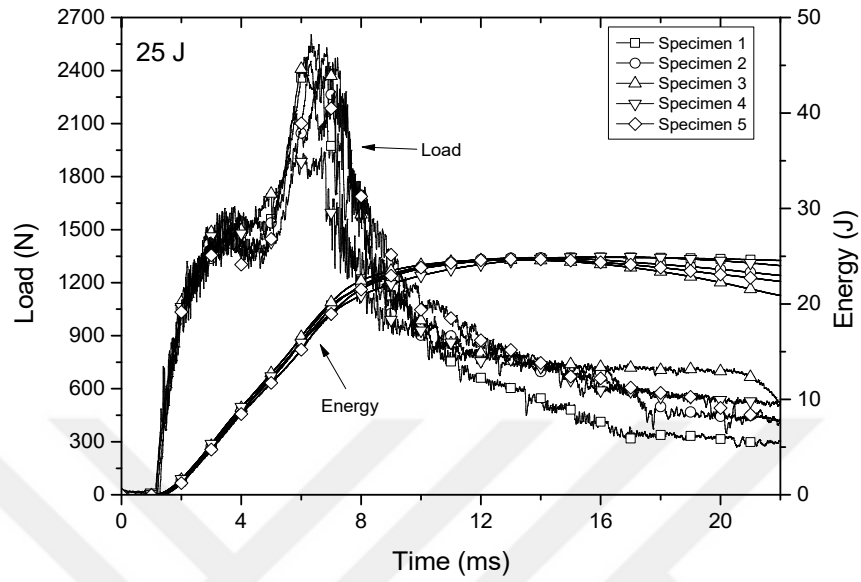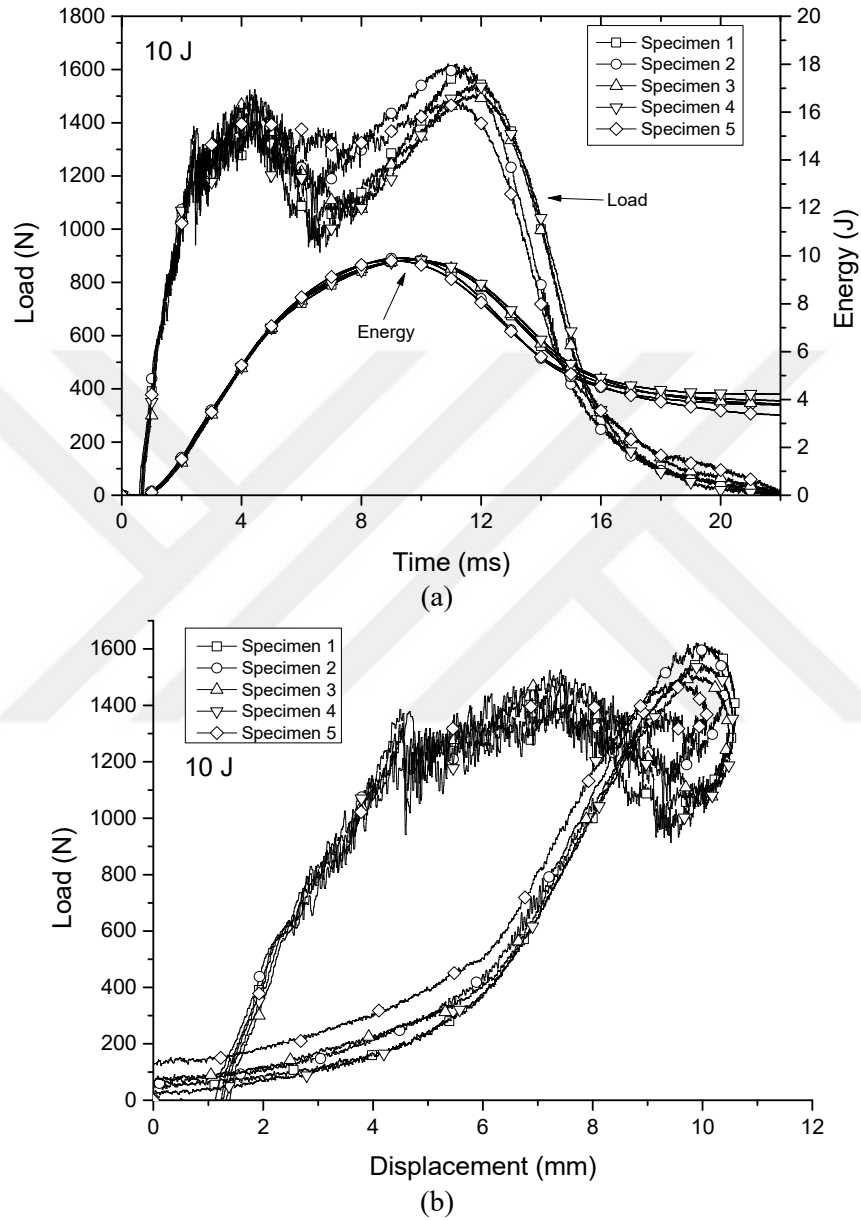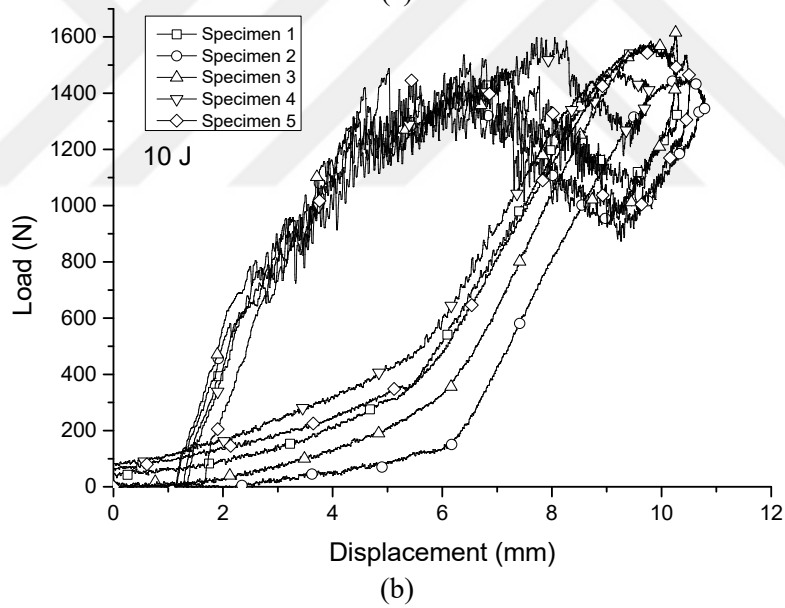
Figure 13. Impact test curves of 2% boron carbide filled sandwich at 17.5 J energy
level: (a) load versus time and energy versus time, (b) load versus
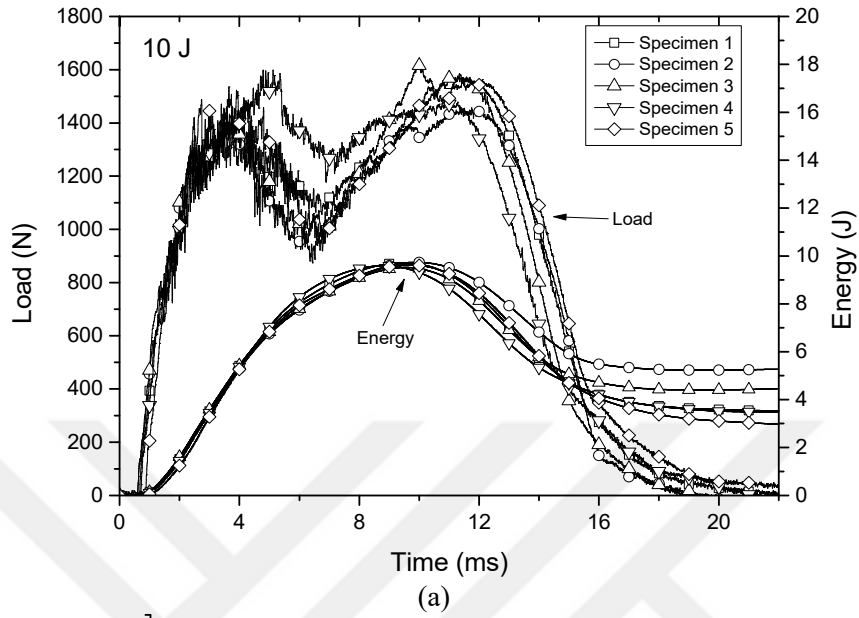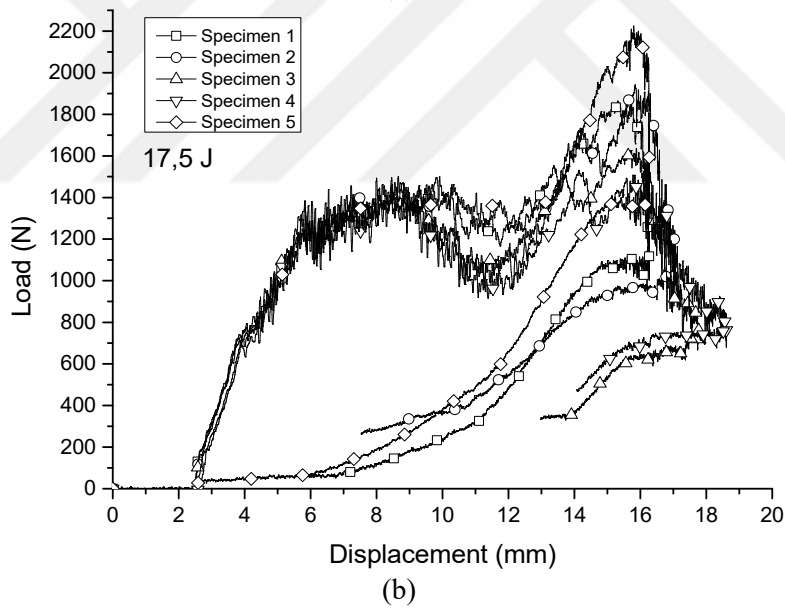displacement

Figure 14. Impact test curves of 5% boron carbide filled sandwich at 17.5 J energy level: (a) load versus time and energy versus time, (b) load versus displacement

Figure 15. Impact test curves of 10% boron carbide filled sandwich at 17.5 J energy level: (a) load versus time and energy versus time, (b) load versus displacement
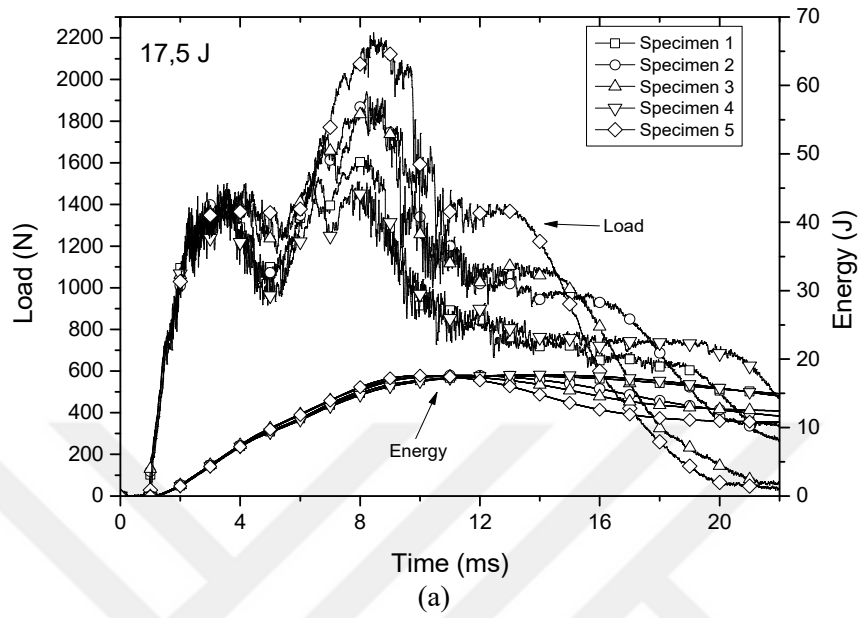
Figure 16. Impact test curves of 2% boron carbide filled sandwich at 25 J energy level: (a) load versus time and energy versus time, (b) load versus displacement

135

Figure 17. Impact test curves of 5% boron carbide filled sandwich at 25 J energy level: (a) load versus time and energy versus time, (b) load versus displacement
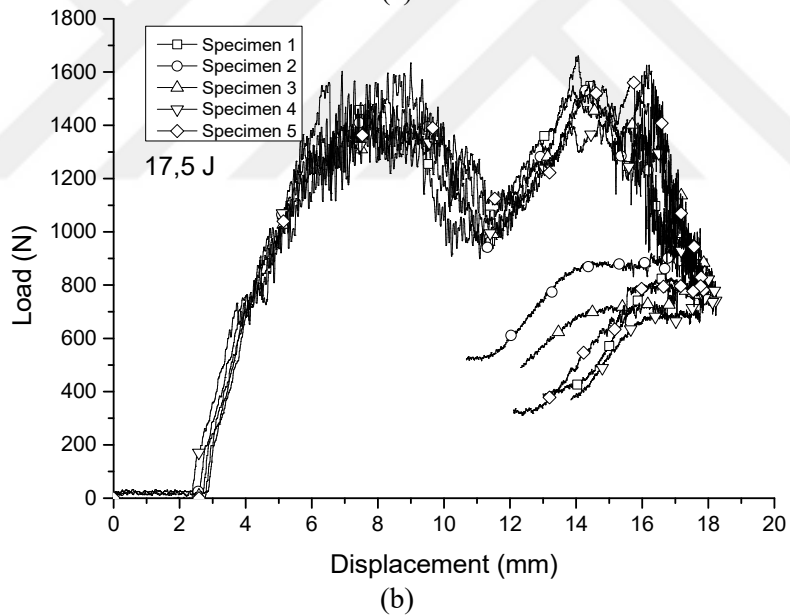
Figure 18. Impact test curves of 10% boron carbide filled sandwich at 25 J energy level: (a) load versus time and energy versus time, (b) load versus displacement

4. Effect of Kaolin Particles

Figure 19. Impact test curves of 2% kaolin filled sandwich at 10 J energy level: (a)
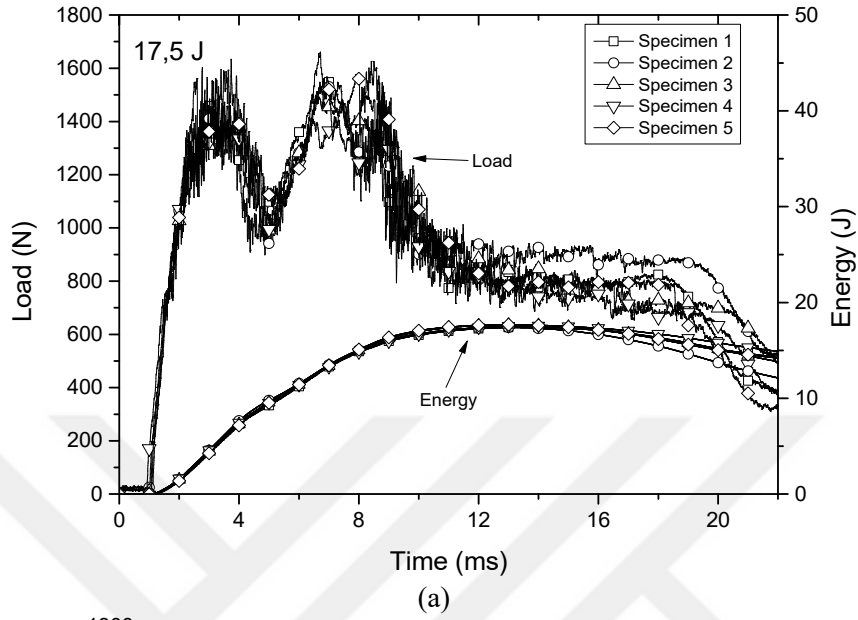load versus time and energy versus time, (b) load versus displacement

Figure 20. Impact test curves of 5% kaolin filled sandwich at 10 J energy level: (a) load versus time and energy versus time, (b) load versus displacement
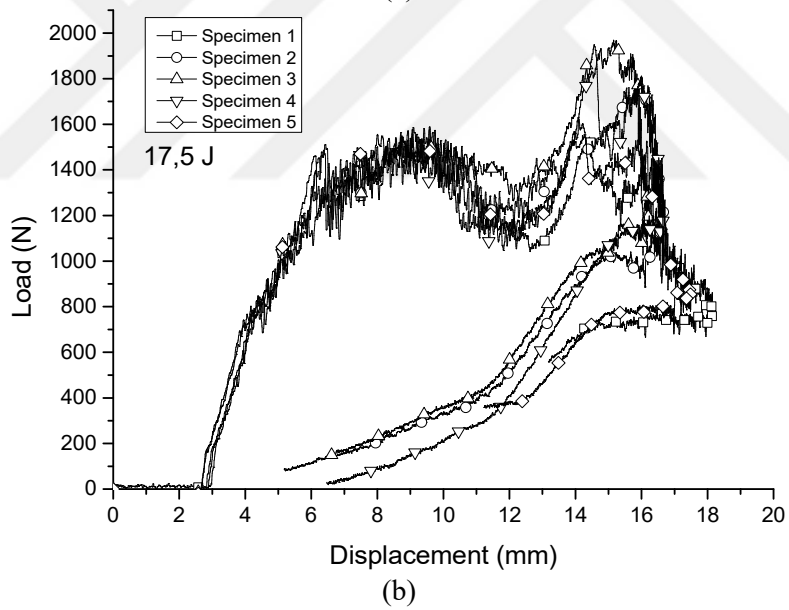
(a)

(b)

Figure 21. Impact test curves of 2% kaolin filled sandwich at 17.5 J energy level: (a) load versus time and energy versus time, (b) load versus displacement
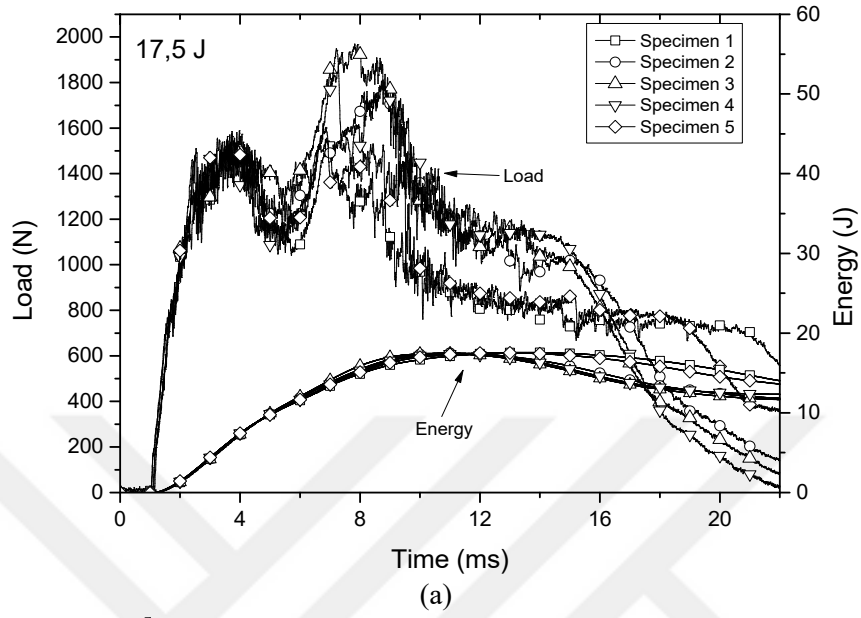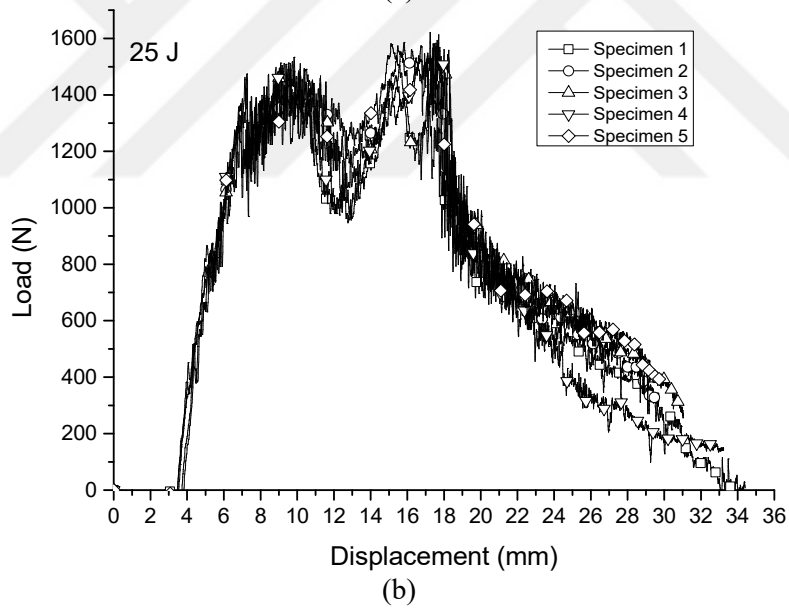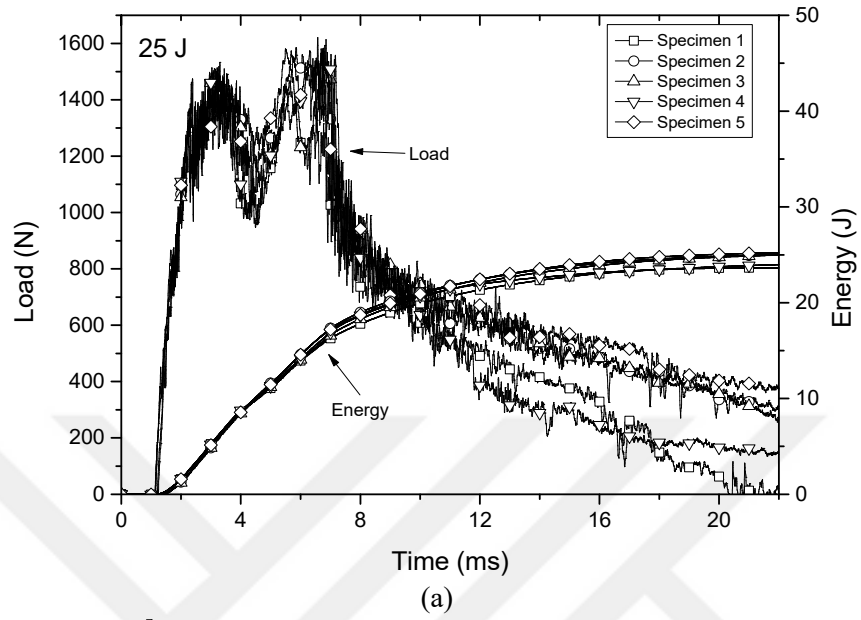
Figure 22. Impact test curves of 5% kaolin filled sandwich at 17.5 J energy level: (a) load versus time and energy versus time, (b) load versus displacement

(a)

(b)

Figure 23. Impact test curves of 10% kaolin filled sandwich at 17.5 J energy level: (a) load versus time and energy versus time, (b) load versus displacement

142

Figure 24. Impact test curves of 2% kaolin filled sandwich at 25 J energy level: (a) load versus time and energy versus time, (b) load versus displacement
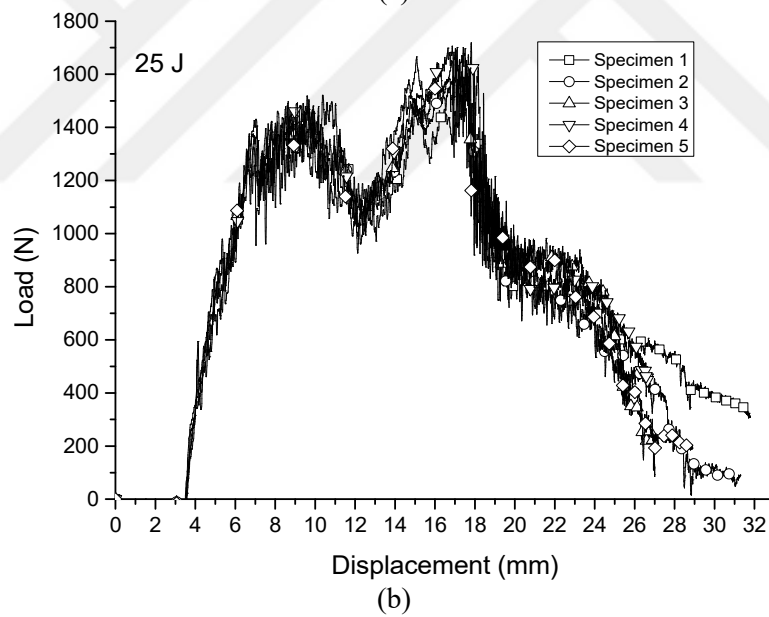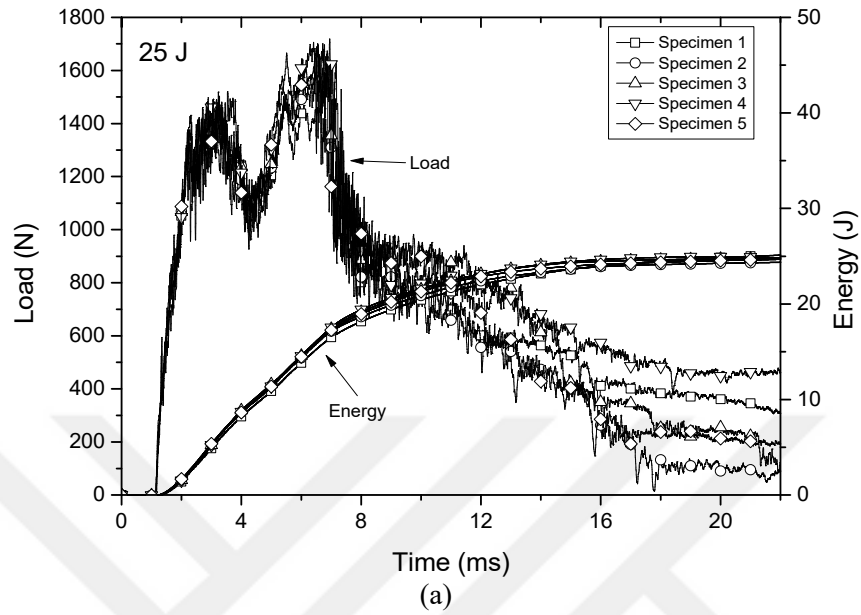
Figure 25. Impact test curves of 5% kaolin filled sandwich at 25 J energy level: (a) load versus time and energy versus time, (b) load versus displacement
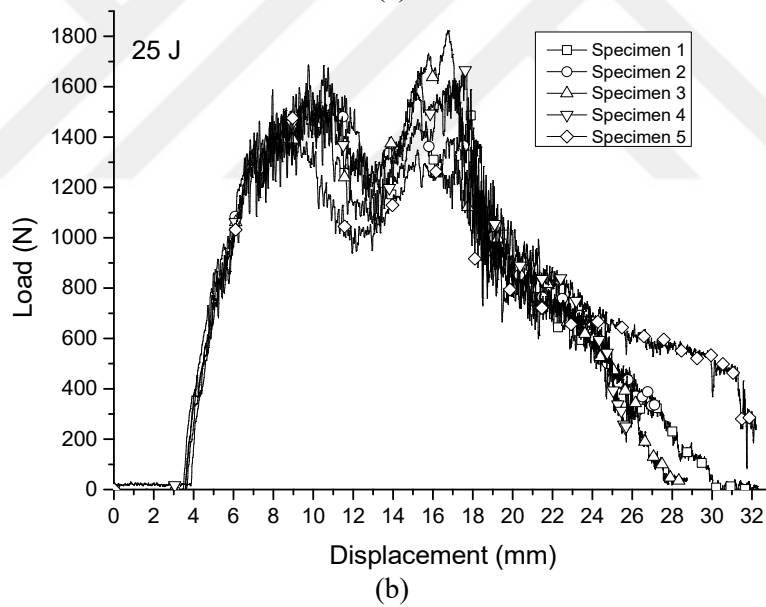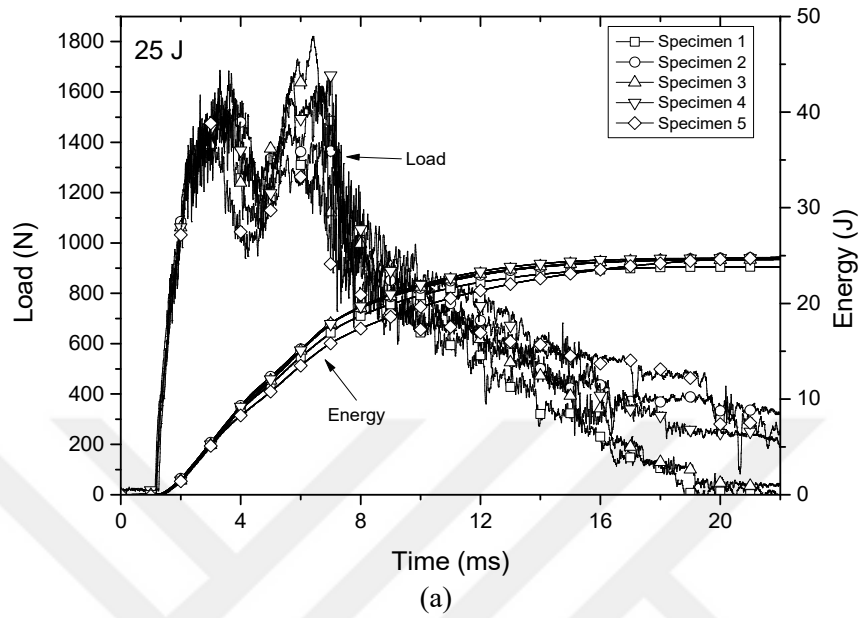
Figure 26. Impact test curves of 10% kaolin filled sandwich at 25 J energy level: (a) load versus time and energy versus time, (b) load versus displacement